

Design Methods for In-Stream Flow Control Structures

DETAILS

90 pages | 8.5 x 11 | PAPERBACK

ISBN 978-0-309-30821-2 | DOI 10.17226/22237

AUTHORS

Fotis Sotiropoulos and Panayiotis Diplas

BUY THIS BOOK

FIND RELATED TITLES

Visit the National Academies Press at NAP.edu and login or register to get:

- Access to free PDF downloads of thousands of scientific reports
- 10% off the price of print titles
- Email or social media notifications of new titles related to your interests
- Special offers and discounts



Distribution, posting, or copying of this PDF is strictly prohibited without written permission of the National Academies Press. (Request Permission) Unless otherwise indicated, all materials in this PDF are copyrighted by the National Academy of Sciences.

NATIONAL COOPERATIVE HIGHWAY RESEARCH PROGRAM

NCHRP REPORT 795

**Design Methods for In-Stream
Flow Control Structures**

Fotis Sotiropoulos

ST. ANTHONY FALLS LABORATORY
DEPARTMENT OF CIVIL, ENVIRONMENTAL, AND GEO-ENGINEERING
UNIVERSITY OF MINNESOTA
Minneapolis, MN

Panayiotis Diplas

DEPARTMENT OF CIVIL AND ENVIRONMENTAL ENGINEERING
LEHIGH UNIVERSITY
Bethlehem, PA

Subscriber Categories

Hydraulics and Hydrology

Research sponsored by the American Association of State Highway and Transportation Officials
in cooperation with the Federal Highway Administration

TRANSPORTATION RESEARCH BOARD

WASHINGTON, D.C.

2014

www.TRB.org

NATIONAL COOPERATIVE HIGHWAY RESEARCH PROGRAM

Systematic, well-designed research provides the most effective approach to the solution of many problems facing highway administrators and engineers. Often, highway problems are of local interest and can best be studied by highway departments individually or in cooperation with their state universities and others. However, the accelerating growth of highway transportation develops increasingly complex problems of wide interest to highway authorities. These problems are best studied through a coordinated program of cooperative research.

In recognition of these needs, the highway administrators of the American Association of State Highway and Transportation Officials initiated in 1962 an objective national highway research program employing modern scientific techniques. This program is supported on a continuing basis by funds from participating member states of the Association and it receives the full cooperation and support of the Federal Highway Administration, United States Department of Transportation.

The Transportation Research Board of the National Academies was requested by the Association to administer the research program because of the Board's recognized objectivity and understanding of modern research practices. The Board is uniquely suited for this purpose as it maintains an extensive committee structure from which authorities on any highway transportation subject may be drawn; it possesses avenues of communications and cooperation with federal, state and local governmental agencies, universities, and industry; its relationship to the National Research Council is an insurance of objectivity; it maintains a full-time research correlation staff of specialists in highway transportation matters to bring the findings of research directly to those who are in a position to use them.

The program is developed on the basis of research needs identified by chief administrators of the highway and transportation departments and by committees of AASHTO. Each year, specific areas of research needs to be included in the program are proposed to the National Research Council and the Board by the American Association of State Highway and Transportation Officials. Research projects to fulfill these needs are defined by the Board, and qualified research agencies are selected from those that have submitted proposals. Administration and surveillance of research contracts are the responsibilities of the National Research Council and the Transportation Research Board.

The needs for highway research are many, and the National Cooperative Highway Research Program can make significant contributions to the solution of highway transportation problems of mutual concern to many responsible groups. The program, however, is intended to complement rather than to substitute for or duplicate other highway research programs.

NCHRP REPORT 795

Project 24-33
ISSN 0077-5614
ISBN 978-0-309-30821-2
Library of Congress Control Number 20149455582

© 2014 National Academy of Sciences. All rights reserved.

COPYRIGHT INFORMATION

Authors herein are responsible for the authenticity of their materials and for obtaining written permissions from publishers or persons who own the copyright to any previously published or copyrighted material used herein.

Cooperative Research Programs (CRP) grants permission to reproduce material in this publication for classroom and not-for-profit purposes. Permission is given with the understanding that none of the material will be used to imply TRB, AASHTO, FAA, FHWA, FMCSA, FTA, or Transit Development Corporation endorsement of a particular product, method, or practice. It is expected that those reproducing the material in this document for educational and not-for-profit uses will give appropriate acknowledgment of the source of any reprinted or reproduced material. For other uses of the material, request permission from CRP.

NOTICE

The project that is the subject of this report was a part of the National Cooperative Highway Research Program, conducted by the Transportation Research Board with the approval of the Governing Board of the National Research Council.

The members of the technical panel selected to monitor this project and to review this report were chosen for their special competencies and with regard for appropriate balance. The report was reviewed by the technical panel and accepted for publication according to procedures established and overseen by the Transportation Research Board and approved by the Governing Board of the National Research Council.

The opinions and conclusions expressed or implied in this report are those of the researchers who performed the research and are not necessarily those of the Transportation Research Board, the National Research Council, or the program sponsors.

The Transportation Research Board of the National Academies, the National Research Council, and the sponsors of the National Cooperative Highway Research Program do not endorse products or manufacturers. Trade or manufacturers' names appear herein solely because they are considered essential to the object of the report.

Published reports of the

NATIONAL COOPERATIVE HIGHWAY RESEARCH PROGRAM

are available from:

Transportation Research Board
Business Office
500 Fifth Street, NW
Washington, DC 20001

and can be ordered through the Internet at:

<http://www.national-academies.org/trb/bookstore>

Printed in the United States of America

THE NATIONAL ACADEMIES

Advisers to the Nation on Science, Engineering, and Medicine

The **National Academy of Sciences** is a private, nonprofit, self-perpetuating society of distinguished scholars engaged in scientific and engineering research, dedicated to the furtherance of science and technology and to their use for the general welfare. Upon the authority of the charter granted to it by the Congress in 1863, the Academy has a mandate that requires it to advise the federal government on scientific and technical matters. Dr. Ralph J. Cicerone is president of the National Academy of Sciences.

The **National Academy of Engineering** was established in 1964, under the charter of the National Academy of Sciences, as a parallel organization of outstanding engineers. It is autonomous in its administration and in the selection of its members, sharing with the National Academy of Sciences the responsibility for advising the federal government. The National Academy of Engineering also sponsors engineering programs aimed at meeting national needs, encourages education and research, and recognizes the superior achievements of engineers. Dr. C. D. Mote, Jr., is president of the National Academy of Engineering.

The **Institute of Medicine** was established in 1970 by the National Academy of Sciences to secure the services of eminent members of appropriate professions in the examination of policy matters pertaining to the health of the public. The Institute acts under the responsibility given to the National Academy of Sciences by its congressional charter to be an adviser to the federal government and, upon its own initiative, to identify issues of medical care, research, and education. Dr. Victor J. Dzau is president of the Institute of Medicine.

The **National Research Council** was organized by the National Academy of Sciences in 1916 to associate the broad community of science and technology with the Academy's purposes of furthering knowledge and advising the federal government. Functioning in accordance with general policies determined by the Academy, the Council has become the principal operating agency of both the National Academy of Sciences and the National Academy of Engineering in providing services to the government, the public, and the scientific and engineering communities. The Council is administered jointly by both Academies and the Institute of Medicine. Dr. Ralph J. Cicerone and Dr. C. D. Mote, Jr., are chair and vice chair, respectively, of the National Research Council.

The **Transportation Research Board** is one of six major divisions of the National Research Council. The mission of the Transportation Research Board is to provide leadership in transportation innovation and progress through research and information exchange, conducted within a setting that is objective, interdisciplinary, and multimodal. The Board's varied activities annually engage about 7,000 engineers, scientists, and other transportation researchers and practitioners from the public and private sectors and academia, all of whom contribute their expertise in the public interest. The program is supported by state transportation departments, federal agencies including the component administrations of the U.S. Department of Transportation, and other organizations and individuals interested in the development of transportation. **www.TRB.org**

www.national-academies.org

COOPERATIVE RESEARCH PROGRAMS

CRP STAFF FOR NCHRP REPORT 795

Christopher W. Jenks, *Director, Cooperative Research Programs*
Christopher Hedges, *Manager, National Cooperative Highway Research Program*
David A. Reynaud, *Senior Program Officer*
Megan A. Chamberlain, *Senior Program Assistant*
Eileen P. Delaney, *Director of Publications*
Doug English, *Editor*

NCHRP PROJECT 24-33 PANEL Soils and Geology—Mechanics and Foundations

Michael Fazio, *City of Bluffdale, Utah, Bluffdale, UT (Chair)*
Eric R. Brown, *Federal Highway Administration, Baltimore, MD*
Petronella L. DeWall, *Minnesota DOT, Oakdale, MN*
Stanley C. Hopfe, *Texas DOT, Austin, TX*
Peggy A. Johnson, *Pennsylvania State University, University Park, PA*
Andrew T. Nottingham, *North Carolina DOT, Raleigh, NC*
David Stolpa, *TRC Companies Inc., Austin, TX*
Kornel Kerenyi, *FHWA Liaison*
Stephen F. Maher, *TRB Liaison*

AUTHOR ACKNOWLEDGMENTS

The research reported herein was performed under NCHRP Project 24-33 by the St. Anthony Falls Laboratory (SAFL) at the University of Minnesota (UMN). UMN was the contractor for this study.

Dr. Fotis Sotiropoulos, James L. Record Professor of Civil Engineering and Director of the St. Anthony Falls Laboratory, was the Principal Investigator. Dr. Panayiotis Diplas, P. C. Rossin Professor and Chair, Water Resources Engineering, Lehigh University (formerly Professor of Civil Engineering at Virginia Tech for the duration of this study) was the co-Principal Investigator. Other contributors to this report were Dr. Jessica Kozarek, Research Associate at SAFL, Ali Khosronejad, Research Associate at SAFL, Craig Hill (SAFL), Dr. Seokkoo Kang (former PhD student, SAFL), Read Plott (former MS student, Virginia Tech), Rajan Jha (former MS student, Virginia Tech), Ryan Radspinner (former MS student, Virginia Tech), and Dr. Anne Lightbody (former Research Associate, SAFL).

FOREWORD

By David A. Reynaud

Staff Officer

Transportation Research Board

This report presents design guidelines for in-stream flow control structures that are often used to limit lateral migration and reduce bank erosion. The guidelines include a description of conditions under which in-stream flow control structures are either successful or not effective in providing protection against erosion and scour and in performing applicable habitat restoration functions. Unlike rip-rap, which strengthens the bank to withstand the applied hydrodynamic forces, in-stream flow control structures alter the stream-flow patterns to shift the high-velocity thread away from the bank. This report will be valuable to hydraulic engineers by facilitating the use of an alternative method to reduce stream-bank erosion and scour.

To design economic in-stream flow control structures with confidence, hydraulic engineers need sound engineering design, installation, and maintenance criteria. These criteria must be supported by quantitative optimization of parameters, such as the amount of construction materials, life-cycle cost, size, spacing, and foundation depth, and their influence on the stream habitat, scour depth, sediment transport, and long-term structure and channel stability.

The objective of NCHRP Project 24-33 was to develop quantitative engineering guidelines, design methods, and recommended specifications for in-stream, low-flow structures that address (1) erosion protection, channel stability, sediment transport, and scour stability of the stream; (2) cost-effectiveness, as well as long-term performance in terms of the low-flow structure stability, durability, and survivability; (3) recommended installation practices; and (4) maintenance requirements.

To develop these guidelines, researchers at the University of Minnesota's St. Anthony Falls Laboratory and Virginia Tech coupled an in-depth review of the current use of in-stream structures with a comprehensive study of five of the most commonly used in-stream structures using physical and numerical experiments. They conducted physical experiments at two scales: a laboratory-scale straight-channel flume and an outdoor field-scale meandering experimental channel. After extensive validation using the physical experimental results, a state-of-the-art coupled hydrodynamic and bed morphodynamic model was used to investigate the performance of various structure configurations under different geomorphic settings. This model, dubbed the Virtual Stream Lab (VSL3D), is capable of simulating the complex three-dimensional flows around in-stream structures and their interaction with the bed.

C O N T E N T S

1	Summary
2	Chapter 1 Background
4	Chapter 2 Research Approach
4	2.1 Rock Vanes
5	2.2 J-Hook Vanes
6	2.3 Bendway Weirs/Stream Barbs
6	2.4 Cross Vanes
7	2.5 W-Weirs
9	Chapter 3 Numerical Methodology for Developing Design Guidelines for Single-Arm Structures
12	3.1 VSL3D Results for Rock Vanes
20	3.2 VSL3D Results for J-Hook Vanes
25	3.3 VSL3D Results for Bendway Weirs/Stream Barbs
35	Chapter 4 Numerical Methodology for Developing Design Guidelines for Sill Structures
35	4.1 VSL3D Results for Cross Vanes
41	4.2 VSL3D Results for W-Weirs
44	Chapter 5 Comparison of In-Stream Flow Control Structure Types
44	5.1 Bank Protection
44	5.2 Scour Hole Dimensions
46	5.3 Flanking Potential
46	5.4 Hydrodynamic Forces on Rock Structures
49	5.5 Backwater and Water Surface Elevation Impacts
54	Chapter 6 Evaluation of Current Guidelines
54	6.1 Length of Bank Protection in Meandering Channels
54	6.2 Spacing and Number of Structures
56	6.3 Footer Rock Depths
58	Chapter 7 Compilation of Experimental and Numerical Results to Develop Design Guidelines
58	7.1 Rock Vanes/J-Hooks
60	7.2 Bendway Weirs/Stream Barbs
62	7.3 Sill Structures (Cross Vanes/W-Weirs)
62	7.4 Structure Selection
64	References
66	Appendix F Design Guidelines for In-Stream Flow Control Structures

Appendices A through E and G are posted on the project web page at <http://apps.trb.org/cmsfeed/TRBNetProjectDisplay.asp?ProjectID=1641>.

LIST OF ABBREVIATIONS AND VARIABLES

A: cross-sectional area (of rock)
B: width
 BW: bendway weir
C_d: drag coefficient
 CV: cross vane (U-shaped)
 CVA: cross vane (A-shaped)
*D*₅₀: median grain size
*D*₁₀₀: largest rock size
F: drag force on a single rock
F_o: representative drag force on a single rock using bulk velocity
H: flow depth
 ISL: indoor StreamLab
 JH: J-hook
L: distance along structure
L_d: downstream bank length
L_e: effective length perpendicular to flow
L_s: structure length
L_u: upstream bank length
 OSL: outdoor StreamLab
Q_{bf}: bankfull discharge
R_c: radius of curvature
 RV: rock vane
S_{C_{MAX}}: maximum scour compared to average bed elevation in baseline channel
S_{ct}: scour at the structure tip
S: slope
 TKE: turbulence kinetic energy
u: local velocity magnitude
V_s: structure spacing
 WW: W-weir
Z_{bed}: time-averaged quasi-equilibrium bed elevation (*Z_{bed}* = 0 at initial flat bed)
 ΔZ : *Z_{bed}* with structure minus *Z_{bed}* for baseline case
Z_{rms}: RMS of bed elevation
 ϕ : angle of repose
 ρ : density of water
 λ : wavelength

S U M M A R Y

Design Methods for In-Stream Flow Control Structures

In-stream flow control structures have been promoted as an alternative to traditional engineering methods employed for protecting rivers and streams against erosion and scour, thus stabilizing them against lateral migration. These structures work in a fundamentally different way that provides a more sustainable solution to the problem of bank erosion. Instead of strengthening the bank to withstand the applied hydrodynamic forces, as rip-rap and similar protection techniques do, they shift the high-velocity thread away from the bank by altering the stream-flow patterns. Furthermore, they typically use less construction material and have the potential for enhancing the availability of stream habitat. Researchers at St. Anthony Falls Laboratory (SAFL) and Virginia Tech coupled an in-depth review of the current use of in-stream structures with a comprehensive study of five of the most commonly used in-stream structures using physical and numerical experiments. Physical experiments were conducted at two scales, a laboratory-scale straight-channel flume and a field-scale meandering experimental channel. After extensive validation using the physical experimental results, a state-of-the-art coupled hydrodynamic and bed morphodynamic model developed by researchers at SAFL was used to investigate the performance of various structure configurations under different geomorphic settings. This model, dubbed the Virtual StreamLab (VSL3D), is capable of simulating the complex three-dimensional flows around in-stream structures and their interaction with the streambed.

Shallow, low-flow structures can span all (sill structures) or part (single-arm structures) of a stream channel. Single-arm structures (rock vanes, J-hook vanes, and bendway weirs) were evaluated for their ability to provide bank protection, redirect the channel thalweg, and provide scour pool habitat. Sill structures (cross vanes and W-weirs) were evaluated for their ability to provide bank protection, grade control, and scour pool habitat. Failure mechanisms for all structures were evaluated, including structure undermining, rock displacement, and flanking (or circumvention behind the structure). Structure configurations were optimized using a systematic approach, first evaluating structure angle, then evaluating spacing and number of structures and location in representative sand and gravel rivers. Results from the review, practitioner survey, field case studies, physical experiments, and numerical investigations were integrated to develop in-stream structure design guidelines.

CHAPTER 1

Background

Efforts to stabilize and restore streams and rivers across the nation have grown dramatically in recent decades, with over \$1 billion spent annually on projects with goals including stabilizing banks, improving water quality, and improving aquatic habitat (Bernhardt et al., 2005). In-stream structures, constructed of rock or wood in various configurations, are often used to limit lateral migration, reduce bank erosion, and create diverse aquatic habitat (Radspinner et al., 2010).

In-stream structures can be classified into two fundamental categories: sills and single-arm structures (Figure 1-1). Sills are structures that span the entire channel width, while single-arm structures extend from one bank into the channel without reaching the opposite bank. Single-arm structures can be further subdivided into deflector, redirective, and retard types, depending on the function of each structure configuration [National Resources Conservation Service (NRCS), 2007].

Proper structure design and placement are necessary to avoid channel aggradation, local bed scour, and bank erosion, all of which can result in structure failure and cause significant harm to the stream and nearby property. Furthermore, failure of these structures will accelerate the adverse effects they were initially installed to prevent, such as lateral migration and infrastructure endangerment (see Table 1-1); however, stream restoration and river training measures today rely heavily on empirical methods

that emphasize a prescribed design approach rather than the application of physically based hydraulic engineering principles to attain performance-based criteria (Simon et al., 2007; Slate et al., 2007). The lack of a comprehensive physics-based design approach can be attributed to the unsteady, three-dimensional (3-D) character of the flow in the vicinity of structures and the fact that the complex interactions of stream hydrodynamics in the water column with streambed sediments are poorly understood. Consequently, the effects of various site-specific conditions on the overall performance and long-term stability of in-stream structures can neither be quantified a priori nor be accounted for in the design process.

In an effort to supplement existing guidelines with comprehensive quantitative analysis of frequently used flow control structures, in this work an in-depth review of current structure use (see Radspinner et al., 2010) is integrated with state-of-the-art physical and numerical modeling and field data collection (Figure 1-2). The result is a set of design guidelines that are based on a state-of-the-art understanding of how turbulence, mobile beds, and sediments interact with and are modified by streams and rivers with flow control rock structures. This report summarizes the methodology employed in this work and presents design guidelines derived by applying this methodology to in-stream flow control structures.

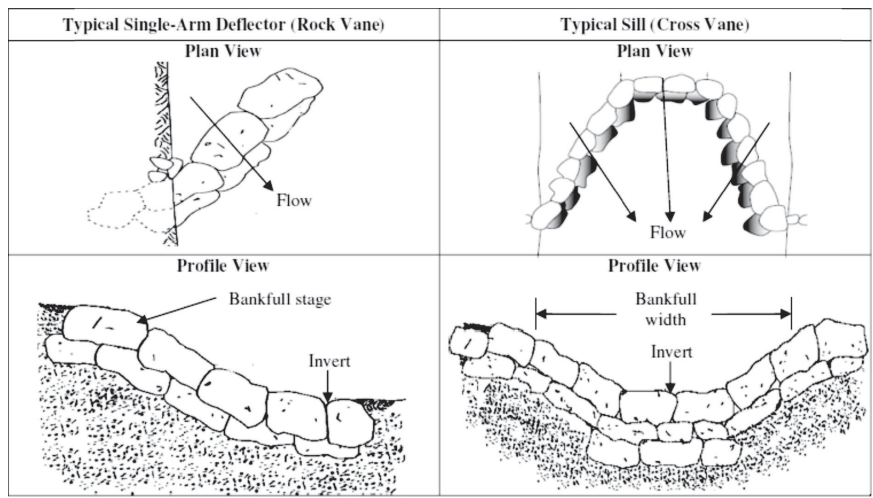


Figure 1-1. Illustrations of typical single-arm deflector structure and typical sill rock structure (from Radspinner et al., 2010).

Table 1-1. Reasons and modes of failure reported in the practitioner survey published in Radspinner et al. (2010).

Structure Type	Channel Characteristics			Failure	
	Aspect Ratio	Sinuosity	Slope	Reasons	Modes
Single-arm structures					
Rock vane (RV)	7–33	n/a	0.003–0.008	Not keyed properly; rock size and shape	Lateral circumvention; winnowing; local scour; aggradation
J-hook vane (JH)	8.8–36	1.1–1.5	0.003–0.02	Not keyed properly; rock size and shape	Lateral circumvention; winnowing; local scour; aggradation
Bendway weir (BW)	8.6–33	1.3–1.5	<0.003	Footer size; build depth	Local scour
Sill structures					
Cross vane (CV and CVA)	7.3–19.6	1.1–1.5	0.001–0.03	Faulty installation; rock size and shape	Lateral circumvention; winnowing; local scour; aggradation; displacement
W-weir (WW)	n/a	n/a	n/a	Faulty installation; rock size and shape	Lateral circumvention; winnowing; local scour; aggradation; displacement

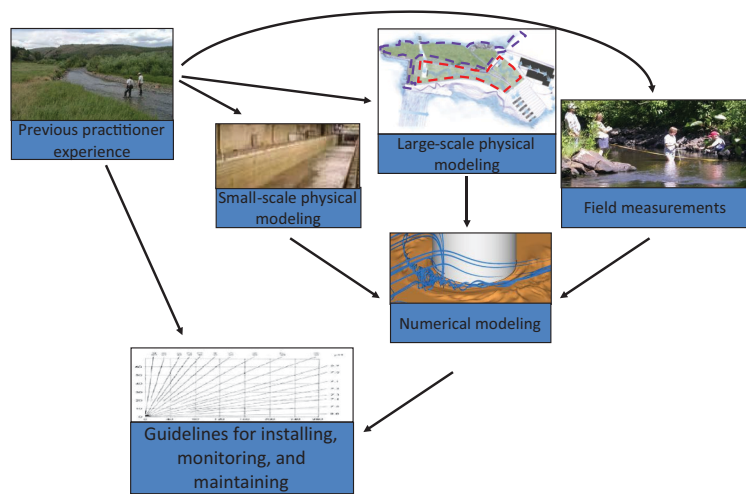


Figure 1-2. Linkages between components used to develop guidelines for the use of in-stream structures to prevent erosion and protect surface transportation.

CHAPTER 2

Research Approach

The objective of this research was to develop comprehensive engineering guidelines, design methods, and recommended specifications for in-stream structure installation, monitoring, and maintenance. Phase I consisted of background research into the current use and success of in-stream structures and their long-term durability and maintenance requirements (Appendix A). In addition to performing a comprehensive literature review, the combined experience of transportation and natural resource departments was used to describe and evaluate existing low-flow structure applications and failure modes (Appendix B). In Phase II, the findings from Phase I were used to develop a comprehensive study using physical and numerical models to explore the most promising structures. Structures that were selected for this project are described in the following.

The Virtual StreamLab (VSL3D) model was used to extend detailed field (Appendix C) and laboratory (Appendix D) measurements to a wider range of channel configurations and flow rates. VSL3D is a state-of-the-art 3-D computational fluid dynamics model developed at St. Anthony Falls Laboratory (SAFL) by Fotis Sotiropoulos and coworkers that is capable of simulating real-life hydraulic engineering flows using advanced numerical techniques and turbulence models that can be coupled with turbulent-free surface and bed-morphodynamics modules. Following validation (Appendix E), this model was used to systematically explore a matrix of structure scenarios in representative gravel and sand channels (Chapter 3). Design guidelines (Appendix F) for in-stream flow control structures based on a combination of laboratory, field, and numerical experiments were developed to inform the choice of structure type, angle of orientation, spacing, and location based on site-specific channel characteristics.

2.1 Rock Vanes

The term “rock vane” (RV) applies to single-arm rock structures that extend out from a stream bank into the flow. These structures gradually slope from the bank to the bed

such that, even at low-flow conditions, the tips of the structure remain submerged (Radspinner et al., 2010). RVs are installed with an upstream angle to minimize erosive flow patterns near the bank by diverting high-velocity flow away from the bank (Maryland Department of the Environment, 2000; Johnson et al., 2002a; see Figure 2-1). Often, RVs and other in-stream rock structures are installed with a secondary goal of improving aquatic habitat by creating flow diversity through the formation of scour pools (Rosgen, 2006). A series of vanes installed for bank protection is intended to move scour to the middle of the channel and enhance deposition along the bank (e.g., Johnson et al., 2001; Bhuiyan et al., 2010). RVs and other in-stream rock structures can reduce or eliminate the need for bank armoring on unstable banks and can improve the effectiveness of other erosion protection measures such as vegetation restoration (McCullah and Gray, 2005). Current guidelines for placement and spacing of RVs are based primarily on practitioner experience (e.g., Maryland Department of the Environment, 2000; Doll et al., 2003; NRCS, 2007).

The Maryland Department of the Environment’s Water Management Administration included design guidelines for rock vanes in its Maryland’s Waterway Construction Guidelines (MWCG) manual (Maryland Department of the Environment, 2000). Included in this document is a summary of the uses of common restoration and stabilization practices. Within this summary, applications for which rock vanes are well suited (e.g., protecting bank toe and redirecting flows), moderately well suited (e.g., providing in-stream habitat), and not well suited (e.g., stabilizing bed and use in bedrock channels) are discussed. Based on the practitioner experience reported in the MWCG, caution should be used in steep stream reaches with gradients that exceed 3%. It is also important to note that the stream bank opposite the RV structures should be monitored closely after installation for any increase in erosion occurring due to the presence of the RV and its ability to direct flow away from the outer bank,

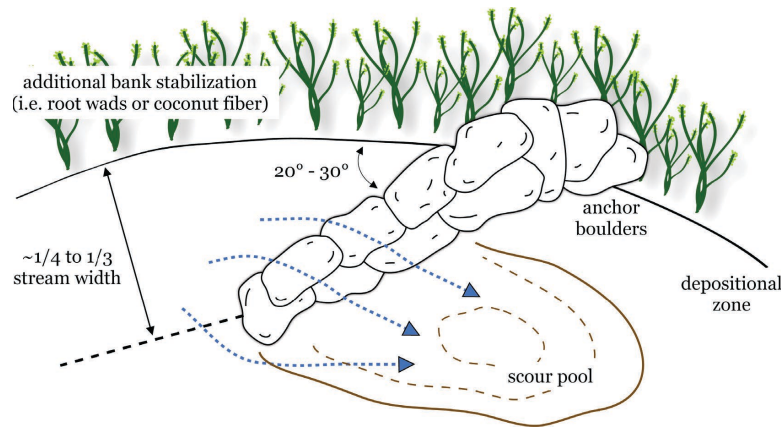


Figure 2-1. Typical rock vane installation (after Rosgen, 2006 and Radspinner et al., 2010).

toward the center of the channel—on occasion negatively affecting the opposite bank.

Several structures use the rock vane as the key component and modify it for various situations. All structures from the rock vane family can be subjected to failure by lateral circumvention, winnowing, local scour, aggradation, and displacement (Johnson et al., 2002b). In addition to Rosgen (2001; 2006) and the MWCG (Maryland Department of the Environment, 2000), rock vane design guidelines can be found in the United States Department of Agriculture (USDA) NRCS *Stream Restoration Design National Engineering Handbook*, Part 654 (NRCS, 2007). Chapter 11 of this design manual, “Rosgen Geomorphic Channel Design,” focuses on the design guidelines for CVs, J-hook (JH) vanes, and W-weir (WW)

structures; however, all of these structures are rock vane variations.

2.2 J-Hook Vanes

JH vanes are a variation of the single-arm RV that include a hook that extends from the tip of the vane approximately perpendicular to flow (Figure 2-2). Similar to the rock vane, the vane portion of these structures gradually slopes from the bank to the bed such that even at low-flow conditions, the tip of the structure remains submerged (Radspinner et al., 2010). JH vanes are also installed with an upstream angle to minimize erosive flow patterns near the bank by diverting high-velocity flow away from the bank (Maryland

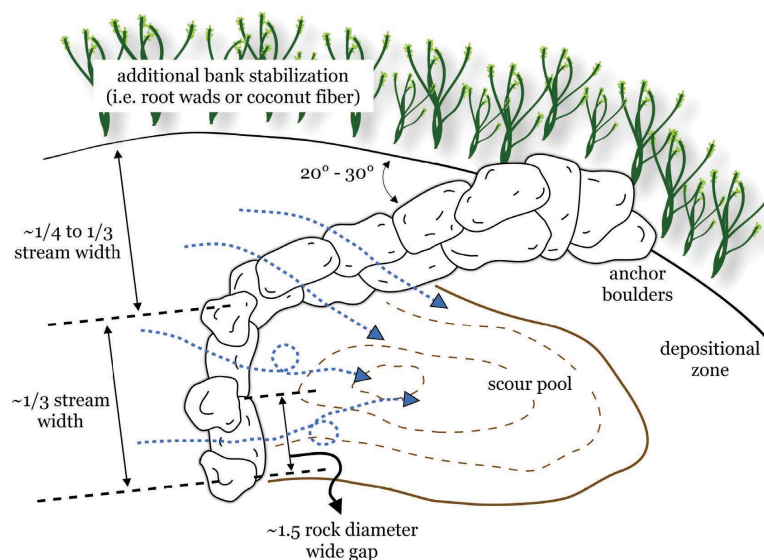


Figure 2-2. Typical J-hook vane installation (after Rosgen, 2006).

Department of the Environment, 2000; Johnson et al., 2002a). Often, rock vanes and other in-stream rock structures are installed with the secondary goal of improving aquatic habitat by creating flow diversity through the formation of scour pools (Rosgen, 2006), and J-hook vanes are expected to provide additional in-stream habitat enhancement in the form of a mid-channel scour pool (Maryland Department of the Environment, 2000). Current guidelines for placement and spacing of JH vanes are similar to those developed for RVs, based primarily on practitioner experience (e.g., Maryland Department of the Environment, 2000; Doll et al., 2003; NRCS, 2007).

Applications for JH vanes are similar to those for RVs, with the exception that JH vanes are expected to provide better in-stream habitat in the form of a deep mid-channel scour hole (Maryland Department of the Environment, 2000). Limitations of J-hook vanes are similar to those for rock vanes. These structures should not be used in steep stream reaches (greater than 3%). With any flow redirection structure, the stream bank opposite the structure should be monitored closely after installation for any increase in erosion occurring due to the presence of the structure. All structures from the rock vane family can be subjected to failure by lateral circumvention, winnowing, local scour, aggradation, and displacement (Johnson et al., 2002b). J-hook design guidelines can be found in Rosgen (2006), the MWCG (Maryland Department of the Environment, 2000), and the USDA NRCS *Stream Restoration Design National Engineering Handbook*, Part 654 (NRCS, 2007). Chapter 11 of this design manual, “Rosgen Geomorphic Channel Design,” focuses on the design guidelines for cross vanes, J-hook vanes, and W-weir structures.

2.3 Bendway Weirs/Stream Barbs

The terms “bendway weir” (BW) and “stream barb” refer to single-arm rock structures extending from the bank that are submerged in all but low flows and are designed to mitigate erosive flow patterns through weir mechanics (Derrick, 1998; Evans and Kinney, 2000; see Figure 2-3). Several state agencies have published technical notes and case studies for bendway weir use under a variety of stream characteristics (e.g., NRCS, 2010; NRCS, 2000). Stream barbs are designed to protect the bank by disrupting velocity gradients in the near-bed regions, deflecting currents toward the tip of the weirs (Matsuura and Townsend, 2004). Guidelines for bendway weir or stream barb design can be found in the U.S. Department of Transportation (U.S. DOT) Federal Highway Administration (FHWA) Hydraulic Engineering Circular (HEC) No. 23, Volume 2 (Lagasse et al., 2009) and the USDA NRCS *Stream Restoration Design National Engineering Handbook*, Part 654, Technical Supplement 14H (NRCS, 2007).

2.4 Cross Vanes

Cross vanes are low-profile, channel-spanning structures designed to provide grade control, divert flow away from unstable banks, and create scour pools for aquatic habitat (Maryland Department of the Environment, 2000). Cross vanes have also been installed upstream of bridge piers to reduce scour. There are two types of cross vane. The first is a U-shaped structure (CV) that has two arms angled upstream at 20° to 30° from the banks that slope downward to the streambed cross piece (Figure 2-4). The second type, an A-shaped structure (CVA), is a modified cross vane with a step located in the upper $\frac{1}{3}$ to $\frac{1}{2}$ of the arm. This step is

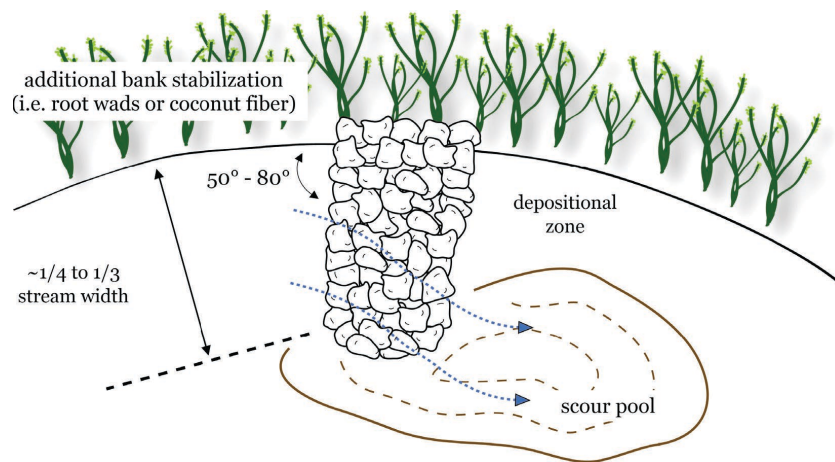


Figure 2-3. Typical bendway weir/stream barb installation (after NRCS, 2007 and Radspinner et al., 2010).

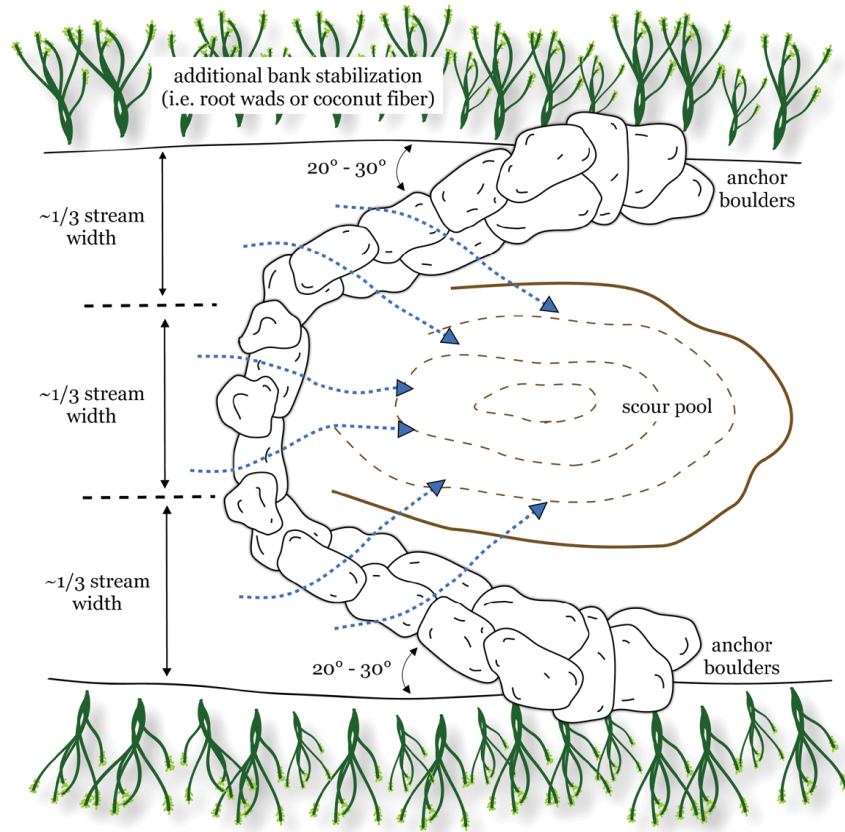


Figure 2-4. Typical cross vane installation (after Rosgen, 2006).

designed to dissipate energy, thereby reducing footer scour and protecting the structure from failure (Rosgen, 2006). Cross vanes are well suited for use in moderate- and high-gradient streams and should be avoided in bedrock channels, streams with unstable bed substrates, and naturally well-developed pool–riffle sequences (Maryland Department of the Environment, 2000). Cross vane design guidelines can be found in Rosgen (2006), the MWCG (Maryland Department of the Environment, 2000), and the USDA NRCS *Stream Restoration Design National Engineering Handbook*, Part 654 (NRCS, 2007). Chapter 11 of this design manual, “Rosgen Geomorphic Channel Design,” focuses on the design guidelines for cross vanes, J-hook vanes, and W-weir structures.

2.5 W-Weirs

Like cross vanes, WWs are low-profile, channel-spanning structures designed to provide grade control, direct flow away from unstable banks, create scour pools for aquatic

habitat, and protect downstream bridge piers (Figure 2-5). WWs are similar to a double cross vane and are typically applicable in larger channels (>12 m or 40 ft in width). They are well suited to protect the bank toe, redirect flow, create flow diversity, and stabilize bed and lateral channel adjustments in channels with highly erodible and steep banks, high design velocity, flashy flows, and high-bedload transport. With proper support, WWs can be used with rigid or fixed banks with limited backwater effects. WWs are not suited for slow-flow or pooled reaches with silt or fine sand beds (Maryland Department of the Environment, 2000). W-weir design guidelines can be found in Rosgen (2006), the MWCG (Maryland Department of the Environment, 2000), and the USDA NRCS *Stream Restoration Design National Engineering Handbook*, Part 654 (NRCS, 2007). Chapter 11 of this design manual, “Rosgen Geomorphic Channel Design,” focuses on the design guidelines for cross vanes, J-hook vanes, and W-weir structures.

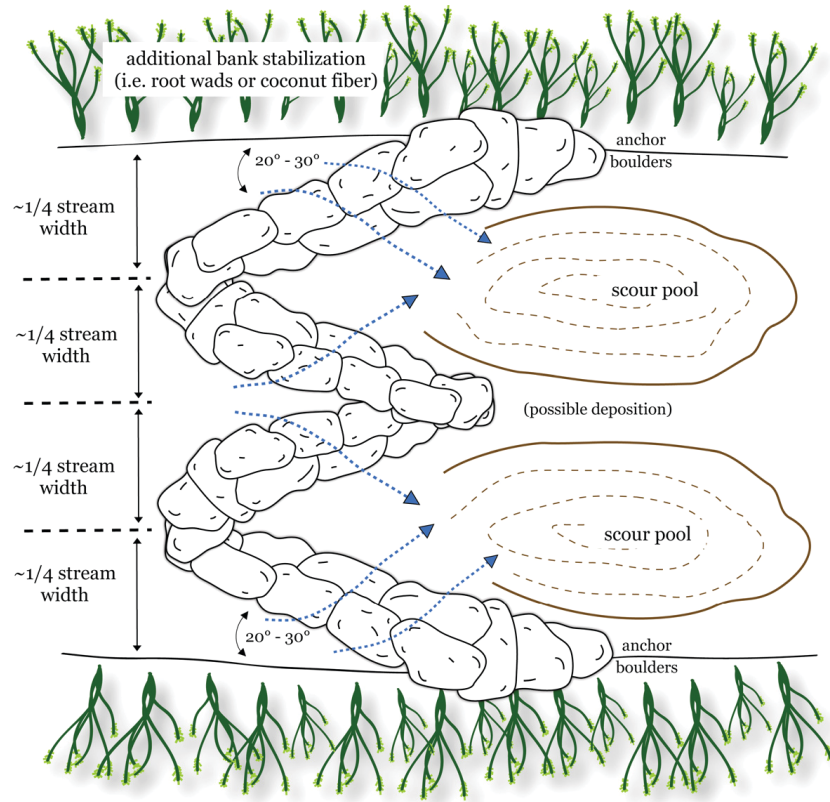


Figure 2-5. Typical W-weir installation (after NRCS, 2007).

CHAPTER 3

Numerical Methodology for Developing Design Guidelines for Single-Arm Structures

Results from case studies and physical experiments (see Appendices C and D) were extended to typical gravel and sand-bed streams using VSL3D (see Appendix E for validation and selection of channel geometry). The goal of these investigations was to determine what structures are most appropriate, how they should be installed (including location of specific structures), how they should be monitored and maintained, and the likely failure mechanisms for each structure installation based on site-specific stream properties (e.g., curvature, slope, bed material).

For each structure type, a systematic approach was used to determine the optimum angle of orientation relative to the bank tangent, spacing, and location for typical sand and gravel channels (Figure 3-1). For single-arm structures (rock vanes, J-hook vanes, and bendway weirs/stream barbs) designed to protect the outer bank of a meander, a single structure was placed at the meander apex, and the angle was varied within a prescribed range defined by current design guidelines for each structure type (Table 3-1). The optimum structure angle was selected as the one that provided the greatest outer bank protection with the least risk to the opposite bank. The risk of structure failure, evaluated by the depth of the scour hole adjacent to the structure, was also included in this evaluation. Optimum spacing for multiple structures was then determined by examining the scour patterns and the location of shear layer reattachment to the outer bank. This process was repeated with additional structures if scour was still present along the outer bank of the test meander. Finally, to examine the effect of structure array location on structure performance, the final structure array was shifted upstream by one channel width. A similar process was employed to evaluate structure angle, location, and multiple structures for channel-spanning sill structures (cross vanes and W-weirs).

The analysis of numerical results focuses on the typical bed morphology of meandering channels for sand and gravel channels (Figure 3-2). Single-arm structures designed to protect the outer bank from scour were first analyzed by exam-

ining the quasi-equilibrium bed topography and comparing this topography to the structure-free quasi-equilibrium bed topography for sand (VSL-S) and gravel (VSL-G) (Figure 3-3). The length of bank protection was defined along the outer bank where the difference between the quasi-equilibrium bed topography for the case with a structure and the baseline case (with no structure) was positive, indicating less scour along the outer bank (Figure 3-3). Three criteria were used to evaluate each single-arm structure case: (1) length of bank protection, (2) depth of scour hole, and (3) threat to inner bank stability. The second two criteria were used to filter out unfavorable configurations where structure failure (due to undermining from excessive scour) and larger channel instability (due to erosion on the inner bank) were likely. With these exceptions, the length of bank protection was the primary factor to differentiate structure performance.

Once the optimum angle of orientation relative to the outer bank tangent was determined for each structure type, additional structures were systematically added to the array as needed by determining the length of the separation zone downstream of the structure to identify the reattachment point or the location where the high-velocity core reattaches to the outer bank. Flow around a meander bend is subject to 3-D helical flow patterns and one or more secondary flow cells that create scour along the outer bank (Chang, 1988; see Kang and Sotiropoulos, 2011; Kang and Sotiropoulos, 2012a, 2012b for detailed discussion of complex flow phenomena in meandering channels.) The location of the high-velocity core and associated high shear stress [see Figure 3-4 for an outdoor StreamLab (OSL) example] moves toward the outer bank of the meander. The location of the high-velocity core attachment to the outer bank varies depending on the channel geometry (Kashyap et al., 2012).

Flow-training structures are used to protect river banks by redirecting or deflecting the high-velocity core away from river banks and interrupting secondary flow patterns. Redirecting the flow results in a flow separation zone defined by a shear layer (Figure 3-5a). Structure geometry, such as length, height,

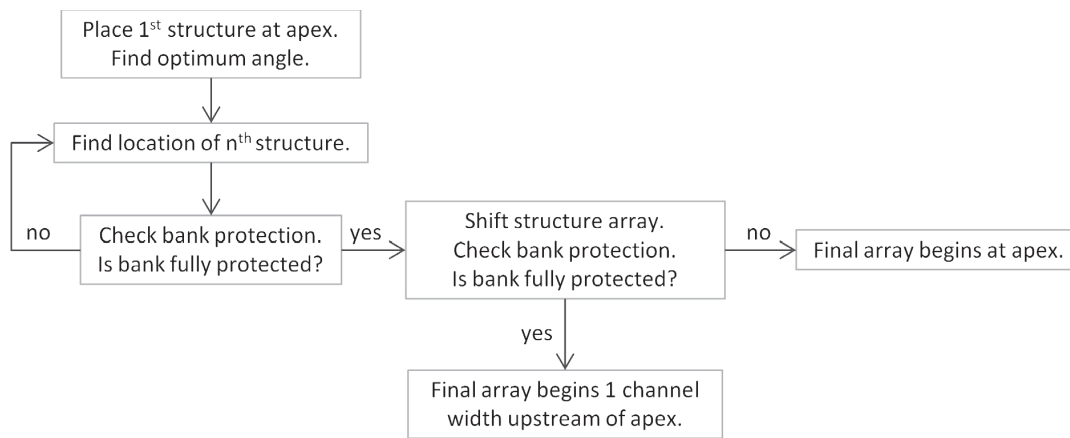


Figure 3-1. Systematic approach for numerical experiments to determine the optimal configuration of single-arm structures for each channel type, gravel (VSL-G), and sand (VSL-S).

Table 3-1. Rock structure geometry used in the VSL3D simulations. B , H , and ϕ are channel width, flow depth, and angle of repose, respectively.

	Single-Arm Structures			Sill Structures		
	Rock vane	Bendway weir	J-hook vane	Cross vane	Cross vane-A	W-weir
Top slope	2%–7%	0%	2%–7%	2%–7%	2%–7%	2%–7%
Side slope	vertical	1:2	vertical	vertical	vertical	vertical
Slope at the tip	vertical	\emptyset	vertical	n/a	n/a	n/a
Top width	D_{100}	$2D_{100}$	D_{100}	D_{100}	D_{100}	D_{100}
Bottom width	D_{100}	$2H + D_{100}$	D_{100}	D_{100}	D_{100}	D_{100}
Max. height of structure	H	$H/2$	H	H	H	H
Effective length span	$B/3$	$B/4$	$2/3 B$	B	B	B
Single rock size (D_{100})	1.2 m	0.569 m	1.2 m	1.2 m	1.2 m	1.2 m
Angle	20°–30°	30°–80°	20°–30°	20°–30°	20°–30°	20°–30°

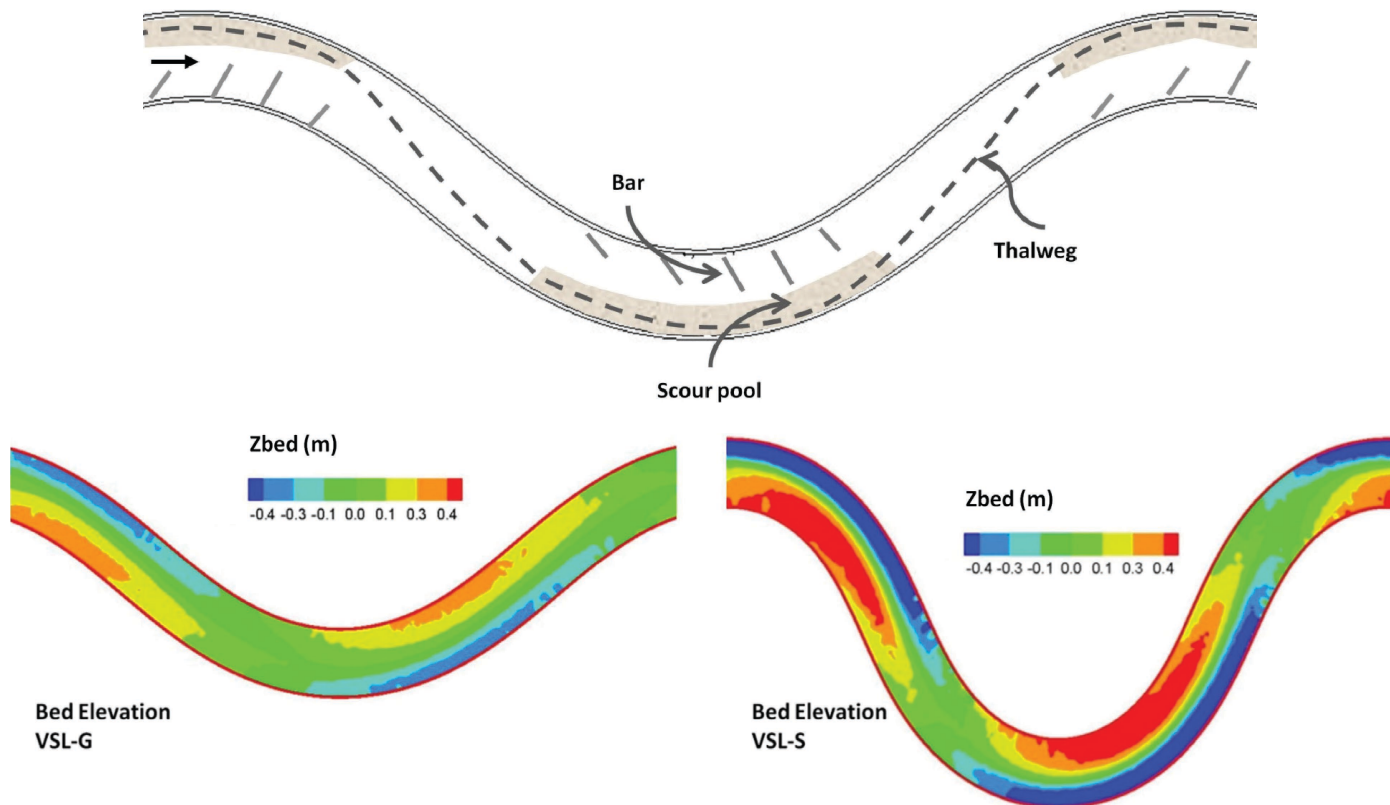


Figure 3-2. Top: typical bed morphology at a simple meander bend in plan view (after Dietrich, 1987); bottom: VSL3D gravel (VSL-G) and sand (VSL-S) bed morphology. Flow is from left to right.

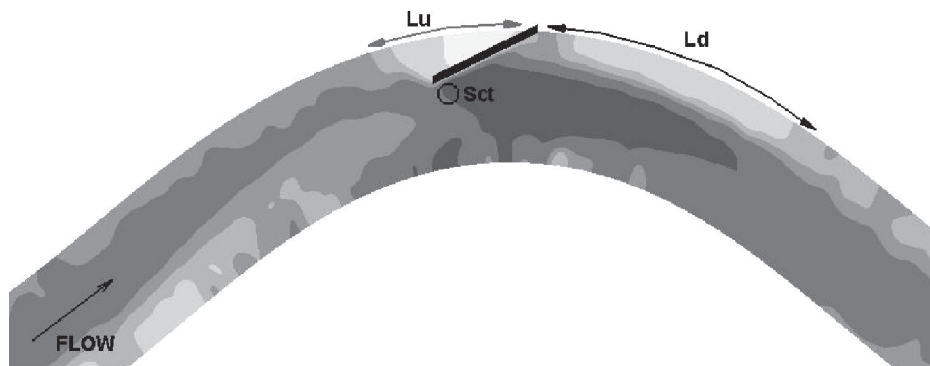


Figure 3-3. Upstream bank protection length, L_u , downstream bank protection length, L_d , and maximum scour at vane tip, S_{ct} , determined from the difference between the time-averaged baseline bed (no structure; Figure 3-2) and the time-averaged bed for each structure case. Darker colors indicate scour, and lighter colors indicate deposition.

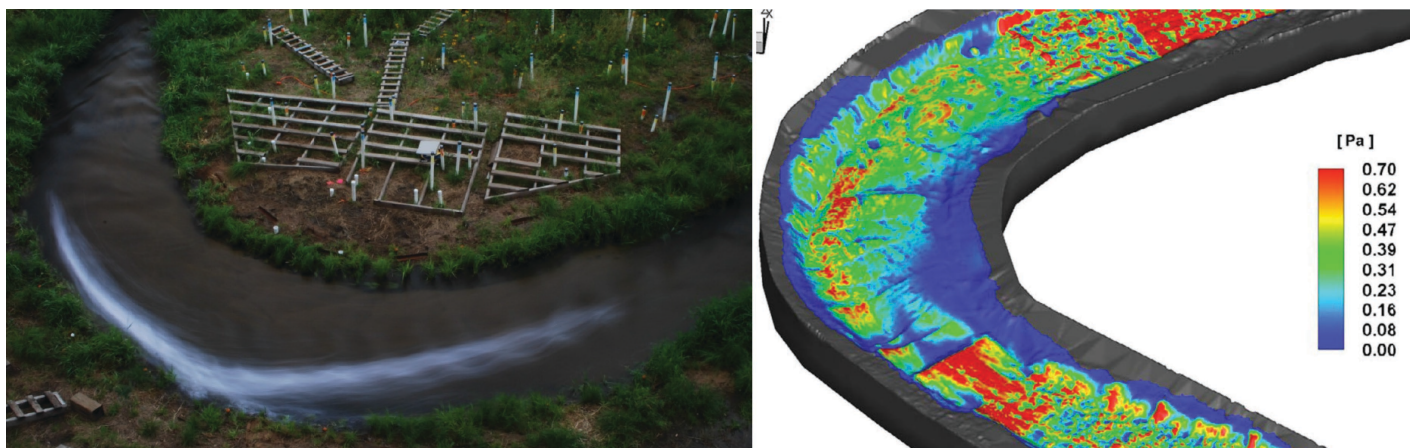


Figure 3-4. The high-velocity core was visualized using confetti and long-exposure photography in the OSL (left). Contours of the mean boundary shear stress (right; flow from bottom to top; Kang and Sotiropoulos, 2011).

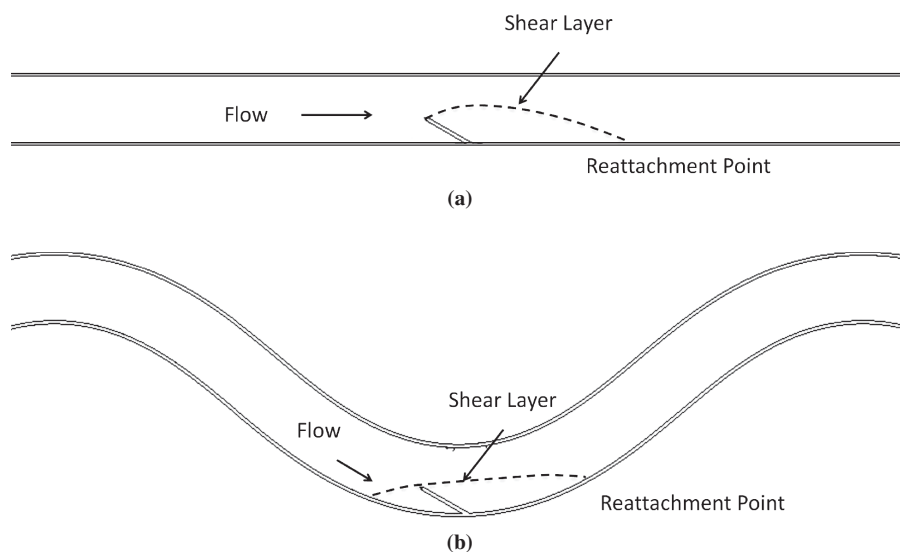


Figure 3-5. Flow separation zone defined by a shear layer in (a) a straight channel and (b) a meandering channel.

width, shape, angle of orientation, submergence, and top angle, affect the flow separation zones present upstream and downstream of a structure (Rajaratnam and Nwachukwu, 1983; Ettema and Muste, 2004; Papanicolaou et al., 2011). In general, the area inside the flow separation zone defined by a shear layer is an area of sediment deposition in recirculating flow, while the area outside of the flow separation zone is subject to scour (Fox et al., 2005). In meandering channels, the flow separation zone is also dependent on the location of the structure within the meander (Sharma and Mohapatra, 2012; see Figure 3-5b). The shear layer can be identified by high turbulence kinetic energy (TKE), where the fast-moving flow around the structure interacts with the slower recirculating flow adjacent to the bank (Figure 3-6). Non-dimensionalized TKE profiles were used in combination with the location of maximum scour along the outer bank to identify the reattachment point or the optimum location for subsequent structures until the entire outer bank was protected from possible bank erosion due to the presence of high shear flow. TKE was non-dimensionalized by mean flow velocity squared.

The following sections present the systematic analysis of each single-arm structure type: rock vane, J-hook vane, and bendway weir/stream barb, following the approach in Figure 3-1. First, the general scour and deposition patterns are analyzed to determine the appropriate angle of orientation for bank projection. Then, spacing and number of structures are determined by an analysis of the TKE patterns and maximum scour along the outer bank. Finally, the location of the final array is examined by shifting the array upstream by one channel width, B .

3.1 VSL3D Results for Rock Vanes

Single Rock Vane Scour and Deposition

A single RV was placed at the meander apex of the VSL-G and VSL-S channels, and the VSL3D model was applied to simulate the resulting bed morphodynamics for the two different angles oriented relative to the tangent to the bank. These two angles were determined based on existing RV guidelines, which suggest RV structure angles in the range of 20° to 30° (NRCS, 2007; Doll et al., 2003; Maryland Department of the Environment, 2000; Brown, 2000). The computed results are shown in Figures 3-7 and 3-8 for VSL-G and VSL-S, respectively. For each case, the time-averaged quasi-equilibrium bed elevation (Z_{bed}), the root-mean-squared (RMS) fluctuations of the bed elevation (Z_{rms}), and the difference between the Z_{bed} with a structure and Z_{bed} with no structure (baseline case shown in Figure 3-2) are shown as elevation difference (ΔZ). Z_{rms} is important to help quantify the changes in bed elevation due to the continuous formation, migration, and merging of bed forms. The computed results indicate that for a single RV, a larger angle provides greater bank protection at the cost of a deep scour hole located adjacent to the RV tip. While the scour hole in VSL-G was deeper for the 20° case than the 30° RV case, there was no scour immediately adjacent to the tip of the structure in either 20° RV case in VSL-G or VSL-S.

Optimum Angle and Spacing

Based on VSL3D results for a single RV structure, a combination of scour and flow field results were used to determine

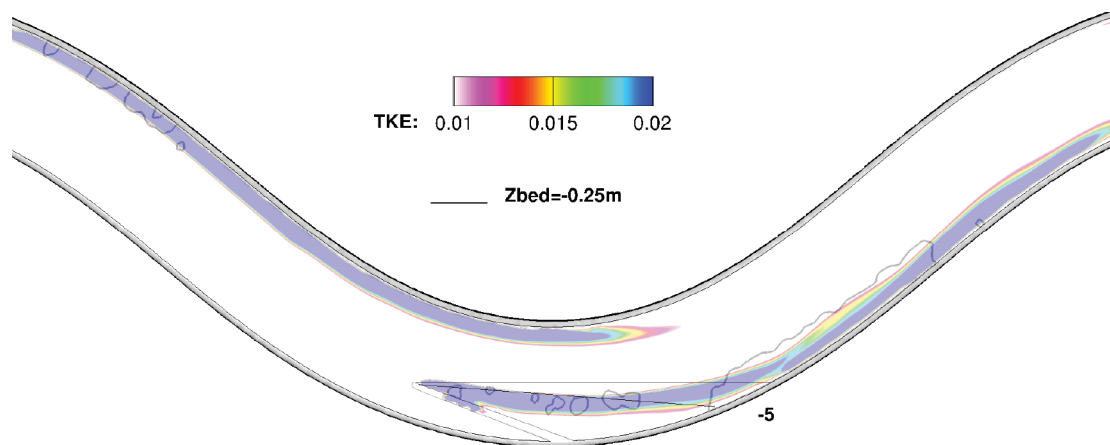


Figure 3-6. Determination of the shear layer downstream of a rock vane using both the zone of high TKE and outer bank scour to identify the reattachment point. In this case the reattachment point is 5° less than the line drawn parallel to the bank tangent at the structure tip. The color map shows the steady-state non-dimensionalized depth-averaged TKE. TKE is non-dimensionalized by mean flow velocity squared. The high-TKE region indicates the location of a shear layer. Contours indicate the deepest scour holes. Flow is from left to right.

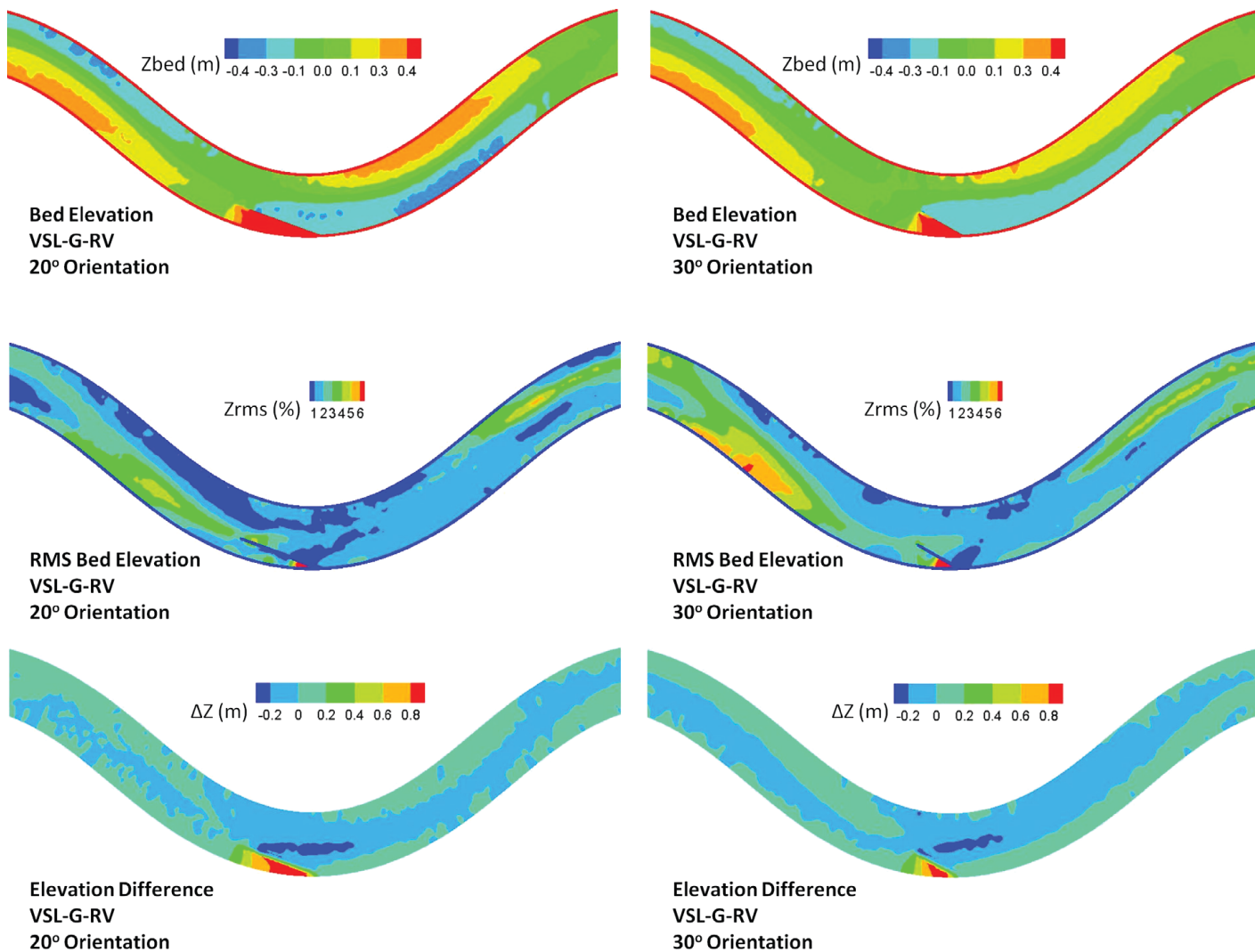


Figure 3-7. *Zbed* for a single rock vane located at the meander apex for VSL-G. The RMS of *Zrms* is non-dimensionalized by the flow depth and multiplied by 100. The ΔZ represents the *Zbed* of the baseline case (with no rock structure; Figure 3-2) subtracted from the *Zbed* of this case. Flow is from left to right.

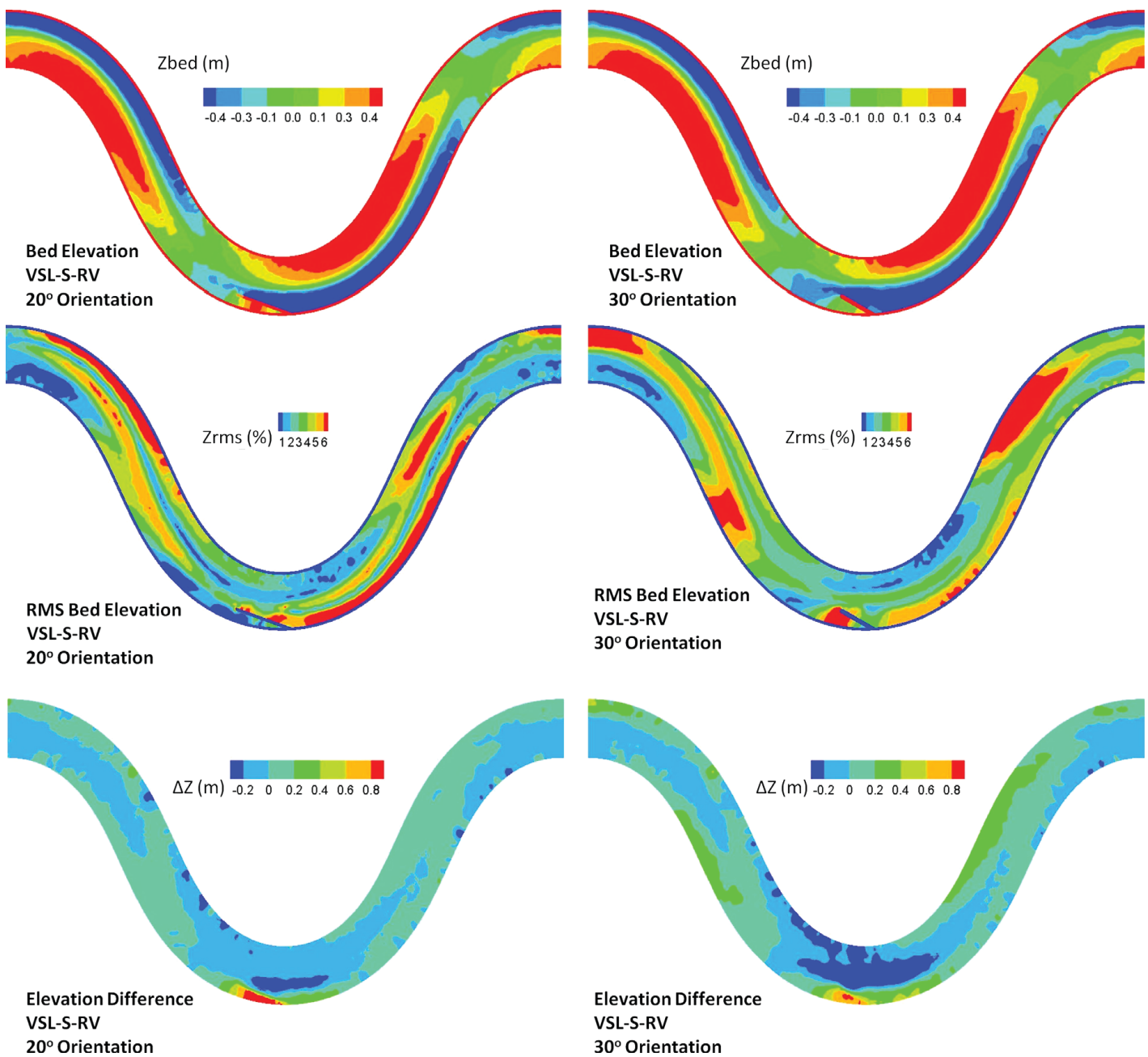


Figure 3-8. *Zbed* for a single rock vane located at the meander apex for VSL-S. The RMS of *Zrms* is non-dimensionalized by the flow depth and multiplied by 100. The ΔZ represents the *Zbed* of the baseline case (with no rock structure; Figure 3-2) subtracted from the *Zbed* of this case. Flow is from left to right.

the optimum angle of orientation and location of a second structure for multiple RVs. For the VSL-G channel with a single RV placed at the meander apex, the 30° RV provided protection over a greater length of the outer bank. A 30° RV uses less material because it is shorter in length to reach $\frac{1}{3}$ of the channel width. In the VSL-G channel, the presence of a single 30° RV did not endanger the inner bank; therefore, 30° was selected as the optimum angle in VSL-G. For the VSL-S channel, the 30° RV was deemed to endanger the stability of the inner bank (see bed elevation difference in Figure 3-8). The 30° RV resulted in more scour of the inner point bar. Therefore, the 20° RV is recommended for the more sinuous VSL-S channel.

Because a single RV did not protect the entire length of outer bank within the meander for either VSL-S or VSL-G, an additional structure was needed to protect the downstream outer bank. To find the optimum location of the second structure

within the VSL-S and VSL-G channels, depth-averaged TKE was used to define the shear layer downstream of the RV (Figures 3-9 and 3-10) to identify the location where the shear layer reattaches to the outer bank. The location of the shear layer attachment corresponded well with the location of the deep scour hole downstream of the RVs (Figures 3-9 and 3-10). The optimum location of the downstream RV for VSL-G was defined as the location where a line extended from the RV tip at -5° and 5° from the tangent to the outer bank intersected with the outer bank for the 20° and 30° RV structures, respectively. The optimum location of the downstream RV for VSL-S was also defined as the location where a line extended from the RV tip at -5° from the tangent to the outer bank intersected with the outer bank for both the 20° and 30° RV structure. Table 3-2 summarizes the optimum angle of orientation and location of a downstream RV for each channel.

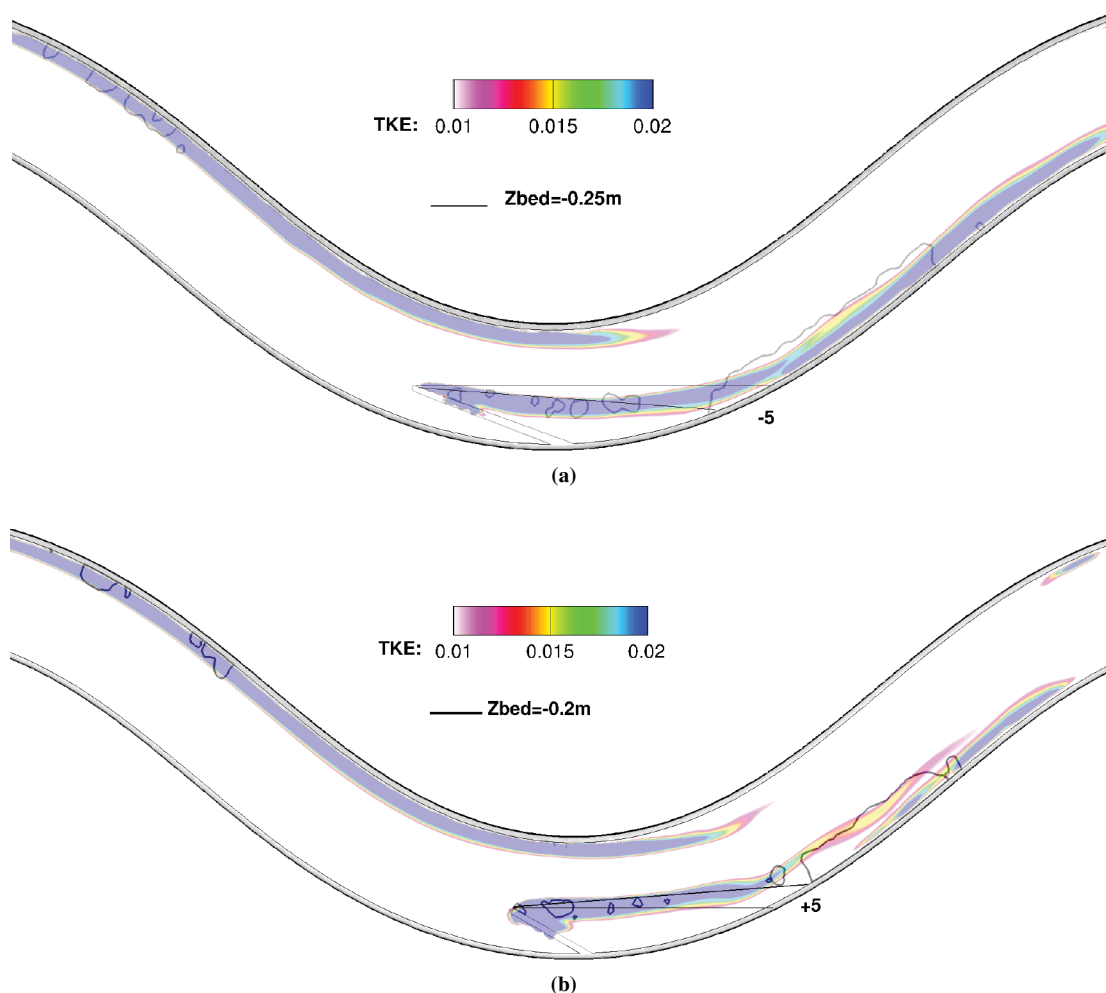


Figure 3-9. Color map of steady-state non-dimensionalized depth-averaged TKE overlaying contours of Z_{bed} downstream of (a) 20° and (b) 30° rock vane in the VSL-G channel. TKE is non-dimensionalized with the square of mean flow velocity. The high-TKE region indicates the location of the shear layer, and contours illustrate the location of the deepest scour holes. Flow is from left to right.

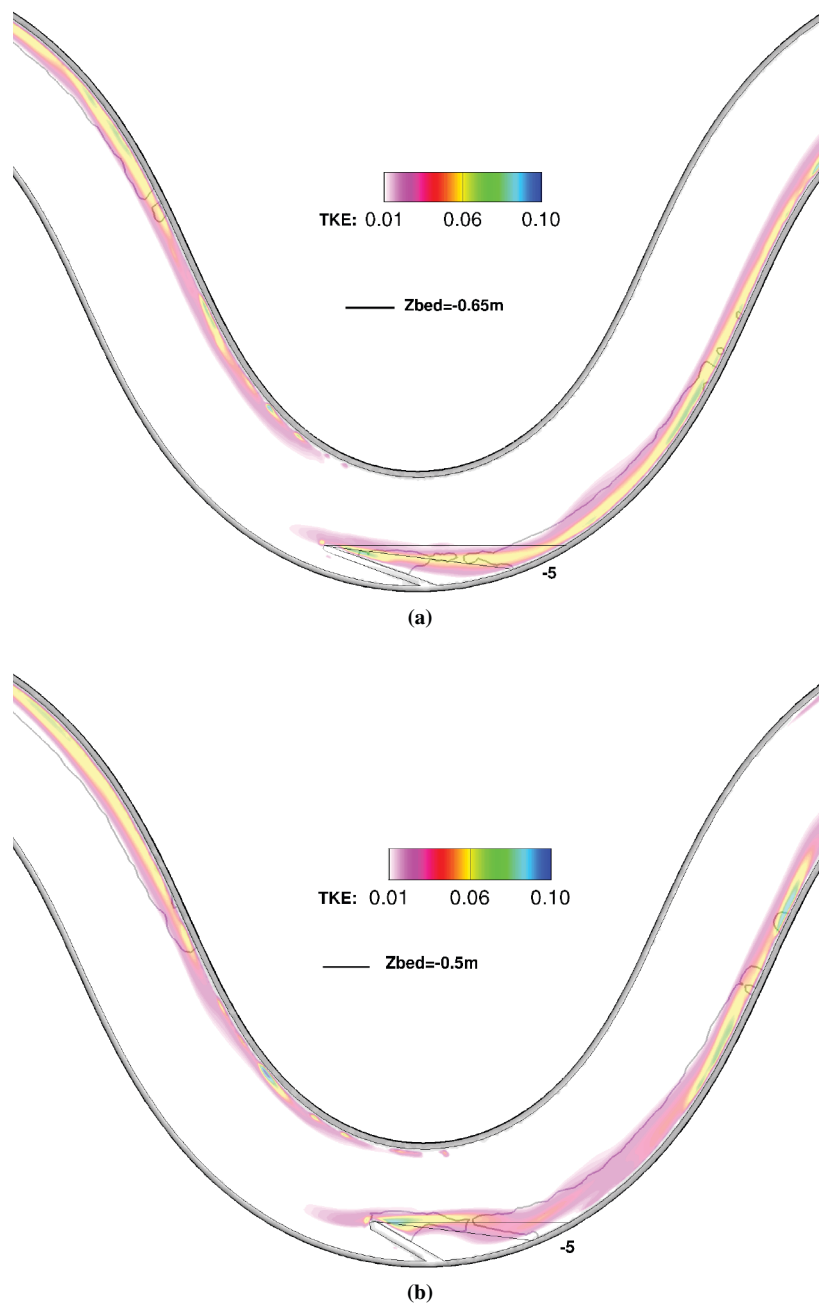


Figure 3-10. Color map of steady-state non-dimensionalized depth-averaged TKE overlaying contours of Z_{bed} downstream of (a) 20° and (b) 30° rock vane in the VSL-S channel. TKE is non-dimensionalized with the square of mean flow velocity. The high-TKE region indicates the location of the shear layer, and contours illustrate the location of the deepest scour holes. Flow is from left to right.

Table 3-2. Angle of orientation and optimum location of second downstream rock vane.

	Optimum Angle	Optimum Location
VSL-G	30°	+5° from the first RV tip
VSL-S	20°	-5° from the first RV tip

Optimum Number of Structures

Based on the numerical results for a single RV structure, the researchers defined the path of the highest TKE, which coincides with the location of the deepest scour region. The point at which the shear layer reattaches to the outer bank was selected for the next RV structure to be installed. The calculated quasi-equilibrium time-averaged bed results for two RVs in VSL-G and VSL-S are shown in Figures 3-11 and 3-12, respectively. The hydrodynamic and live-bed morphodynamic simulations were carried out for approximately 2 months for both cases.

As shown in Figures 3-11 and 3-12, for both channel types, use of the second RV downstream of the apex provides significant bank protection at locations where deep scour holes were observed with a single structure (Figures 3-7 and 3-8).

For both channels, sediment deposition occurred upstream of the second RV. The second structure clearly shifted the thalweg away from the outer bank and extended its length downstream compared to the single RV. Of note is the maximum scour depth adjacent to the tip on the downstream side of the RV in VSL-S. As shown in Figure 3-12, the deep scour hole near the second RV can potentially lead to some serious structural stability problems; however, this large scour hole was not present in the case of VSL-G (see Figure 3-11).

Based on the simulation results for VSL-G (Figure 3-11), with two RVs installed following the arrangement shown in Table 3-2, appropriate protection is provided for the outer bank, and the extent of the realigned channel thalweg is located in its entirety along the centerline of the channel. Therefore, two RV structures were deemed to be sufficient, and no additional structures were added to VSL-G.

For VSL-S, as shown in Figure 3-12, the second RV provided limited bank protection, leaving the rest of the downstream bank clearly exposed to erosion (see the bed elevation contours in the left side of Figure 3-12). In order to further analyze the risk to the outer bank for this simulation, in Figure 3-13 the

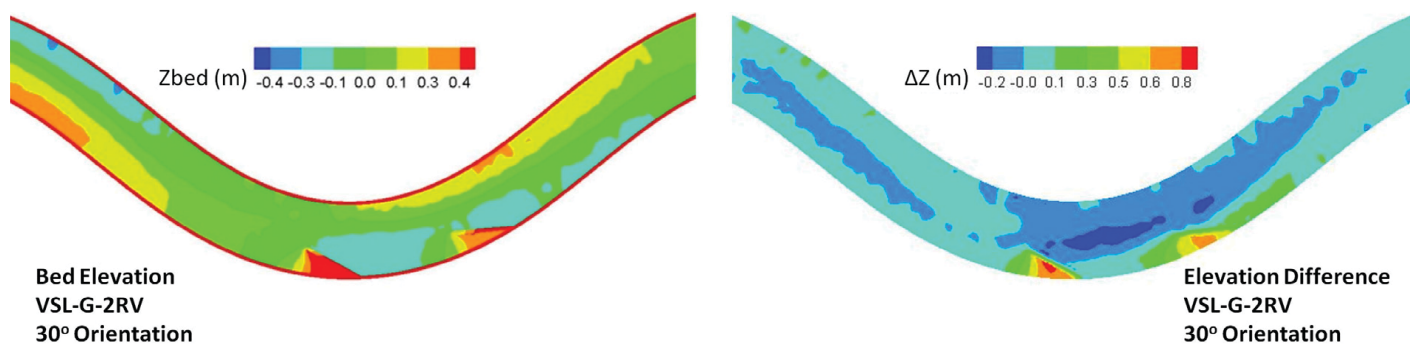


Figure 3-11. *Zbed* for a two-RV array starting at the meander apex for VSL-G. The ΔZ represents the *Zbed* of the baseline case (with no rock structure; Figure 3-2) subtracted from the *Zbed* of this case. Flow is from left to right.

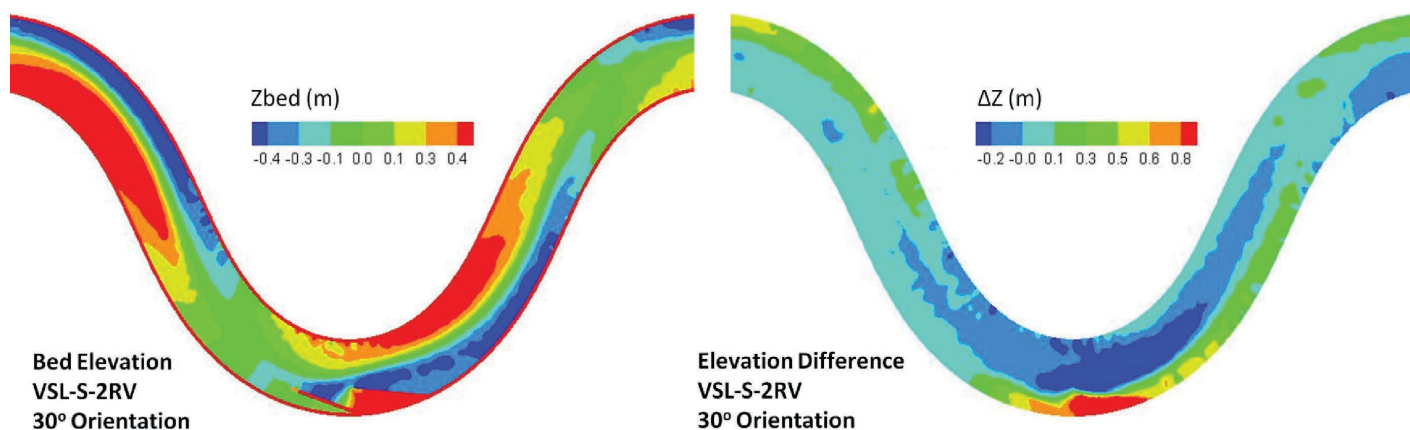


Figure 3-12. *Zbed* for a two-RV array starting at the meander apex for VSL-S. The ΔZ represents the *Zbed* of the baseline case (with no rock structure; Figure 3-2) subtracted from the *Zbed* of this case. Flow is from left to right.

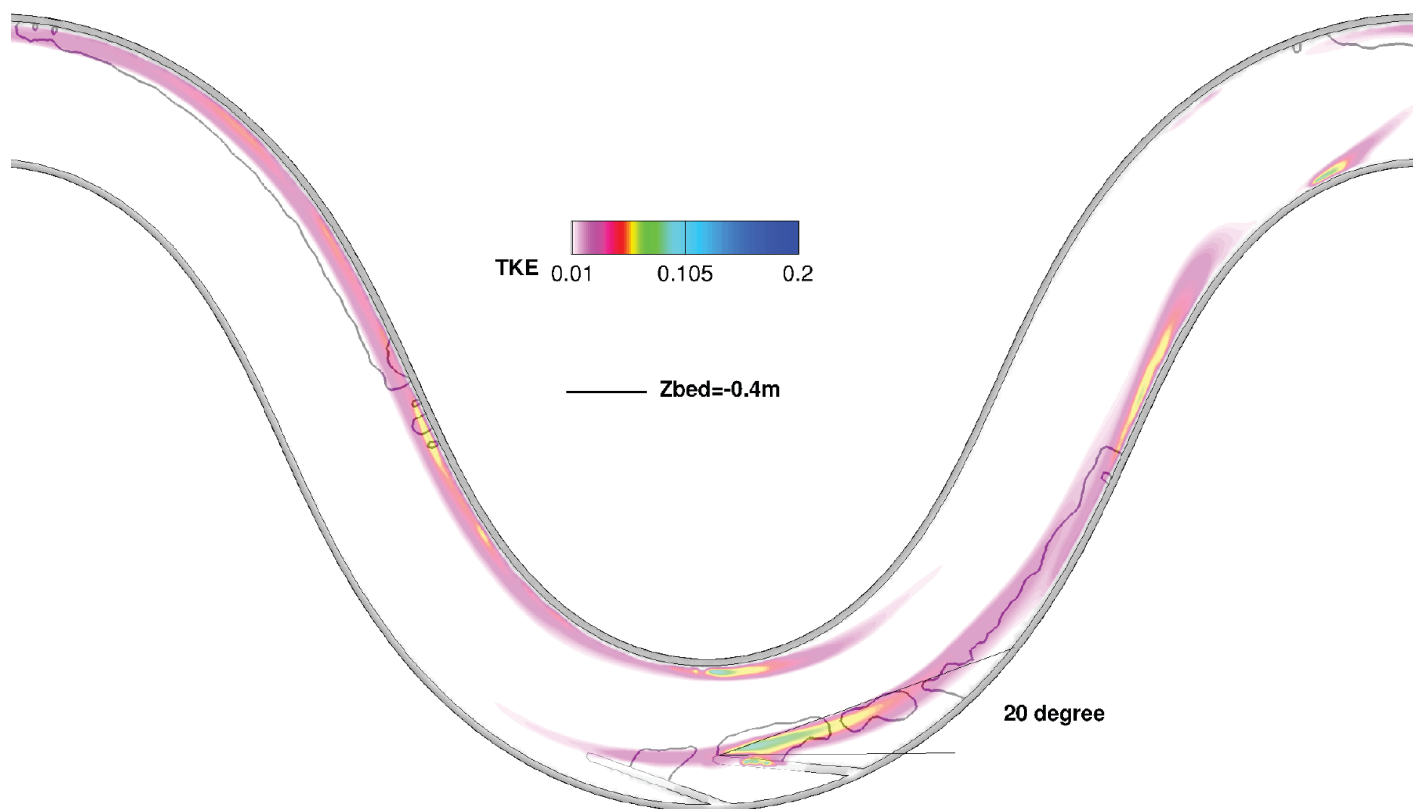


Figure 3-13. Color map of steady-state non-dimensionalized depth-averaged TKE overlaying contours of Z_{bed} downstream of a two-RV array in the VSL-S channel. TKE is non-dimensionalized with the square of mean flow velocity. The high-TKE region indicates the location of the shear layer, and contours illustrate the location of the deepest scour holes. Flow is from left to right.

depth-averaged TKE contours are plotted over the bed elevation contours. As shown in Figure 3-13, the deepest scour regions are located exactly below the shear layer and where the shear layer impinges on the outer bank. The result of this analysis clearly suggests that the protection of the downstream part of the outer bank requires the installation of another RV structure in the more sinuous VSL-S. In Figure 3-13, a horizontal line radiated from the tip of the second structure was used to determine the offset angle of the shear layer. The location where the deflected shear layer hits the outer bank was used to determine the location to install the third RV. As shown in this figure, the third structure is needed where a line drawn at a 20° offset from the tip of the second rock structure intersects with the outer bank (see Table 3-3).

A third RV structure was installed based on the arrangements of Tables 3-2 and 3-3 in the VSL-S. Figure 3-14 illustrates the time-averaged results of flow and morphodynamics under live-bed simulations. The addition of the third RV pro-

vides significant protection along the outer bank and at the same time creates a longer and deeper thalweg located along the channel centerline. Therefore, no additional RVs were deemed necessary in VSL-S.

Evaluation of Structure Array Location

In order to investigate the effect of location of the RV arrays in each channel, the series of RVs (two and three RVs for VSL-G and VSL-S, respectively) were shifted upstream by a length equal to the channel width (B). In this scenario for VSL-G, the first RV is installed a length of B upstream of the meander apex and the second one downstream of the apex. Figure 3-15 illustrates the time-averaged bed morphologic results of this rearrangement study for the VSL-G.

Although the new arrangement provides some protection to the outer bank, a closer examination of the results reveals that (a) the stream banks downstream of the second RV are exposed to significant scour, and (b) a portion of the outer bank, approximately $0.5B$ long immediately downstream of the first vane, was subject to significant erosion. Based on these observations, the shifting of RVs for the VSL-G resulted in less favorable bank protection.

The same approach was used for VSL-S with an array of three RVs with the arrangements shown in Tables 3-2 and 3-3. This

Table 3-3. Angle of orientation and optimum location of third downstream rock vane.

	Angle	Optimum Location
VSL-G	n/a	None required
VSL-S	20°	20° from horizontal line from second RV tip

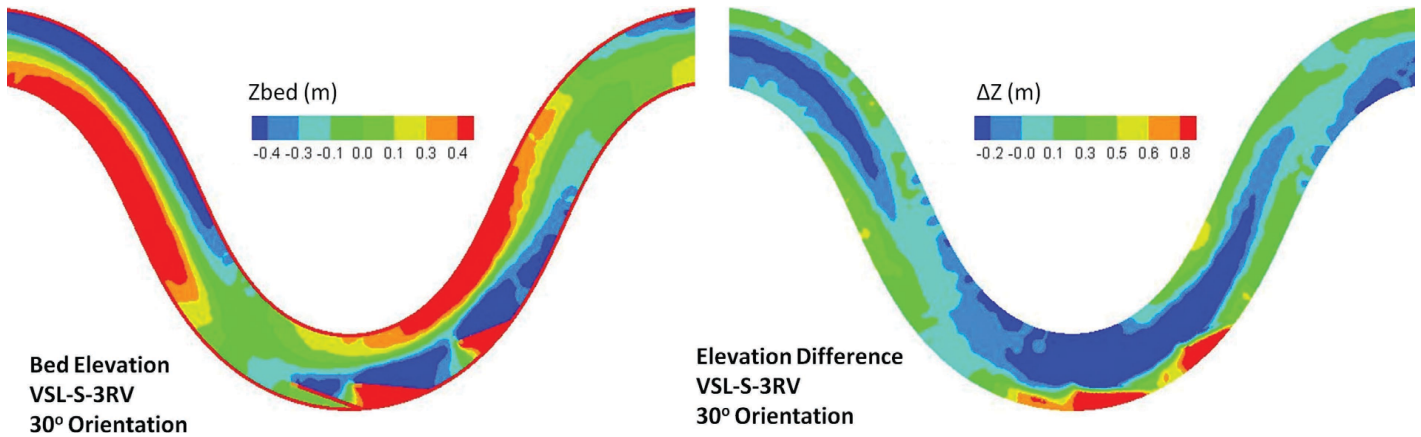


Figure 3-14. *Zbed* for a three-RV array starting at the meander apex for VSL-S. The ΔZ represents the *Zbed* of the baseline case (with no rock structure; Figure 3-2) subtracted from the *Zbed* of this case. Flow is from left to right.

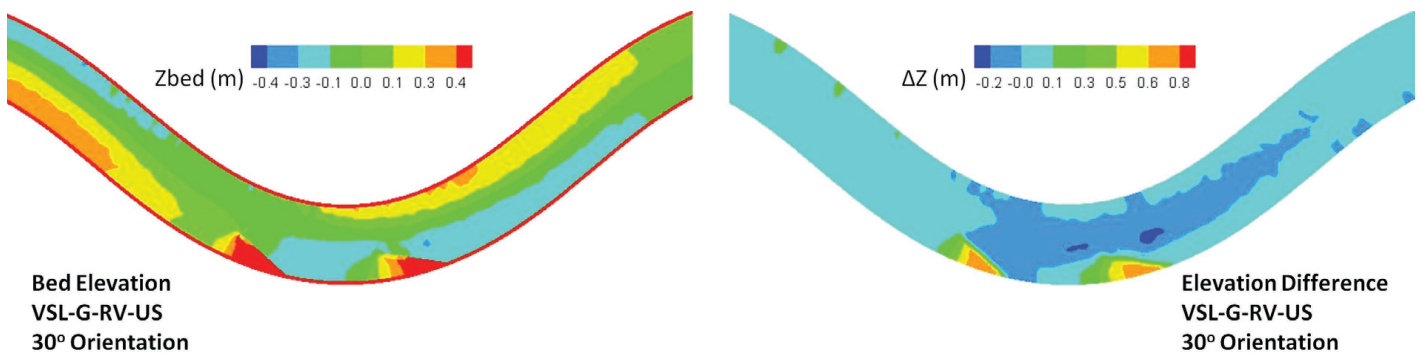


Figure 3-15. *Zbed* for a two-RV array in VSL-G shifted upstream of the meander apex by a length equal to one channel width. The ΔZ represents the *Zbed* of the baseline case (with no rock structure; Figure 3-2) subtracted from the *Zbed* of this case. Flow is from left to right.

array was shifted upstream by a length of one channel width (B). The calculated bed morphology at quasi-equilibrium is shown in Figure 3-16.

For VSL-S, by comparing Figure 3-14 (original arrangement) and 3-16 (shifted arrangement), it was concluded that shifting the RV array shows several advantages. These include

(a) less deposition of sediment at the upstream corner of each RV, (b) the maximum thalweg scour depth is less than the non-shifted case, and (c) the protected length of the outer bank is extended farther upstream [see Figure 3-16 (right)]. The first two advantages are especially important for the structural integrity of the RVs, and the last one is important

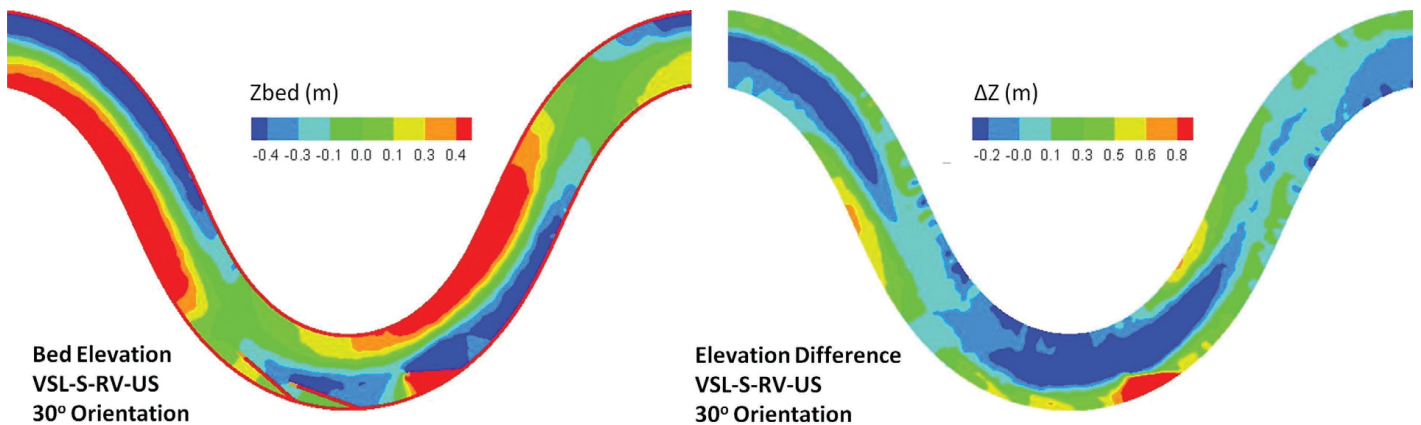


Figure 3-16. *Zbed* for a three-RV array in VSL-S shifted upstream of the meander apex by a length equal to one channel width. The ΔZ represents the *Zbed* of the baseline case (with no rock structure; Figure 3-2) subtracted from the *Zbed* of this case. Flow is from left to right.

for the stream bank stability. Based on these observations, unlike VSL-G, the shifted arrangement of the RV array proved to be more effective for VSL-S.

3.2 VSL3D Results for J-Hook Vanes

Single J-Hook Vane Scour and Deposition

A single JH vane was placed at the meander apex of the VSL-G and VSL-S channels at angles of orientation of 20° and 30° . J-hooks are an adaptation of RVs with a J-shaped hook placed at the tip of the RV. The two angles were selected to span the range of typical J-hook guidelines (NRCS, 2007; Doll et al., 2003; Maryland Department of the Environment, 2000; Brown, 2000). The computed results are shown in Figures 3-17 and 3-18 for VSL-G and VSL-S, respectively. For each case, the Zbeds and their difference (ΔZ) with the corresponding Zbed obtained for the baseline case (with no structure; Figure 3-2). JHs yielded different results for VSL-G and VSL-S. For VSL-G, the computed results indicated that for a single JH, a larger angle provided greater bank protection with less risk to the inner bank. For VSL-S, the smaller angle, 20° , JH provided protection over a greater length of the bank downstream.

Optimum Angle and Spacing

Based on the numerical results for a single JH structure, a combination of scour and flow field results were used to deter-

mine the optimum angle of orientation and location of a second structure. For a single JH placed at the meander apex, the optimum angle of orientation was determined to be the same as that for RVs. For the VSL-G channel, an angle of 30° was selected because (1) a larger structure angle uses less material, (2) the scour hole formed downstream of the structure was located near the centerline of the channel, and (3) there was less risk of scour to the inner bank (see Figure 3-17). For the VSL-S channel, an angle of 20° was selected for a JH because the smaller angle offered more outer bank protection and less risk to the inner bank (see Figure 3-18).

A single JH vane did not protect the entire length of the outer bank within the meander bend for either VSL-S or VSL-G; therefore, an additional structure was needed. In the VSL-G and VSL-S channels, the depth-averaged TKE was used to define the shear layer downstream of the JH (Figures 3-19 to 3-21) to identify the location where the shear layer reattaches to the outer bank. For JHs, because of the highly turbulent nature of the flow, the shear layer was not well defined, and therefore the location of its impingement on the outer bank could not be clearly identified. The location of the second JH vane was defined by first creating a tangent line to the outer bank at the apex. A parallel line extended from the structure tip (in this case, from the vane portion of the structure) was used to create a line with offset angles of 5° and -5° for VSL-G and VSL-S, respectively. The location where this line intersected the outer bank corresponded approximately to the location of the edge of

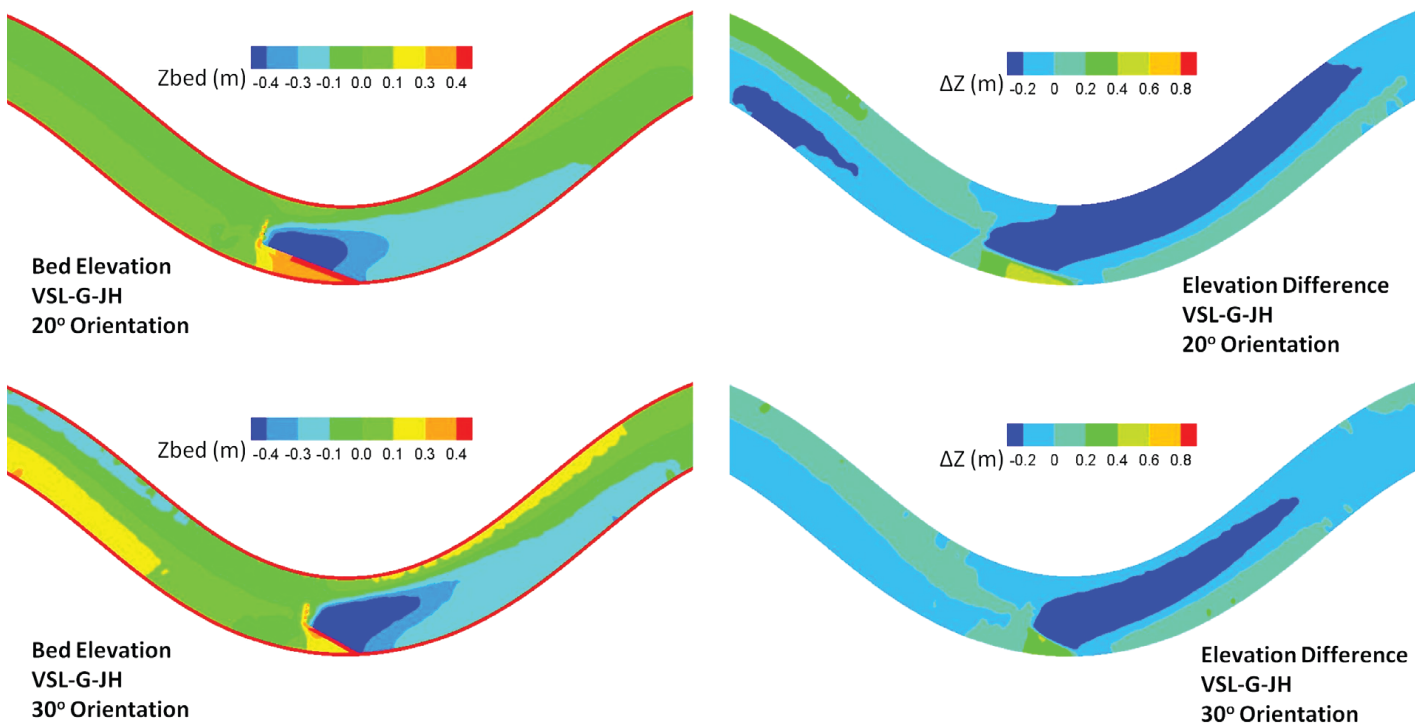


Figure 3-17. Zbed for a J-hook vane located at the meander apex for VSL-G. The ΔZ represents the Zbed of the baseline case (with no rock structure; Figure 3-2) subtracted from the Zbed of this case. Flow is from left to right.

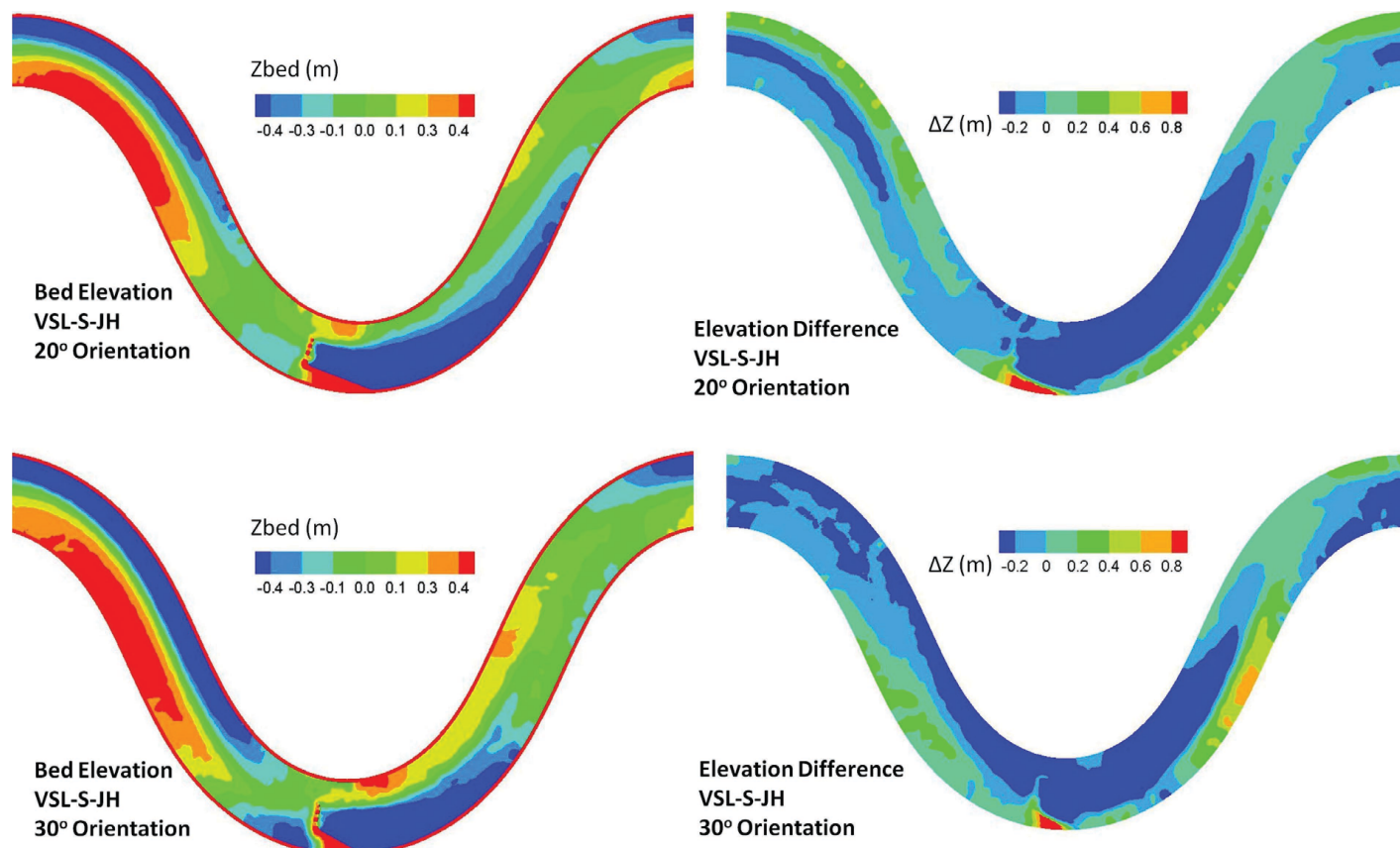


Figure 3-18. Z_{bed} for a J-hook vane located at the meander apex for VSL-S. The ΔZ represents the Z_{bed} of the baseline case (with no rock structure; Figure 3-2) subtracted from the Z_{bed} of this case. Flow is from left to right.

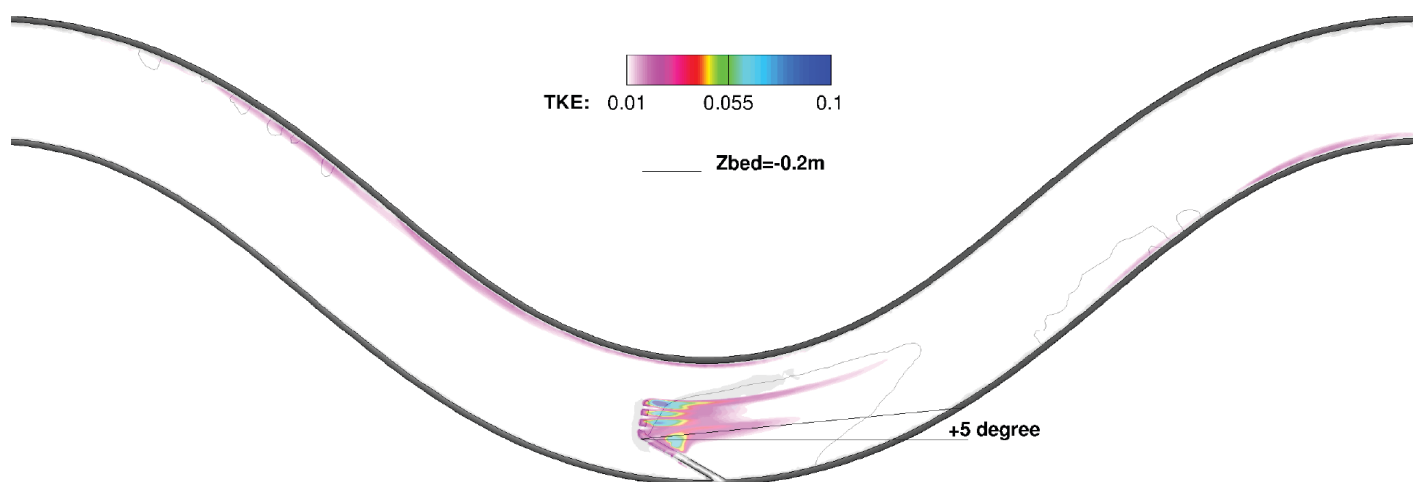


Figure 3-19. Color map of steady-state non-dimensionalized depth-averaged TKE overlaying contours of Z_{bed} downstream of a JH vane in the VSL-G channel. TKE is non-dimensionalized with the square of mean flow velocity. The high-TKE region indicates the location of the shear layer, and contours illustrate the location of the deepest scour holes. Flow is from left to right.

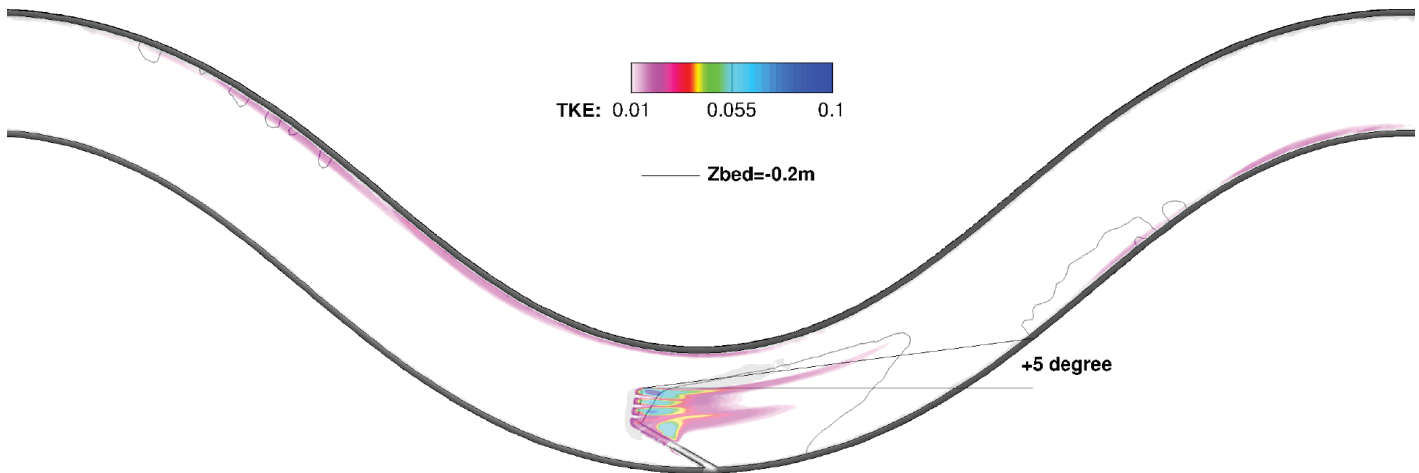


Figure 3-20. Color map of steady-state non-dimensionalized depth-averaged TKE overlaying contours of Z_{bed} downstream of a JH vane in the VSL-G channel. TKE is non-dimensionalized with the square of mean flow velocity. The high-TKE region indicates the location of the shear layer, and contours illustrate the location of the deepest scour holes. Flow is from left to right. The location of the maximum scour hole does not coincide with the projected shear layer in this case.

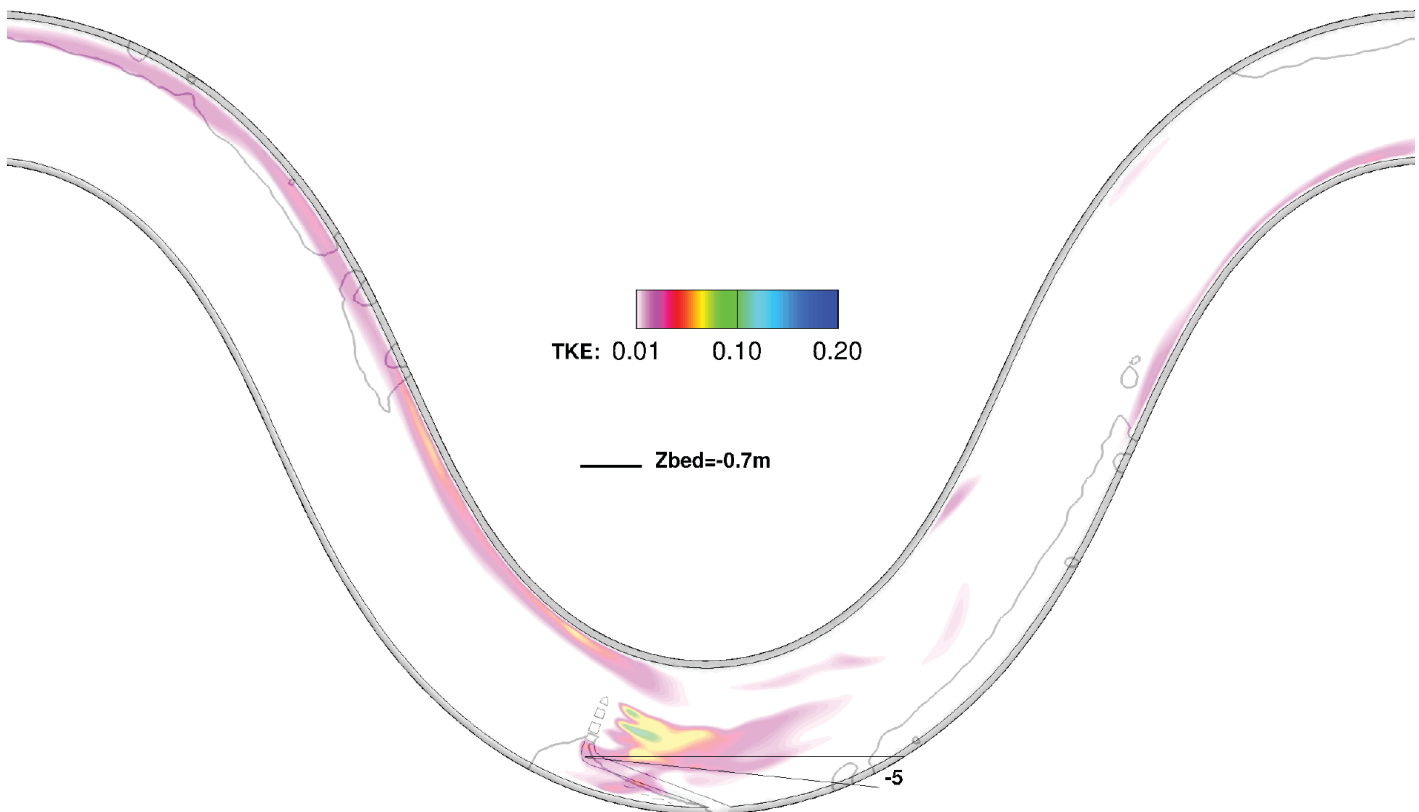


Figure 3-21. Color map of steady-state non-dimensionalized depth-averaged TKE overlaying contours of Z_{bed} downstream of a JH vane in the VSL-S channel. TKE is non-dimensionalized with the square of mean flow velocity. The high-TKE region indicates the location of the shear layer, and contours illustrate the location of the deepest scour holes. Flow is from left to right.

Table 3-4. Angle of orientation and optimum location of second downstream J-hook vane.

	Angle	Optimum Location
VSL-G	30°	5° from the first JH hook tip
VSL-S	20°	-5° from first JH vane tip

the turbulent region closest to the outer bank (Figures 3-19 to 3-21). For VSL-S, this corresponded to the region of the deepest scour hole near the outer bank (Figure 3-21). For VSL-G, the shear layer did not correspond to the deepest scour, likely because of the poorly defined shear layer. For VSL-G, the location of the deepest scour corresponded to a line 5° from the horizontal line drawn from the hook portion of the structure (Figures 3-19 and 3-20); therefore, this was selected as the optimum location of the next structure for the VSL-G, but both layouts were tested, and the bed elevations are described in the next section. Table 3-4 summarizes the optimum angle of orientation and location of a downstream JH for each channel.

Optimum Number of Structures

The hydrodynamics and bed-morphodynamics for both channels were simulated with two JHs. For the VSL-G, two different spacings were tested, shown in Figures 3-19 and

3-20. For VSL-S, the optimum spacing shown in Table 3-4 was tested. The simulations for both JH structure array cases were carried out for approximately 2 months, and the resulting quasi-equilibrium time-averaged bed elevations are shown in Figures 3-22 and 3-23 for VSL-G and Figure 3-24 for VSL-S.

Based on the simulation results for VSL-G with similar spacing to the RV case (Figure 3-19), the placement of the second structure diverts flow toward the inner side of the bend and creates significant erosion near the same region (~25% of the flow depth). This phenomenon can be clearly seen in Figure 3-22 (left) where the teal color map near the inner bend and between the tip of second (downstream) JH and inner bank indicates scour compared to the mean (flat bed) elevation. Based on this result, the location of the second JH structure was adjusted downstream to reduce the interference with sediment transport within the region of the meander apex. The location of the second J-hook was shifted to where the 5° line from the tip of the hook (instead of the vane) intersected with the outer bend. Comparison between Figures 3-19 and 3-20 clarifies the difference between these two placements. This adjusted location of the second JH coincides with the location of the maximum scour hole on the outer bank downstream of a single JH shown in Figure 3-20.

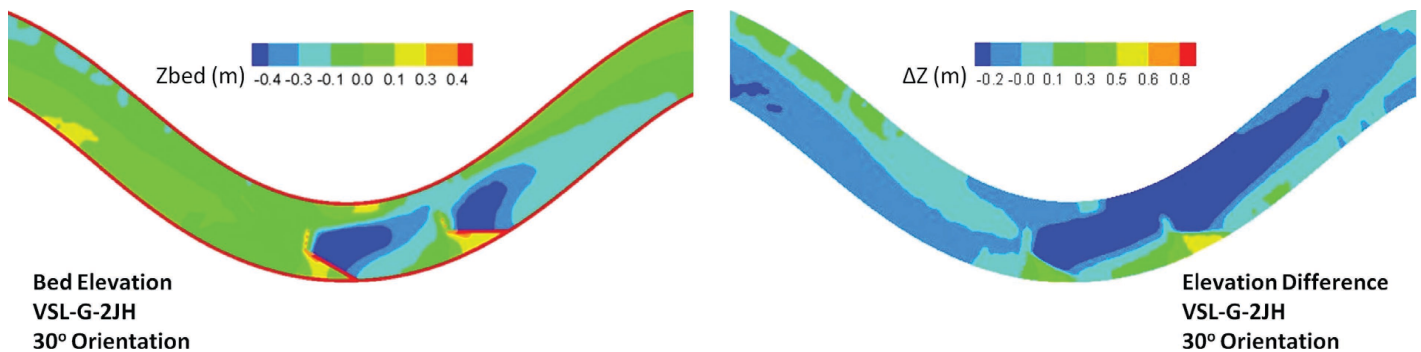


Figure 3-22. *Zbed* for a two-JH vane array starting at the meander apex for VSL-G. The ΔZ represents the *Zbed* of the baseline case (with no rock structure; Figure 3-2) subtracted from the *Zbed* of this case. Flow is from left to right.

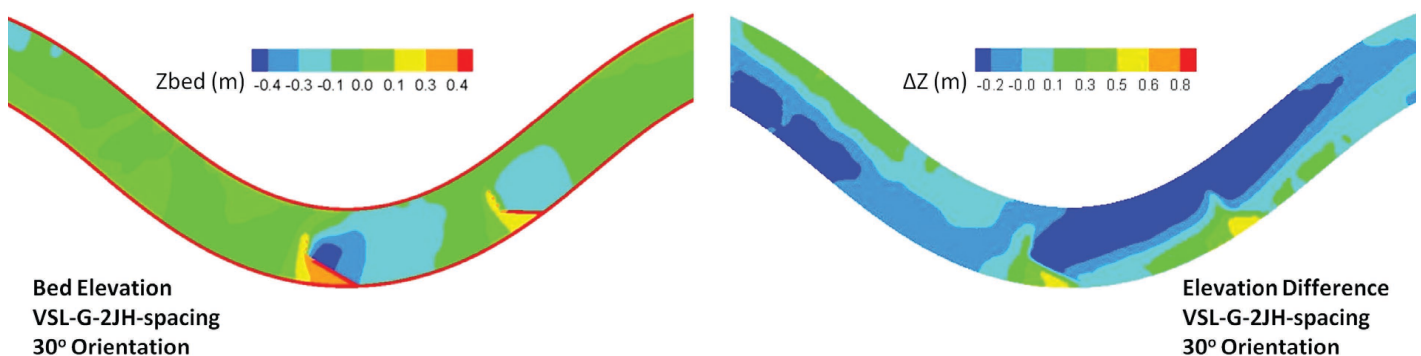


Figure 3-23. *Zbed* for a two-JH vane array starting at the meander apex with increased spacing compared to Figure 3-22 for VSL-G. The ΔZ represents the *Zbed* of the baseline case (with no rock structure; Figure 3-2) subtracted from the *Zbed* of this case. Flow is from left to right.

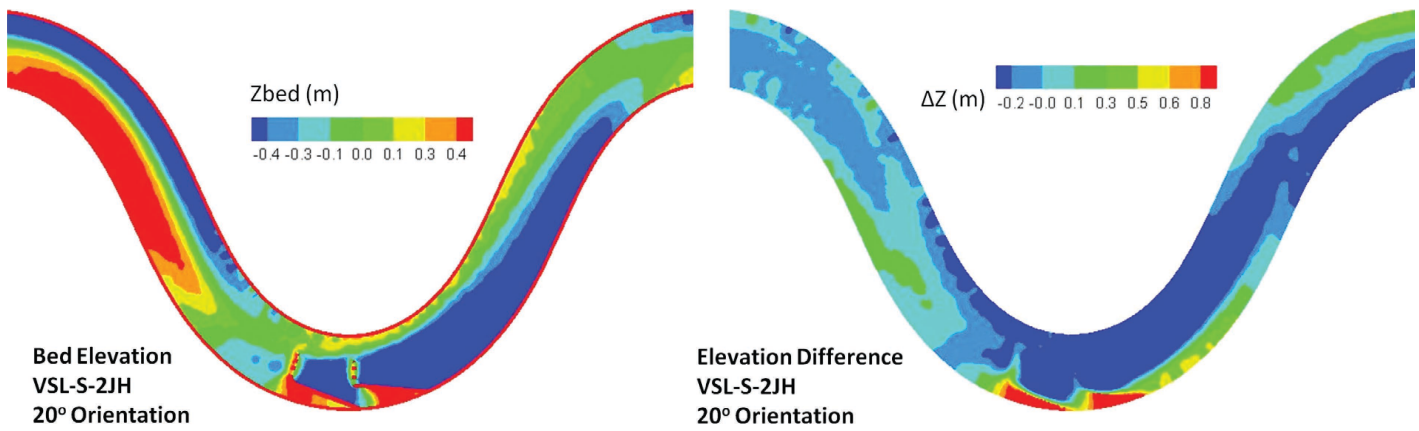


Figure 3-24. Z_{bed} for a two-JH vane array starting at the meander apex for VSL-S. The ΔZ represents the Z_{bed} of the baseline case (with no rock structure; Figure 3-2) subtracted from the Z_{bed} of this case. Flow is from left to right.

The computed VSL-G bed morphology for the new JH arrangement is shown in Figure 3-23. In terms of inner bend erosion, both arrangements provide similar results (see Figures 3-22 and 3-23). However, for the outer bank, the new placement results in approximately 5% greater length of bank protection. Therefore, regardless of the second J-hook structure location, in VSL-G, significant erosion near the inner bank remains a concern. The arrangement from the tip of the hook provided more protection for the outer bank compared to the original arrangement (with spacing similar to RVs). Based on this arrangement, no further structures are needed to protect the outer bank of the meander.

The simulation results of VSL-S show some promising bank protection downstream of the second JH, while at the same time, less erosion is evident near the inner bend than for the single structure case. No further adjustments were deemed necessary regarding the location of the second structure. However, to provide better protection along the outer bank, an additional structure should be added. In order to find the optimal location of the third J-hook structure, the depth-averaged TKE contours were plotted along with the bed bathymetry, as shown in Figure 3-25.

As shown in Figure 3-25, for VSL-S, the TKE contours indicating the shear layer did not align well with the location of

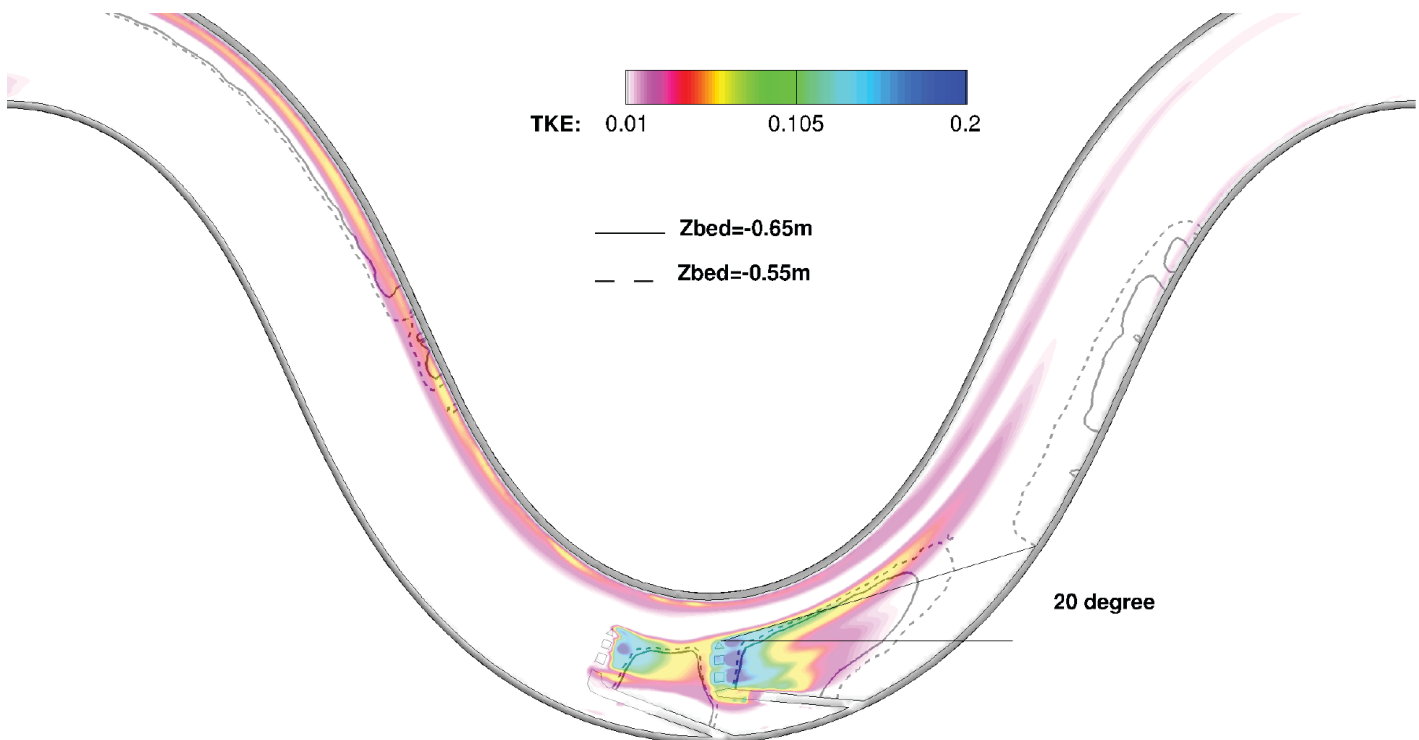


Figure 3-25. Color map of steady-state non-dimensionalized depth-averaged TKE overlaying contours of Z_{bed} downstream of a two-JH vane array in the VSL-S channel. TKE is non-dimensionalized with the square of mean flow velocity. The high-TKE region indicates the location of the shear layer, and contours illustrate the location of the deepest scour holes. Flow is from left to right.

Table 3-5. Angle of orientation and optimum location of third downstream JH vane.

	Angle	Optimum Location
VSL-G	n/a	None required
VSL-S	20°	20° from the hook's tip of second JH

the deepest scour hole downstream of the apex and along the outer bank. This is likely due to the passage of flow through gaps between rocks in the hook portion of the structure creating several adjacent turbulent jet flows. Immediately downstream of the gaps, these jet-like flows created a larger mixing zone. This phenomenon breaks down the large-scale vortical structures and creates a zone of small-scale structures without any specific shear layer. Therefore, due to the absence of any distinct shear layer, the location of the deepest scour hole along the outer bank was used to locate the position of the next JH structure for VSL-S. The third downstream JH was placed where the 20° line from the tip of the hook part intersected with the outer bank (see Figure 3-25). Table 3-5 shows the summary of the third J-hook structure positioning for both stream types. As shown in Figure 3-26, the computed bed morphology for VSL-S with the three JH structures installed based on Table 3-5 shows the effectiveness of the third JH structure in providing bank protection throughout the meander length without need for an additional structure downstream.

Evaluation of Structure Array Location

To investigate the effect of JH structure array location, the series of JHs (two and three JHs for the VSL-G and VSL-S, respectively) were shifted upstream a length equal to the channel width (B). The simulation results obtained for this shift in VSL-G and VSL-S are illustrated in Figures 3-27 and 3-28, respectively.

As shown in Figure 3-27, an upstream shift of the JH array in VSL-G provides less protection for the outer bank at regions near the apex and upstream of the apex; however, it results in

less erosion to the inner bend. Comparison of Figures 3-23 and 3-27 also shows that shifting the J-hooks upstream has led to roughly 10% less scour depth near the structure in each channel. Therefore, the new arrangement is expected to be structurally more stable. Since the structural stability of the rocks for this type of in-stream structure is an important factor for the individual rocks that make up the hook, and because the new arrangement causes less erosion near the inner bend, the J-hook installation shifted upstream one channel width is favorable in VSL-G. For VSL-S (Figure 3-28), the upstream shift of the J-hook array shows a solid improvement in the resultant quasi-equilibrium bed bathymetry. Comparison between Figures 3-26 and 3-28 shows the following improvements with an upstream shift of the JH array in VSL-S: greater outer bank protection, less erosion near the inner bank, bank protection near the outer bank over greater distance, and less deposition depth of sediment material at the upstream of each J-hook structure (which is a key factor for determining flanking potential; see Section 5.3). Therefore, shifting the JH array upstream by one channel width results in a favorable arrangement for VSL-S.

3.3 VSL3D Results for Bendway Weirs/Stream Barbs

Single Bendway Weir/Stream Barb Scour and Deposition

A single BW was placed at the meander apex of the VSL-G and VSL-S channels, and the VSL3D model was applied to simulate the resulting bed morphodynamics for five different angles oriented relative to the tangent to the bank (20°, 30°, 50°, 60°, 80°). These five angles were determined based on the range of angles suggested in current BW and stream barb guidelines, which suggest that such structures be installed at angles in the range of 50° to 80° (NRCS, 2007; NRCS, 2010) or 20° to 30° (NRCS, 2000). To directly compare the function of BWs

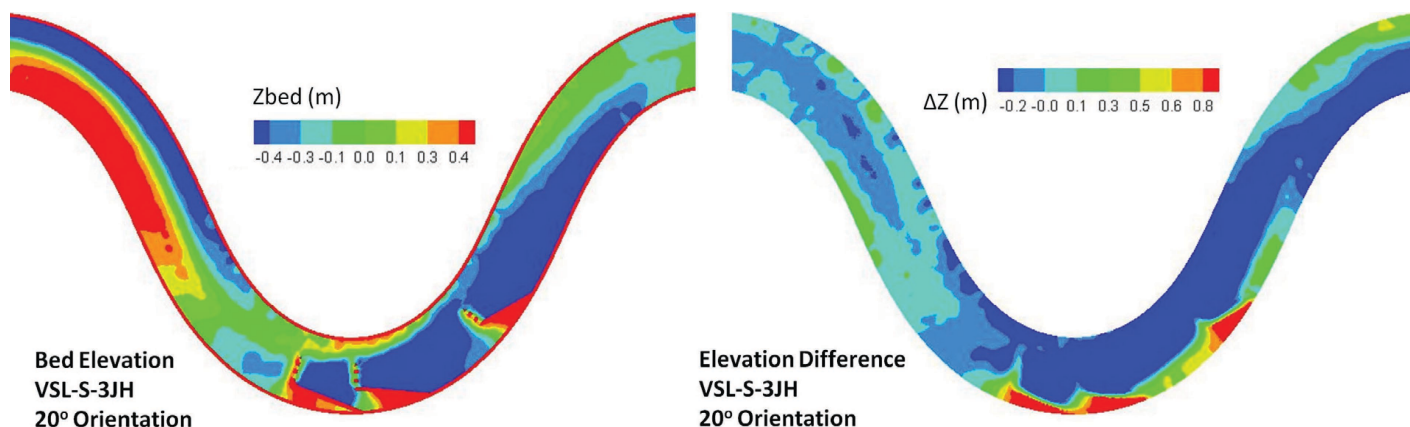


Figure 3-26. Z_{bed} for a three-JH vane array starting at the meander apex for VSL-S. The ΔZ represents the Z_{bed} of the baseline case (with no rock structure; Figure 3-2) subtracted from the Z_{bed} of this case. Flow is from left to right.

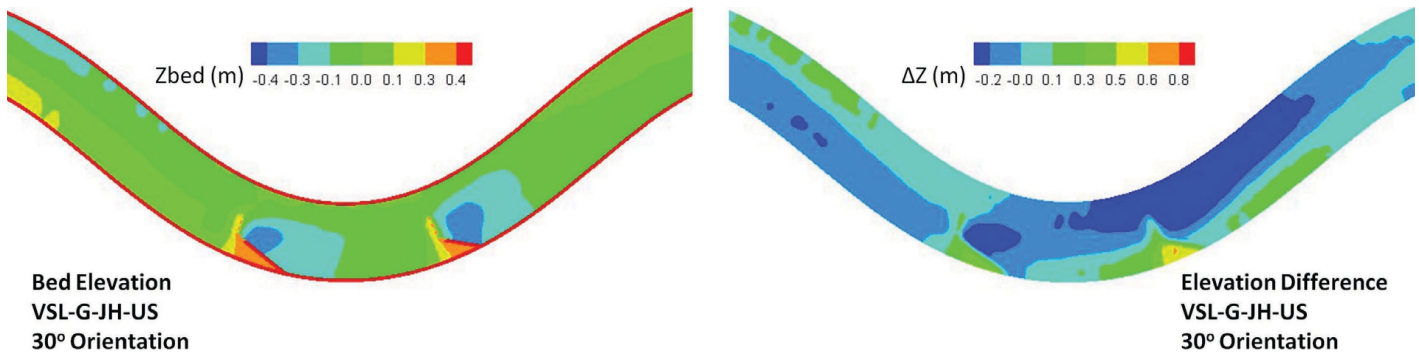


Figure 3-27. *Zbed* for a two-JH vane array in VSL-G shifted upstream of the meander apex by a length equal to one channel width. The ΔZ represents the *Zbed* of the baseline case (with no rock structure; Figure 3-2) subtracted from the *Zbed* of this case. Flow is from left to right.

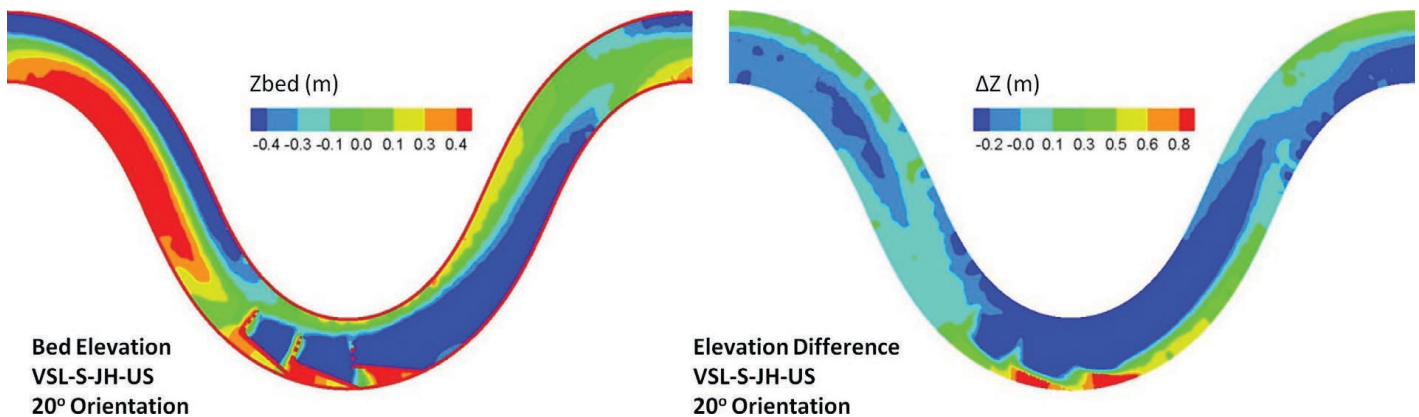


Figure 3-28. *Zbed* for a three-JH vane array in VSL-S shifted upstream of the meander apex by a length equal to one channel width. The ΔZ represents the *Zbed* of the baseline case (with no rock structure; Figure 3-2) subtracted from the *Zbed* of this case. Flow is from left to right.

to RVs and JHs, a range of angles was chosen that covers both ranges and overlap with the 20° and 30° angles of vane-type structures. The computed results are shown in Figures 3-29 and 3-30 for VSL-G and VSL-S, respectively. For each case, the difference between the time-averaged bed elevation with no structure (baseline case for which the simulated bed elevation is shown in Figure 3-2) and the time-averaged bed with a structure are shown. The computed results indicated that smaller angles seem to provide greater protection both upstream and downstream of the structure. It should be noted that smaller angles have longer vanes to reach an effective width of one-quarter of the stream width (B); therefore, the cost of installation will be greater for smaller angles than larger angles. Scour was consistently deeper in VSL-S than VSL-G, but this trend did not appear to be related to structure angle.

Optimum Angle and Spacing

Based on the numerical results for a single BW structure, a combination of scour and flow field results was used to deter-

mine the optimum angle of orientation and location of a secondary structure for multiple BWs. For a single BW placed at the meander apex for both the VSL-G and VSL-S channels, the optimum angle of orientation with respect to the outer bank was determined to be 50°. This orientation required less material to construct a single structure while it protected the bank over a longer distance. As the angle of orientation increases, the ratio of protected bank to channel width decreases (Figure 3-31). When the results from the VSL3D simulations are combined, BWs, which are submerged at most flows, behaved differently than RVs. For BWs in VSL-G and VSL-S, smaller angles resulted in greater bank protection, with one exception for the 60° structure in VSL-S. In this particular case, sediment deposition (generally around 10 cm) was present upstream of the structure extending to the previous meander (see Figure 3-32). The length of protected bank in Figure 3-31a only included the length of protected bank within the meander. As the angle of orientation increases, the length of the structure decreases to maintain a constant one-quarter of the channel width effective length (Figure 3-31b).

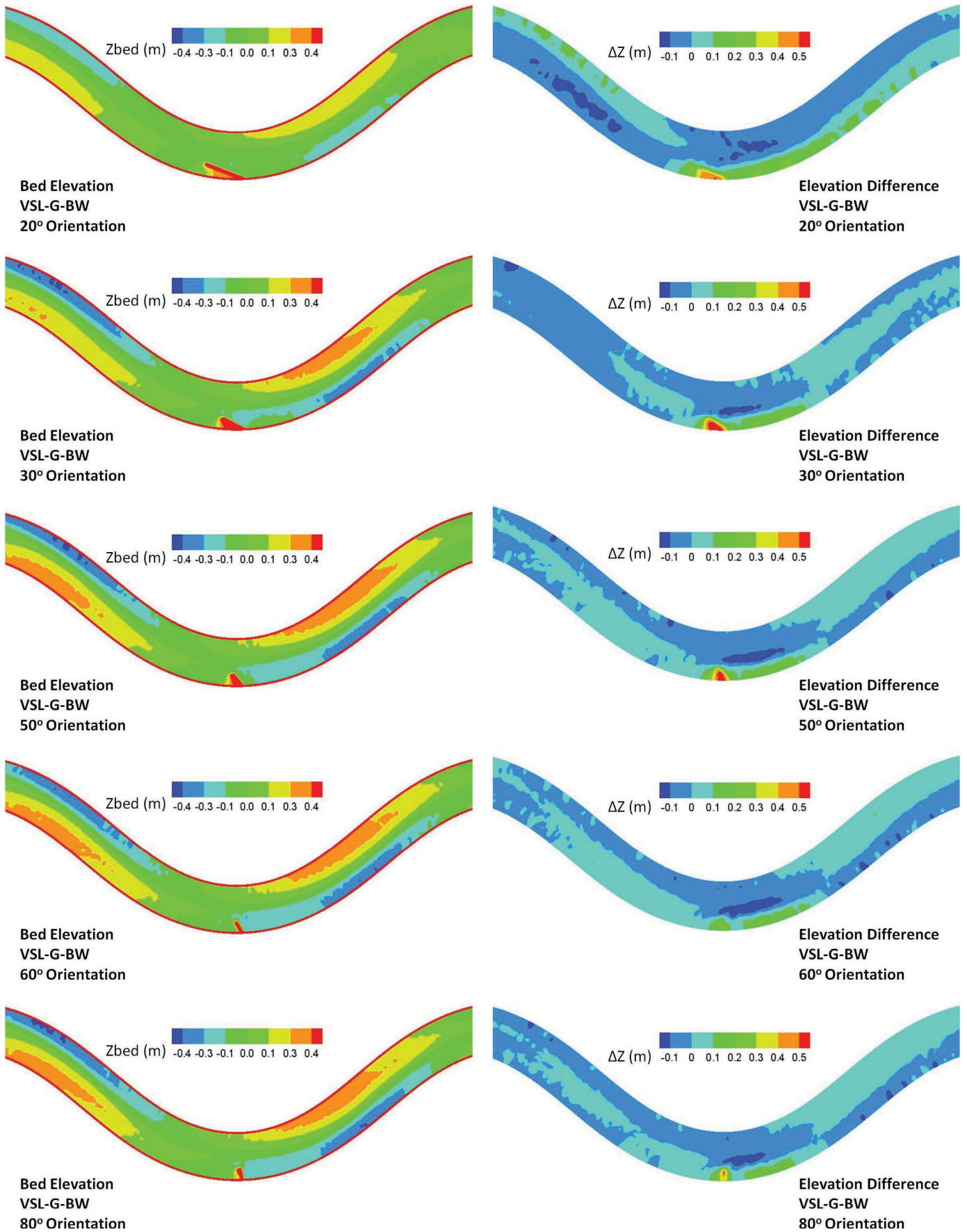


Figure 3-29. Z_{bed} for a bendway weir located at the meander apex for VSL-G. The ΔZ represents the Z_{bed} of the baseline case (with no rock structure; Figure 3-2) subtracted from the Z_{bed} of this case. Flow is from left to right.

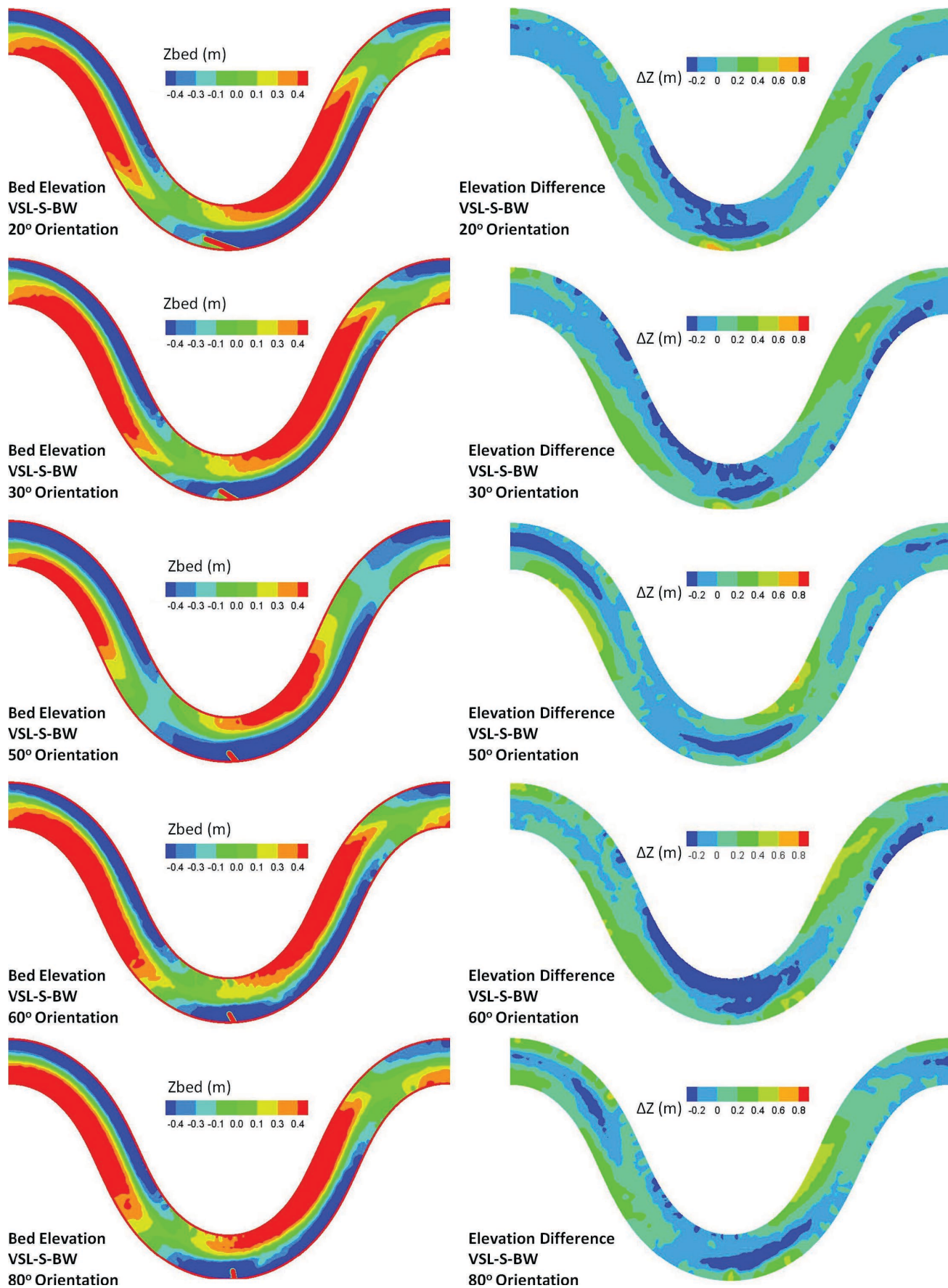


Figure 3-30. *Zbed* for a bendway weir located at the meander apex for VSL-S. The ΔZ represents the *Zbed* of the baseline case (with no rock structure; Figure 3-2) subtracted from the *Zbed* of this case. Flow is from left to right.

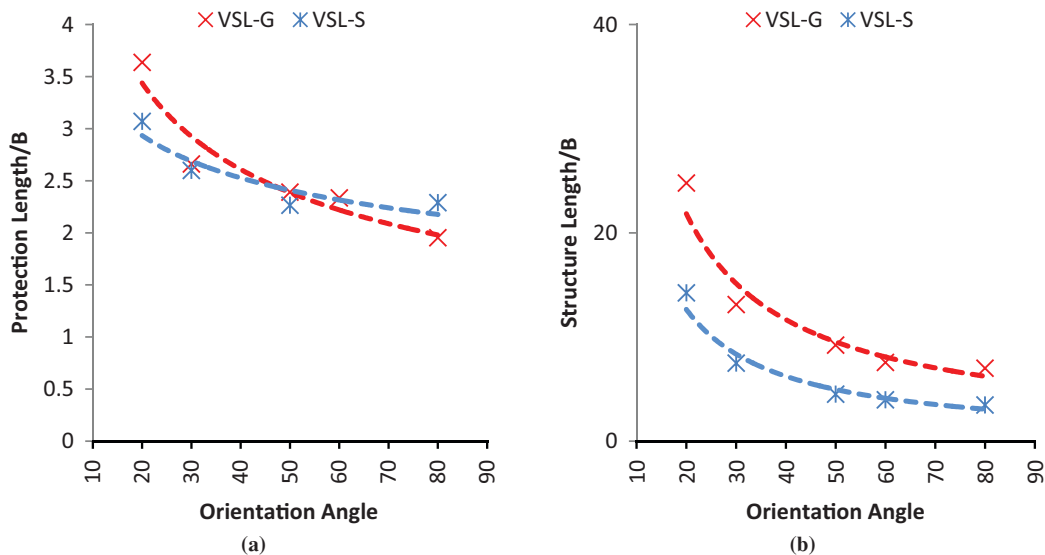


Figure 3-31. (a) Angle of orientation of bendway weirs compared to the ratio of protected bank to channel width, B, and (b) angle of orientation of bendway weirs compared to the ratio of structure length to channel width.

Therefore, an optimum structure angle for a single structure can be selected to strike a balance between structure length (or cost of materials) and protection length (Figure 3-31). For VSL-G and VSL-S, this was found to be approximately 50°.

Similar to RVs and JHs, a single BW did not protect the full outer bank, and additional structures are recommended. To determine the optimum location of the next downstream structure, a horizontal line (tangent to the outer bank) was extended from the tip of the structure to the outer bank. The optimum location of the next structure was defined as the difference

(angle) between this line and the location where the shear layer attached to the outer bank. The shear layer was identified for each channel by the zone of high TKE (Figures 3-33 and 3-34). As shown in Figures 3-33 and 3-34 for both channels, the region of deep scour holes along the outer bank corresponded to the path of the high TKE or the shear layer from the tip of the structures. Based on the extent of the shear layer and the scour pattern, the location of the second BW structure for each channel was determined. The optimum angle and location of downstream BW for each channel are listed in Table 3-6.

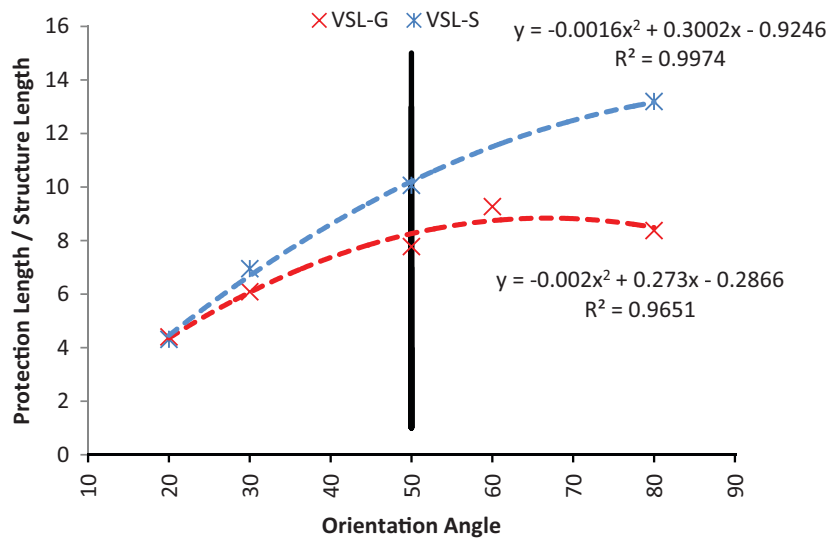


Figure 3-32. Ratio of length of bank protection to structure length (effective length held constant at one-quarter channel width) as a function of orientation angle for bendway weirs in VSL-S and VSL-G.

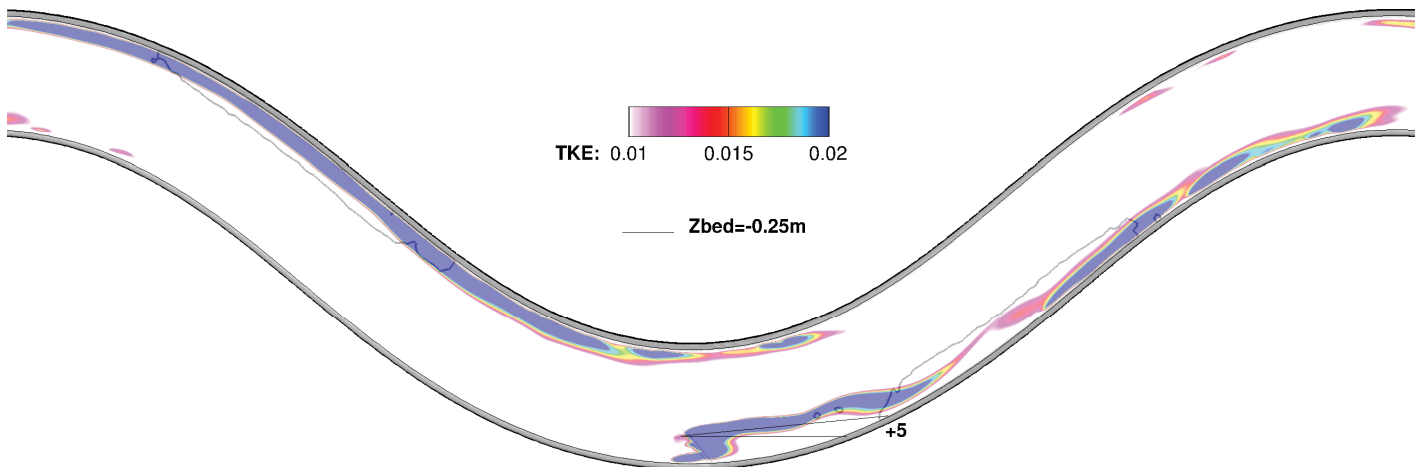


Figure 3-33. Color map of steady-state non-dimensionalized depth-averaged TKE overlaying contours of Z_{bed} downstream of a bendway weir in the VSL-G channel. TKE is non-dimensionalized with the square of mean flow velocity. The high-TKE region indicates the location of the shear layer, and contours illustrate the location of the deepest scour holes. Flow is from left to right.

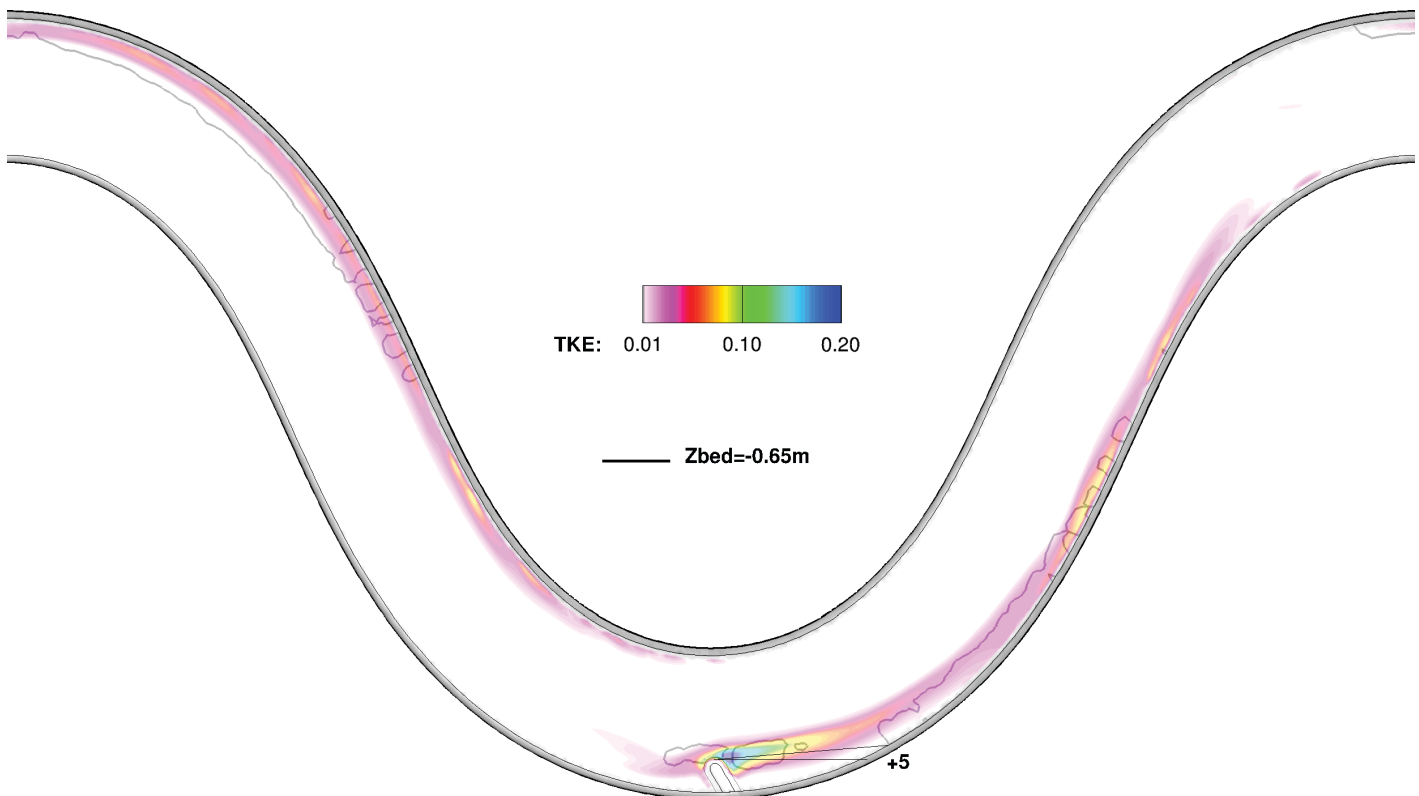


Figure 3-34. Color map of steady-state non-dimensionalized depth-averaged TKE overlaying contours of Z_{bed} downstream of a bendway weir in the VSL-S channel. TKE is non-dimensionalized with the square of mean flow velocity. The high-TKE region indicates the location of the shear layer, and contours illustrate the location of the deepest scour holes. Flow is from left to right.

Table 3-6. Angle of orientation and optimum location of second downstream bendway weir.

	Angle	Optimum Location
VSL-G	50°	+5° from the first BW tip
VSL-S	50°	+5° from the first BW tip

Optimum Number of Structures

An additional BW was installed in each stream based on the layout described in Table 3-6. In Figures 3-35 and 3-36, the results of simulations are shown for the VSL-G and VSL-S, respectively. For both channels, the placement of the second BW structure increased the length of bank protection on the outer bend. The shear layer was diverted toward the middle of the channel instead of impinging to the outer bank. However, from Figures 3-35 and 3-36, it is clear that an additional structure is required in both channels to protect the entire meander outer bank. Therefore, the shear layer was examined along with the bed bathymetry downstream of the second structure for each channel (Figures 3-37 and 3-38).

As shown in Figures 3-37 and 3-38, for both channels, the shear layer downstream of the second structure reattaches to the outer bank and creates another deep scour hole near the bank. To address this problem, installation of the third BW structure was accomplished as shown in Table 3-7.

Simulations with three BW structures in each channel are shown in Figures 3-39 and 3-40. In these figures, the proposed combination of three BWs protected the outer bank of the meander by diverting the shear layer to the middle of each channel. For both channels, VSL-G and VSL-S, the three-structure array arranged as described in Tables 3-6 and 3-7 protected the entire outer bank of the meander.

Evaluation of Structure Array Location

Similar to RV and JH structures, further investigations were carried out to study the effect of shifting the array of three BWs upstream by one channel width (B). Figures 3-41 and 3-42 show the results of this new arrangement of three BW structures in VSL-G and VSL-S, respectively.

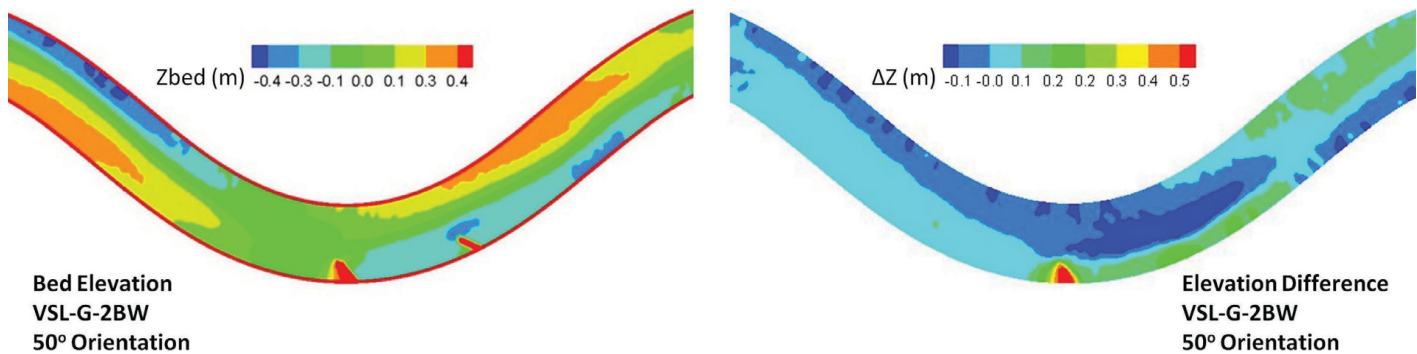


Figure 3-35. *Zbed* for a two-bendway weir array starting at the meander apex for VSL-G. The ΔZ represents the *Zbed* of the baseline case (with no rock structure; Figure 3-2) subtracted from the *Zbed* of this case. Flow is from left to right.

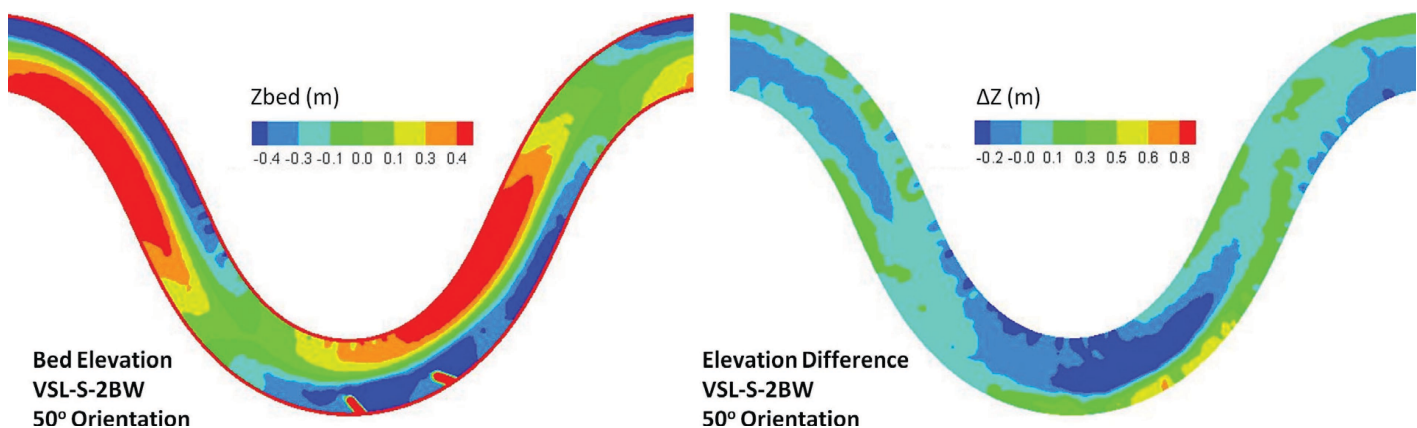


Figure 3-36. *Zbed* for a two-bendway weir array starting at the meander apex for VSL-S. The ΔZ represents the *Zbed* of the baseline case (with no rock structure; Figure 3-2) subtracted from the *Zbed* of this case. Flow is from left to right.

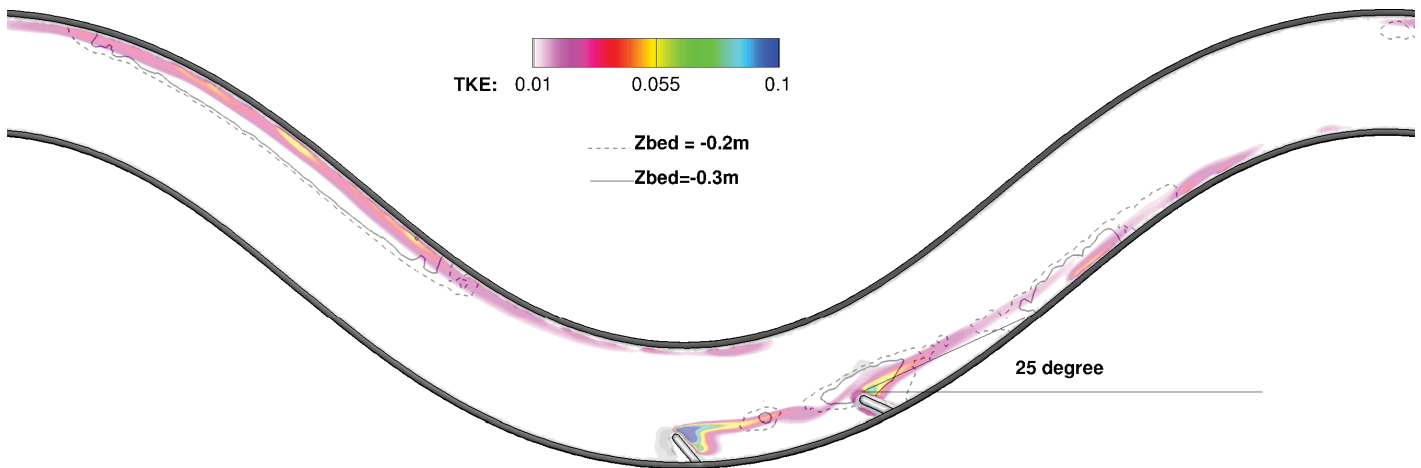


Figure 3-37. Color map of steady-state non-dimensionalized depth-averaged TKE overlaying contours of Z_{bed} downstream of a two-bendway weir array in the VSL-G channel. TKE is non-dimensionalized with the square of mean flow velocity. The high-TKE region indicates the location of the shear layer, and contours illustrate the location of the deepest scour holes. Flow is from left to right.

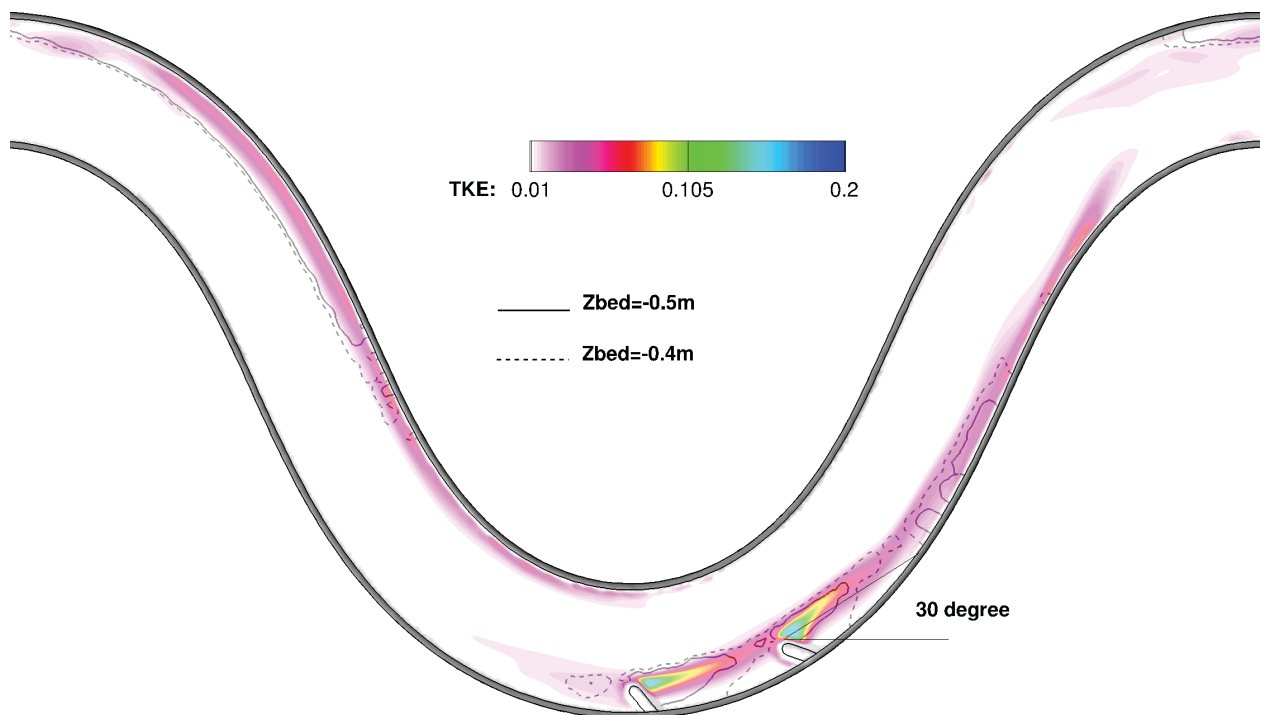


Figure 3-38. Color map of steady-state non-dimensionalized depth-averaged TKE overlaying contours of Z_{bed} downstream of a two-bendway weir array in the VSL-S channel. TKE is non-dimensionalized with the square of mean flow velocity. The high-TKE region indicates the location of the shear layer, and contours illustrate the location of the deepest scour holes. Flow is from left to right.

Table 3-7. Angle of orientation and optimum location of third downstream bendway weir.

	Angle	Optimum Location
VSL-G	50°	+25° from the second BW tip
VSL-S	50°	+30° from the second BW tip

Shifting the BW array upstream led to less bank protection on the outer bank downstream of the structure array without any improvement in bank protection length on the outer bank upstream of the meander apex. Therefore, the original arrangement of BWs with the first structure located at the meander apex was favorable for both VSL-G and VSL-S with spacing as described in Tables 3-6 and 3-7.

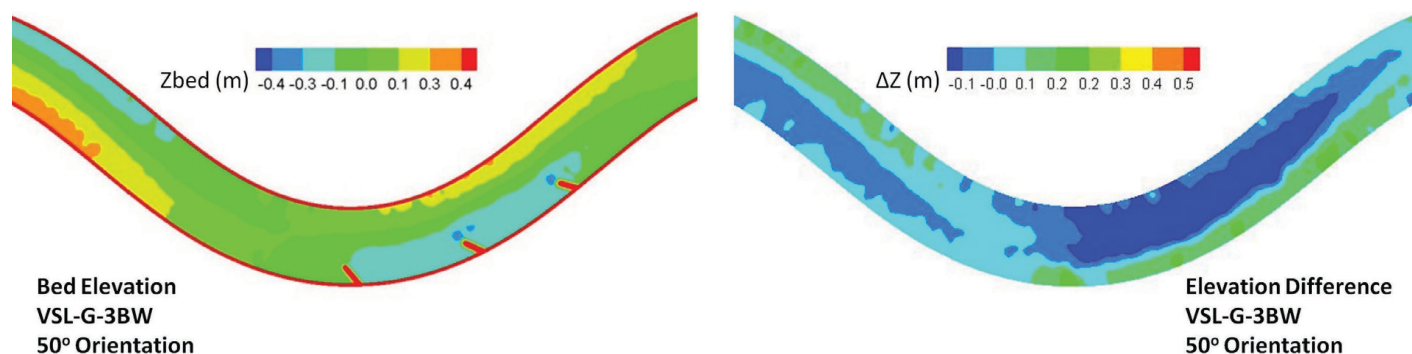


Figure 3-39. *Zbed* for a three-bendway weir array starting at the meander apex for VSL-G. The ΔZ represents the *Zbed* of the baseline case (with no rock structure; Figure 3-2) subtracted from the *Zbed* of this case. Flow is from left to right.

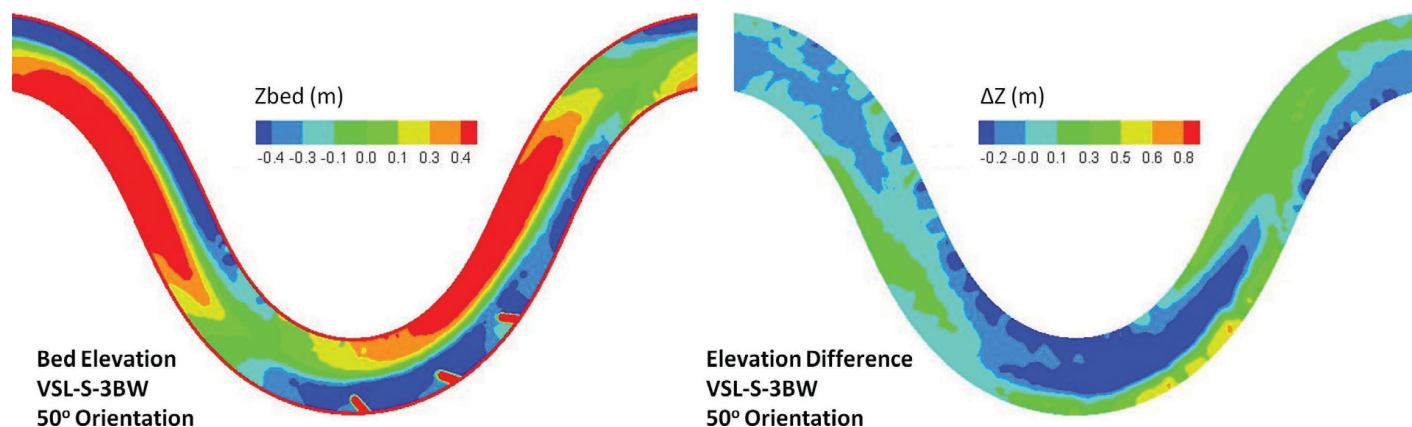


Figure 3-40. *Zbed* for a three-bendway weir array starting at the meander apex for VSL-S. The ΔZ represents the *Zbed* of the baseline case (with no rock structure; Figure 3-2) subtracted from the *Zbed* of this case. Flow is from left to right.

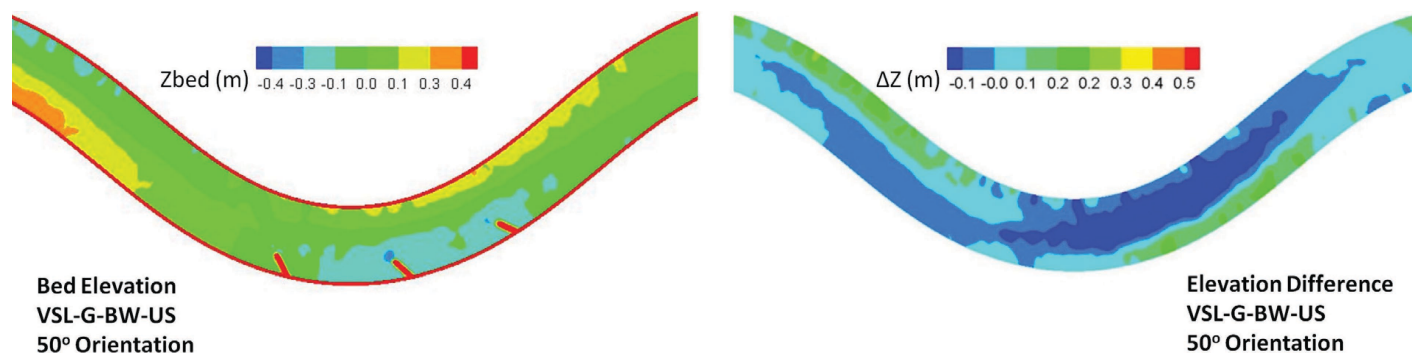


Figure 3-41. *Zbed* for a three-bendway weir array in VSL-G shifted upstream of the meander apex by a length equal to one channel width. The ΔZ represents the *Zbed* of the baseline case (with no rock structure; Figure 3-2) subtracted from the *Zbed* of this case. Flow is from left to right.

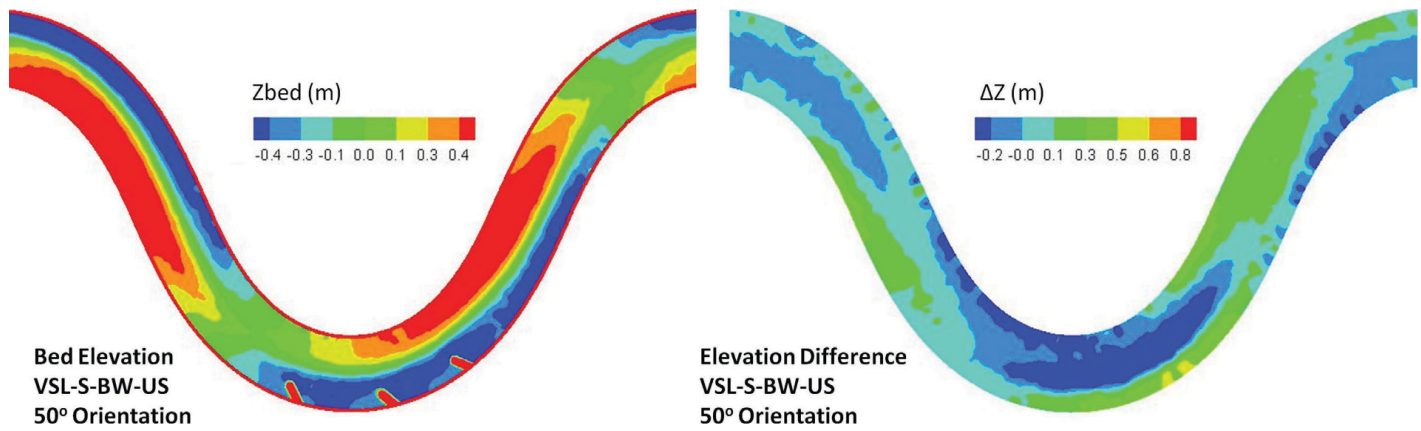


Figure 3-42. *Zbed* for a three-bendway weir array in VSL-S shifted upstream of the meander apex by a length equal to one channel width. The ΔZ represents the *Zbed* of the baseline case (with no rock structure; Figure 3-2) subtracted from the *Zbed* of this case. Flow is from left to right.

CHAPTER 4

Numerical Methodology for Developing Design Guidelines for Sill Structures

Results from case studies and physical experiments (see Appendices C and D) were extended to typical gravel and sand-bed streams using the VSL3D for two channel-spanning or sill structures, cross vanes, and W-weirs. The goal of these investigations was to determine what structures are most appropriate, how they should be installed (including location of specific structures), how they should be monitored and maintained, and the likely failure mechanisms for each structure installation based on site-specific stream properties (e.g., curvature, slope, bed material).

For each structure type, a systematic approach was used to determine the optimum angle of orientation relative to the bank, location, and the effect of multiple structures for typical sand (VSL-S) and gravel (VSL-G) channels. For channel-spanning structures, the optimum angle of orientation was determined using quasi-equilibrium bed elevation (see Table 3-1 for structure geometry). The optimum angle was selected as the configuration that resulted in (1) the most central thalweg, and (2) the least erosion near either bank. Once the optimum angle was selected for each structure configuration for sill structures located at the upstream end of a straight reach, the effect of structure location in a meandering channel was tested by shifting the structure to the downstream end of the straight reach (see Figure 4-1) approximately one channel width (B) downstream of the previous (upstream end) location. The performance of multiple sill structures in meandering sand and gravel channels was investigated. Two sill structures were installed upstream and downstream of a meander of interest bracketing the meander apex (Figure 4-2). Time-averaged quasi-equilibrium bed elevation (Z_{bed}) was analyzed to investigate the influence of a second structure.

4.1 VSL3D Results for Cross Vanes

Single Cross Vane Scour and Deposition

Two configurations of a cross vane structure, a U-shaped cross vane (CV) and an A-shaped cross vane (CVA), were tested

with the VSL-G and VSL-S bed-morphodynamics models. The VSL3D was applied to simulate the resulting bed morphodynamics for two different angles for each CV configuration placed just after a meander and before a straight section of channel. These angles, 20° and 30° , were chosen within the range of angles that define CV and CVA structures (Rosgen, 2006; NRCS, 2007). The computed results are shown in Figures 4-3 and 4-4 for VSL-G and VSL-S, respectively. For each case, the time-averaged bed elevation and the difference between the time-averaged bed elevation and the quasi-equilibrium bed elevation with no structure (see Figure 3-2) are shown. The computed results for the VSL-G channel show very little effect of angle on scour patterns (Figure 4-3). The addition of a step to form a CVA structure results in a larger (longer) scour hole downstream of the structure in both VSL-G and VSL-S. For the VSL-S channel, the effect of angle was more evident, with the 20° structure resulting in greater scour downstream of both CV and CVA structures.

Optimum Angle and Structure Shape

Both CV and CVA structures have been used in the field, although current guidelines (i.e., Rosgen, 2006, NRCS, 2007) recommend the additional step present in the CVA. The field performance of both CV and CVA was evaluated by the U.S. Bureau of Reclamation (U.S. Department of the Interior, Bureau of Reclamation, 2009). The effect of the arm angle of orientation was tested with numerical simulation in the VSL-G and VSL-S channels (Figures 4-3 and 4-4). Differences in scour depth and pattern were small for different structure angles of orientation. However, for the VSL-G and VSL-S channels, the 30° angle of orientation for both A-shaped and U-shaped structures performed better. The criteria for selection included the threat of scour on either bank. A more central scour hole with less scour adjacent to either bank would be preferred over a wide, deep scour hole that extends to the banks. The optimum cross vane shape, U- or A-shaped,

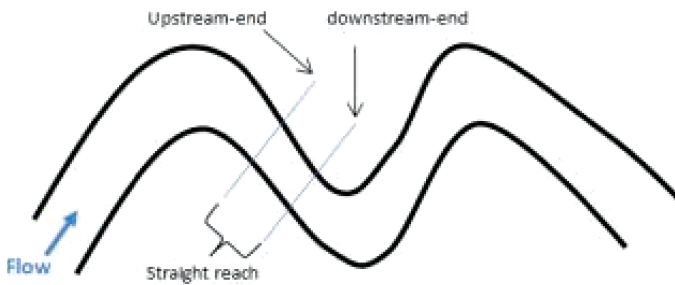


Figure 4-1. Schematic of meandering channel and sill structure locations at upstream and downstream of straight reach.

depends on the project goals. CVA structures were successful in protecting the upper cross piece of the cross vane by preventing deep scour immediately downstream of these rocks. The scour hole downstream of the CVA structure extended to the banks in the VSL-G channel, creating greater risk to the banks. The following sections will investigate both types of cross vanes with the 30° angle of orientation.

Evaluation of Structure Location

To investigate the effect of cross vane location on the sediment transport process, a single cross vane structure (CV or CVA) was placed at the downstream end of the straight reach of VSL-S and VSL-G (see Figure 4-1) approximately one channel width (B) downstream of the previous (upstream end) location. Figures 4-5 and 4-6 show the quasi-equilibrium bed morphology with a CV or a CVA at the downstream end of the straight reach for VSL-G and VSL-S, respectively. The comparisons between this case and the previous case (Figures 4-3 and 4-4) show that shifting the structure's location to the downstream end of the straight reach leads to a shift in the location of the scour hole and point bar within the meander. Shifting the sill structure downstream caused deeper scour near the outer bank around the meander apex (Figures 4-5 and 4-6);

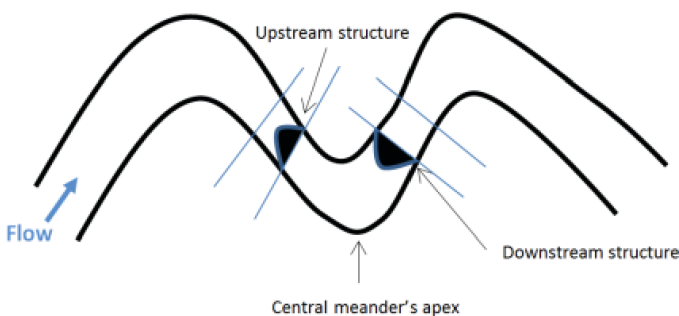


Figure 4-2. Schematic of meander and two sill structure locations. The reach between the two blue lines on each side of the apex shows the straight reaches. The upstream and downstream structures are installed at the downstream end and upstream end of the straight reaches.

however, the point bar was also pushed downstream of the apex as a result of the highly turbulent flow downstream of the sill structure. Comparing Figures 4-3 and 4-4 (upstream) with Figures 4-5 and 4-6 (downstream) indicates that shifting CVs or CVAs downstream by approximately B moves the scour pattern to approximately $0.5B$ downstream. Hence, for meandering streams, the turbulent flow downstream of the sill structure is a potential threat to the stability of the outer bank (especially at regions near the apex); therefore, a single cross vane should be installed at the upstream end of a straight reach in a meandering channel (similar to suggestions by Doll et al., 2003).

Evaluation of Multiple Sill Structures

The performance of multiple sill structures in VSL-G and VSL-S was investigated. Two CV structures were installed upstream and downstream of a meander bracketing the meander apex. Figure 4-7 illustrates the quasi-equilibrium bed morphology of VSL-G with CVs or CVAs bracketing the meander. As shown in this figure, the presence of the second sill structure leads to sediment deposition immediately upstream of the structure; however, the general morphological pattern at the apex region is very similar to that in the previous case with one sill structure (Figure 4-5). The downstream sill structure (for both CV and CVA structures) only influenced the morphological pattern immediately upstream. For example, in Figure 4-5, with one sill structure upstream of the apex, the near-bank scour depth at the apex is comparable with the results with two sill structures in Figure 4-7. This is because the CV configuration with sloping arms allows sediment movement to be transported over the second sill structure. Once the depth of deposited sediment upstream of the second CV was equal to the structure height, the sediment material was easily entrained and moved downstream. Adding a second sill structure resulted in two scour pools, one downstream of each structure. The scour hole downstream of the first structure has similar characteristics to the scour pool downstream of a single CV structure (Figure 4-5) that can cause some structural stability issues downstream of the apex for the inner bank (see Figure 4-7).

In Figure 4-8 the quasi-equilibrium bed morphology of VSL-S with two cross vanes is shown. Like VSL-G, the second sill structure caused sediment deposition immediately upstream of the structure; however, the general morphological pattern at the apex region is similar to that in the previous case with one sill structure (Figure 4-6). The use of the second sill structure did not influence the quasi-equilibrium morphological pattern at the meander's apex and, like VSL-G, the main reason could be the passage of the sediment material over the second sill structure. For VSL-S, the scour hole downstream of the first structure also had similar characteristics to the scour hole in the single sill structure case (Figure 4-6). A second scour hole can cause some structural stability issues downstream of the apex for the inner bank (see Figure 4-8).

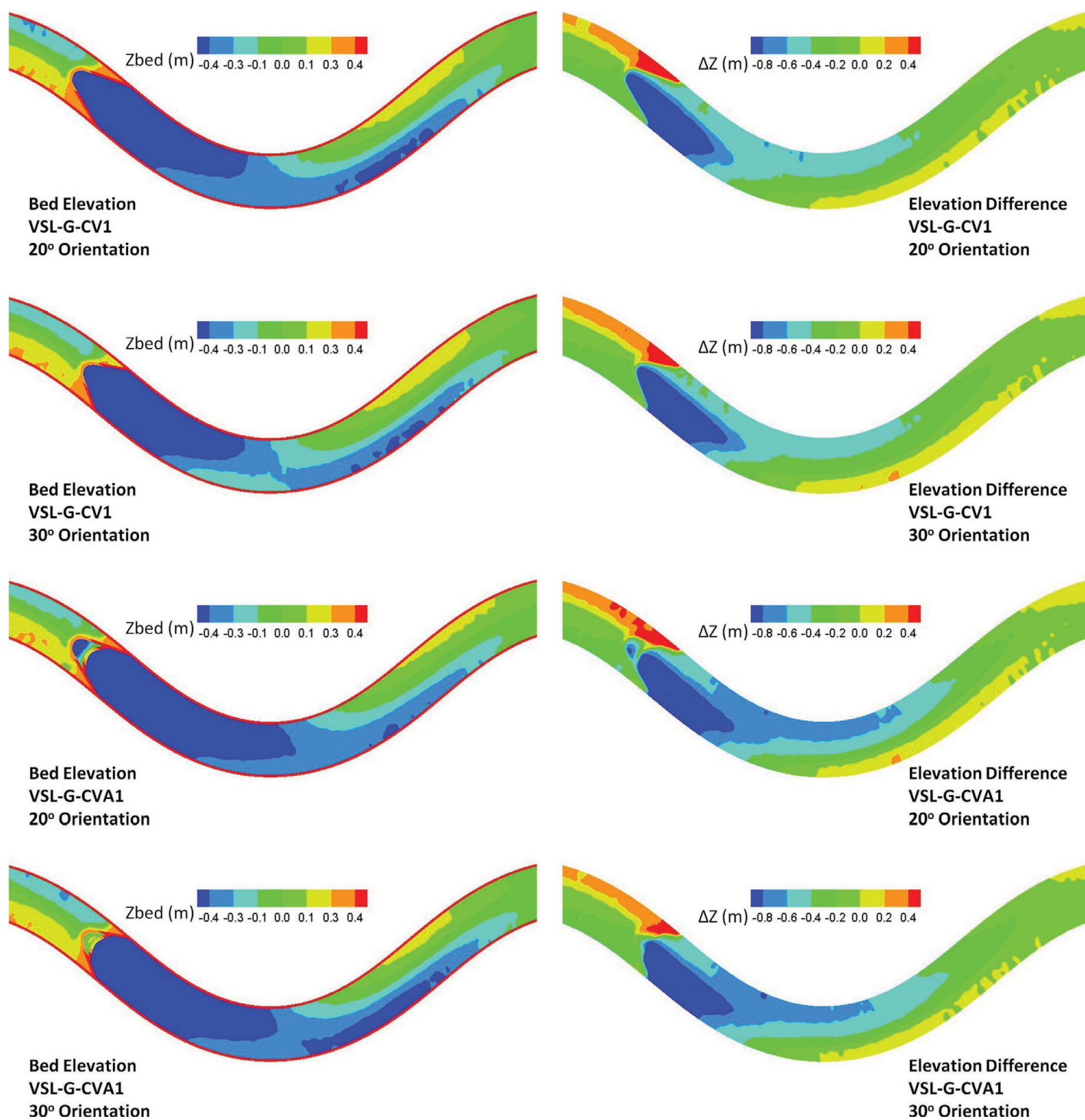


Figure 4-3. Z_{bed} for a standard or U-shaped cross vane and a stepped, A-shaped cross vane located at the upstream end of the straight reach of the VSL-G. The ΔZ represents the Z_{bed} of the baseline case (with no rock structure; Figure 3-2) subtracted from the Z_{bed} of this case. Flow is from left to right.

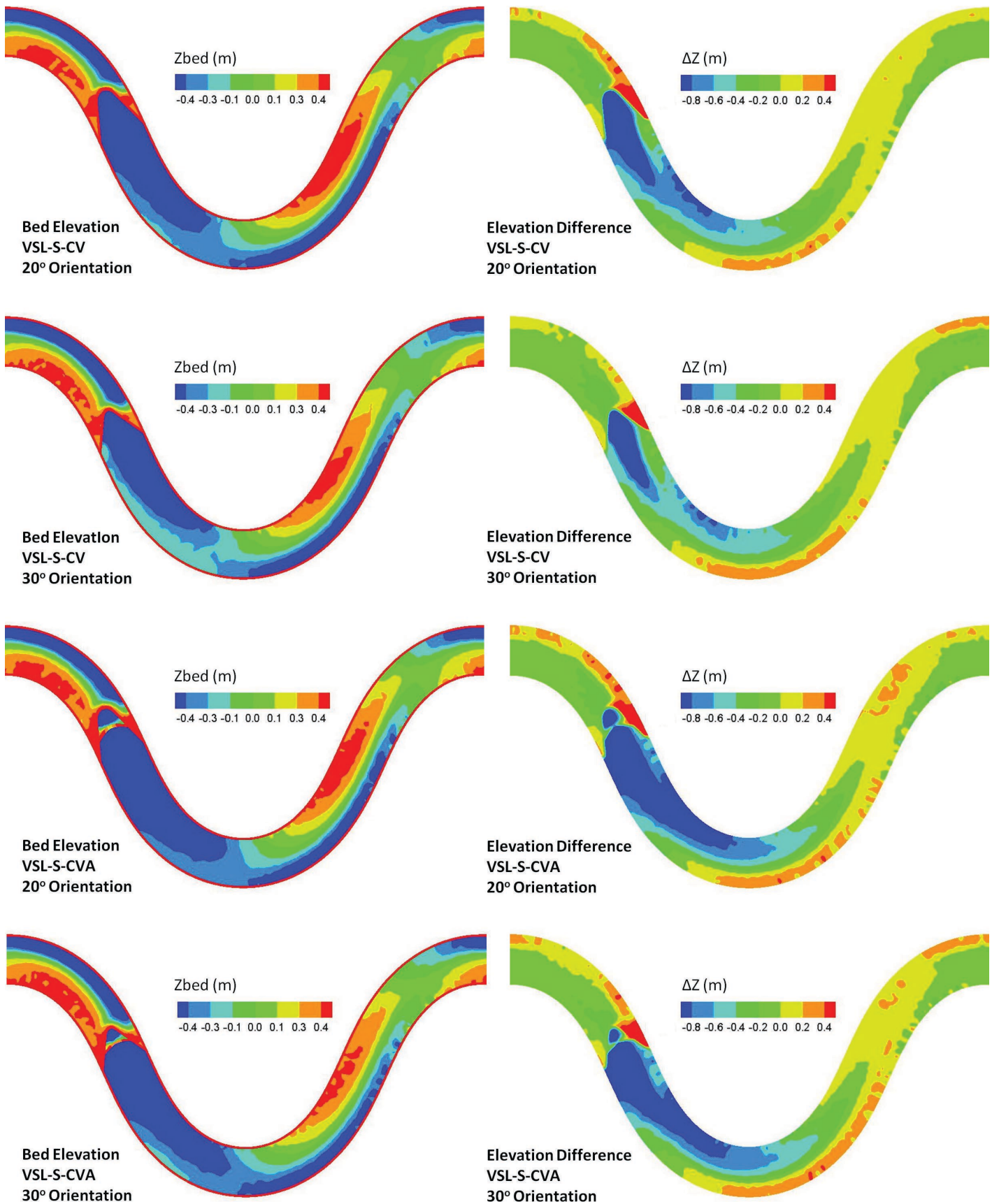


Figure 4-4. Z_{bed} for a U-shaped cross vane and a stepped, A-shaped cross vane located at the upstream end of the straight reach of the VSL-S. The ΔZ represents the Z_{bed} of the baseline case (with no rock structure; Figure 3-2) subtracted from the Z_{bed} of this case. Flow is from left to right.

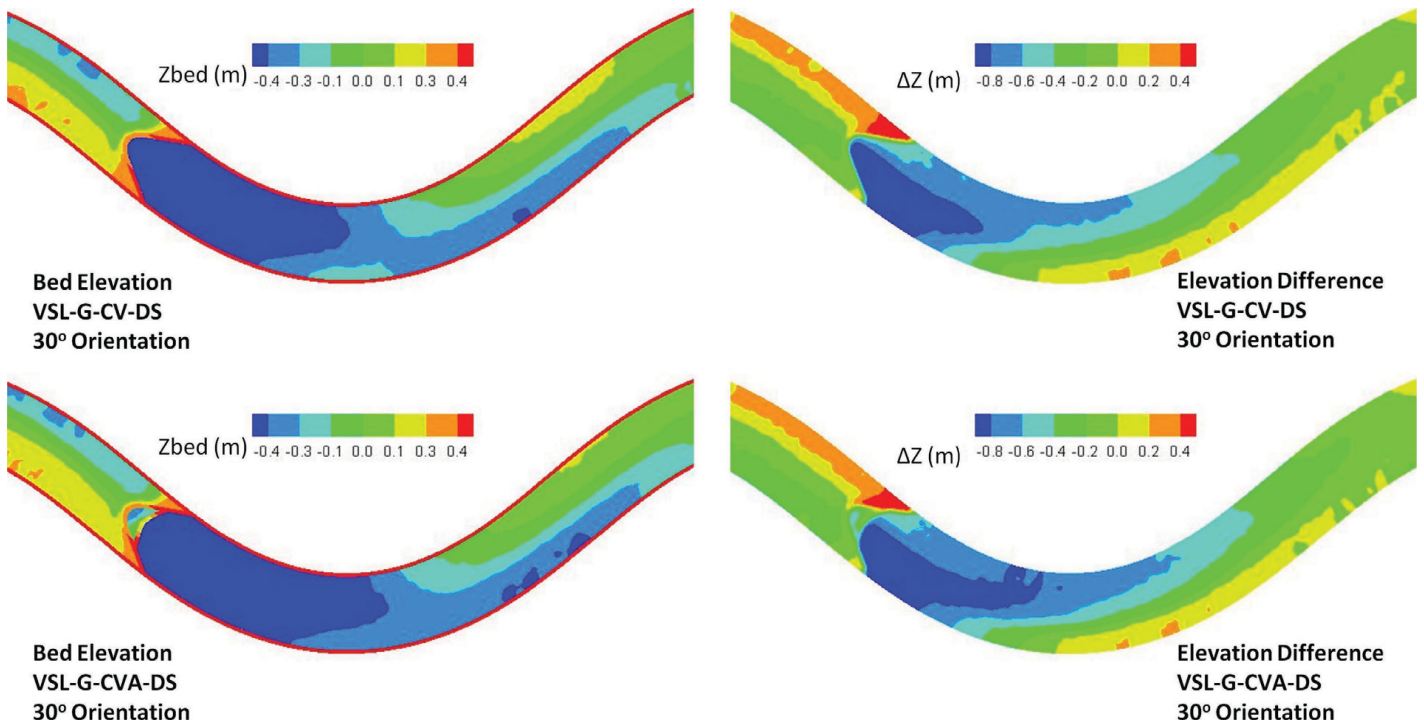


Figure 4-5. *Zbed* for a U-shaped cross vane and a stepped, A-shaped cross vane located at the downstream end of the straight reach of the VSL-G. The ΔZ represents the *Zbed* of the baseline case (with no rock structure; Figure 3-2) subtracted from the *Zbed* of this case. Flow is from left to right.

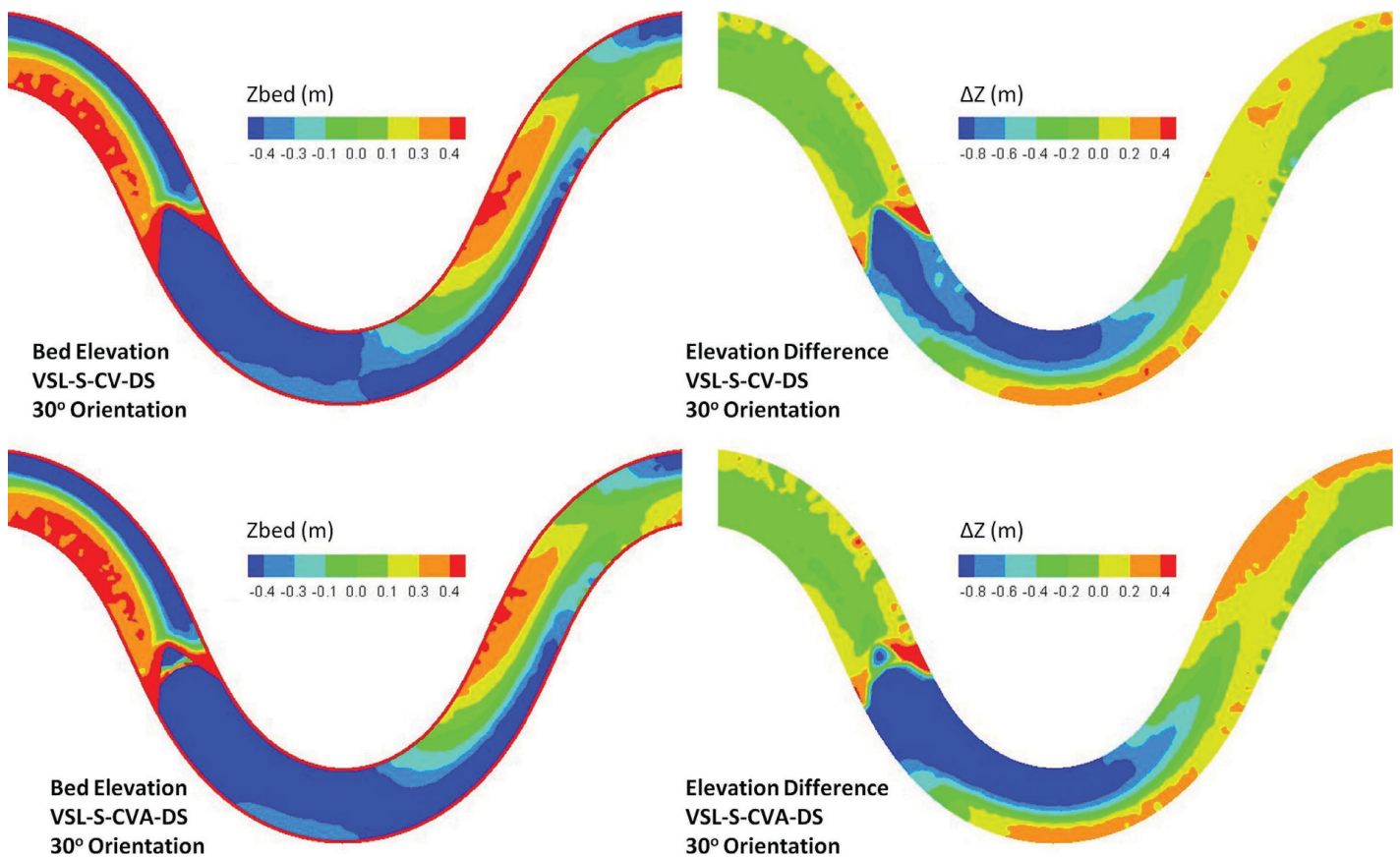


Figure 4-6. *Zbed* for a U-shaped cross vane and a stepped, A-shaped cross vane located at the downstream end of the straight reach of the VSL-S. The ΔZ represents the *Zbed* of the baseline case (with no rock structure; Figure 3-2) subtracted from the *Zbed* of this case. Flow is from left to right.

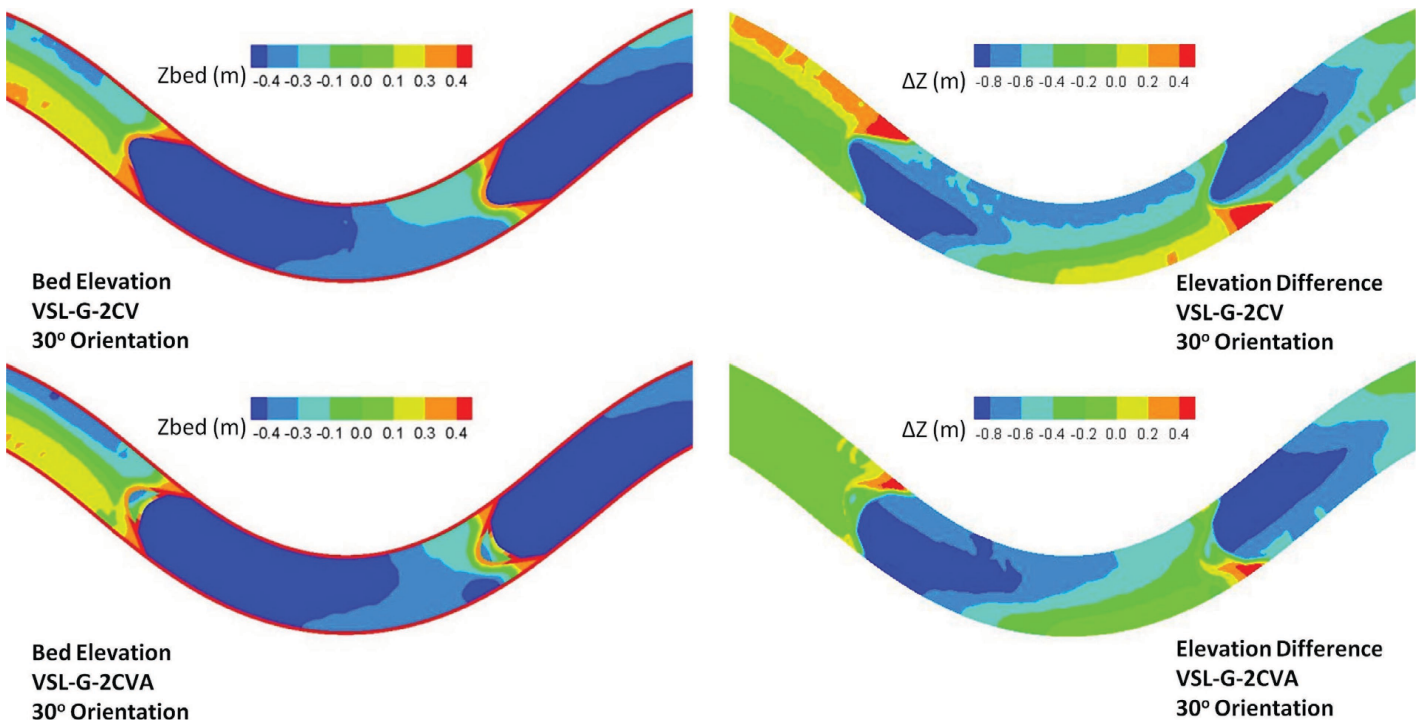


Figure 4-7. *Zbed* for two U-shaped cross vanes and two stepped, A-shaped cross vanes in VSL-G. The ΔZ represents the *Zbed* of the baseline case (with no rock structure; Figure 3-2) subtracted from the *Zbed* of this case. Flow is from left to right.

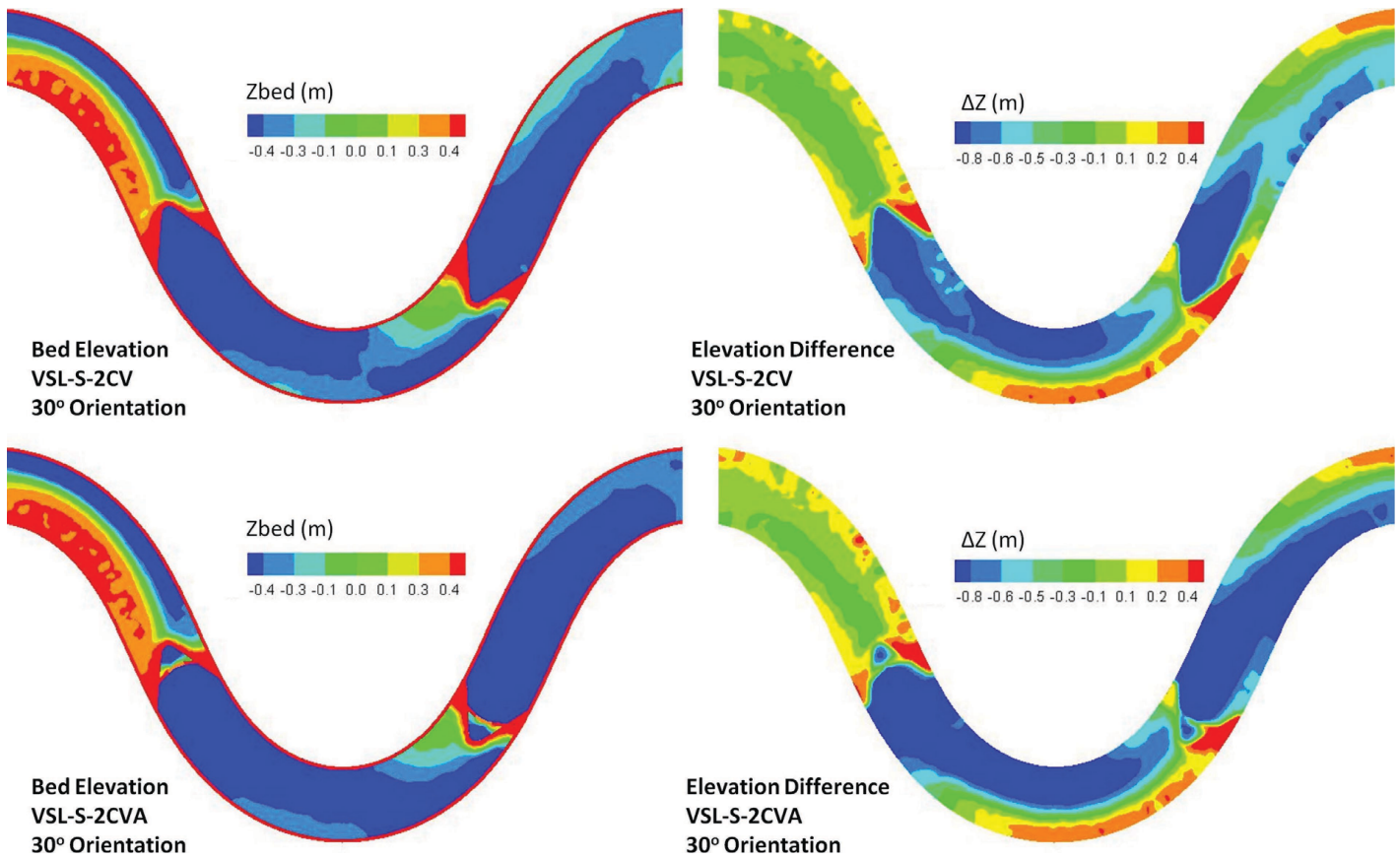


Figure 4-8. *Zbed* for two U-shaped cross vanes and two stepped, A-shaped cross vanes in VSL-S. The ΔZ represents the *Zbed* of the baseline case (with no rock structure; Figure 3-2) subtracted from the *Zbed* of this case. Flow is from left to right.

4.2 VSL3D Results for W-Weirs

Single W-Weir Scour and Deposition

A WW was placed in the VSL-G and VSL-S bed-morphodynamics models just after a meander and before a straight section of channel (see Figure 4-1). VSL3D was applied to simulate the resulting bed morphodynamics for two different angles for each configuration. These angles, 20° and 30° , were chosen within the range of angles in WW guidelines (Rosgen, 2006 and NRCS, 2007). The computed results are shown in Figures 4-9 and 4-10 for VSL-G and VSL-S, respectively. For each case, the time-averaged bed elevation and the difference between the time-averaged bed elevation and the quasi-equilibrium bed elevation with no structure are shown. The computed results for the VSL-G and VSL-S channel show very little effect of angle on scour patterns.

Optimum Angle

The optimum angle of orientation for WWs in the VSL-S and VSL-G channels was determined to be 30° from the banks. This evaluation was based on similar performance criteria as in the CV numerical experiments. The 30° arm angle provided a deep scour hole downstream of the structure with less risk of bank erosion downstream. In addition, significantly less rock material is required to install a 30° arm angle relative to one with 20° arm angle.

Evaluation of Structure Location

In order to investigate the effect of the location of a WW on the final bed topography, the WW was relocated at the downstream end of the straight reach for each meandering channel (see Figure 4-1). The WW structure was moved downstream with a length of approximately B . Figures 4-11 and 4-12 show the quasi-equilibrium bed morphology for VSL-G and VSL-S, respectively, with a WW located at the downstream end of the straight reach.

Figures 4-11 and 4-12 are comparable with Figures 4-9 and 4-10 for 30° WWs. As shown in these figures, shifting the WW structure downstream results in a downstream shift of the scour hole pattern. A downstream shift in structure location of B resulted in a shift in the scour pool of $0.5B$ downstream. This finding is valid for both VSL-G and VSL-S and also for all other types of sill structures tested. Placement of the WW structure at the upstream end of the straight reach can cause less bank erosion near the apex of the downstream meander.

Evaluation of Multiple Sill Structures

The performance a WW structure array was evaluated in VSL-G and VSL-S. WW structures were located upstream and downstream of a meander bracketing the meander apex (see Figure 4-2). Figure 4-13 illustrates the quasi-equilibrium bed morphology of VSL-G. As shown in this figure, the presence of the second sill structure leads to sediment deposition

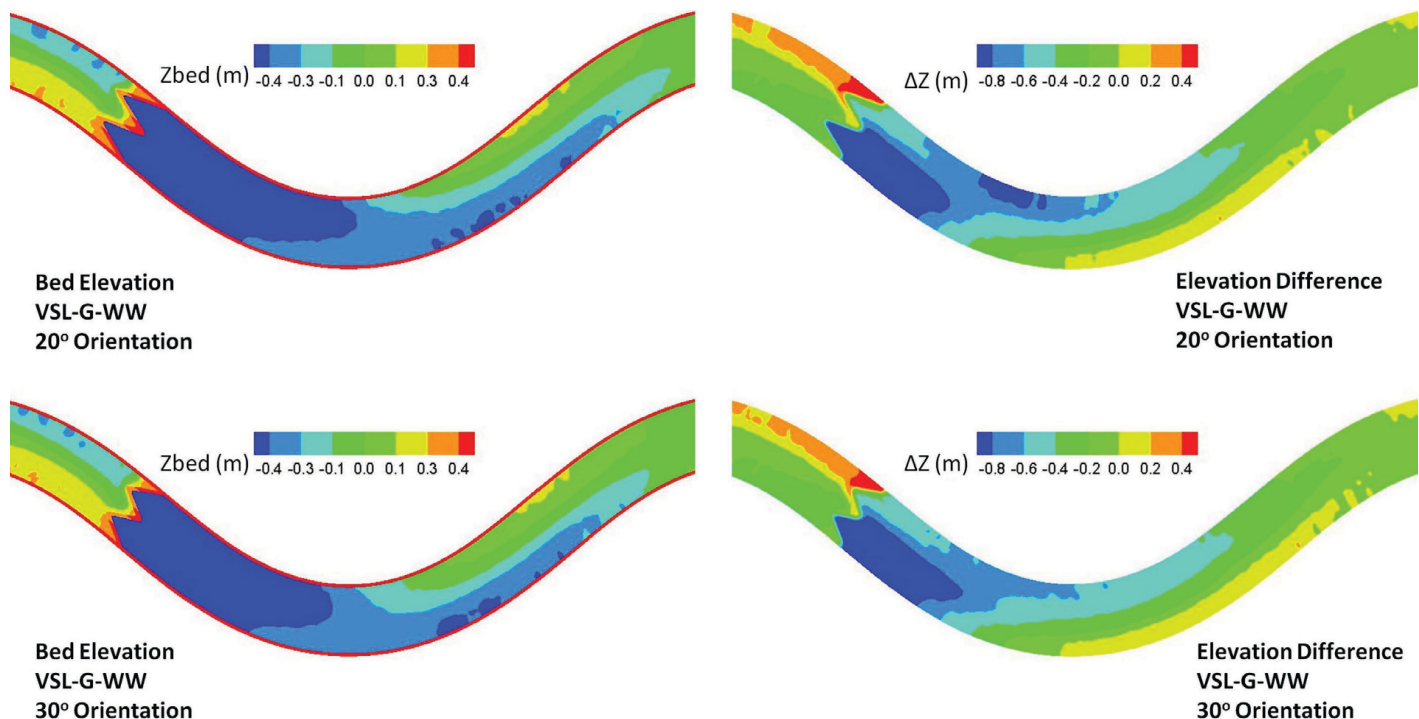


Figure 4-9. Z_{bed} for a single WW located at the upstream end of the straight reach of the VSL-G. The ΔZ represents the Z_{bed} of the baseline case (with no rock structure; Figure 3-2) subtracted from the Z_{bed} of this case. Flow is from left to right.

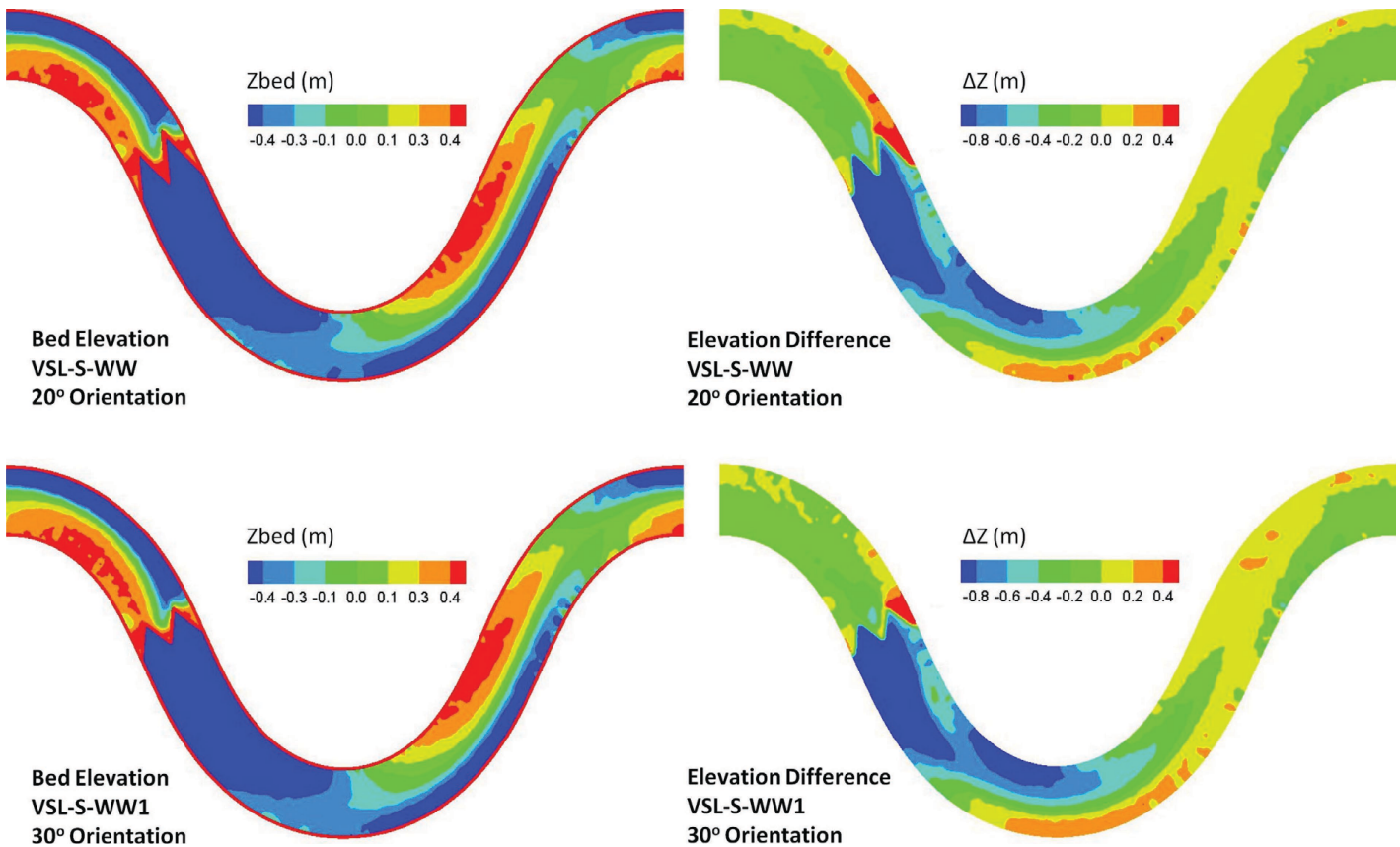


Figure 4-10. *Zbed* for a single WW located at the upstream end of the straight reach of the VSL-S. The ΔZ represents the *Zbed* of the baseline case (with no rock structure; Figure 3-2) subtracted from the *Zbed* of this case. Flow is from left to right.

immediately upstream of the structure; however, the general morphological pattern at the apex region is similar to that in the previous case with one sill structure. The scour hole downstream of the first structure has similar characteristics to the one in the single WW structure case.

Figure 4-14 shows the quasi-equilibrium bed morphology of VSL-S with multiple WWs. The presence of the second

WW structure causes sediment material deposition immediately upstream of the structure; however, the general morphological pattern at the apex region is similar to that in the previous case with one sill structure (Figure 4-12). Like the other two sill structures, use of the second sill structure does not significantly influence the quasi-equilibrium morphological pattern at the meander's apex.

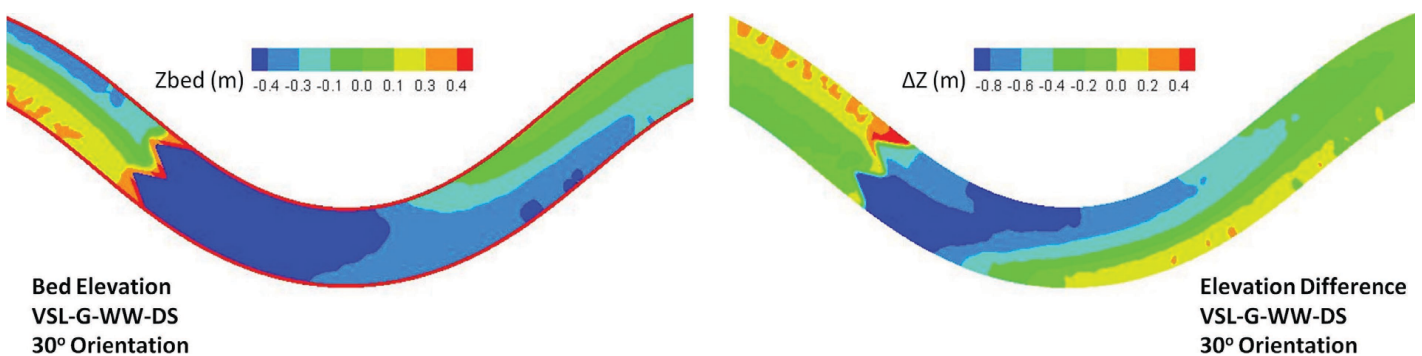


Figure 4-11. *Zbed* for a single WW located at the downstream end of the straight reach of the VSL-G. The ΔZ represents the *Zbed* of the baseline case (with no rock structure; Figure 3-2) subtracted from the *Zbed* of this case. Flow is from left to right.

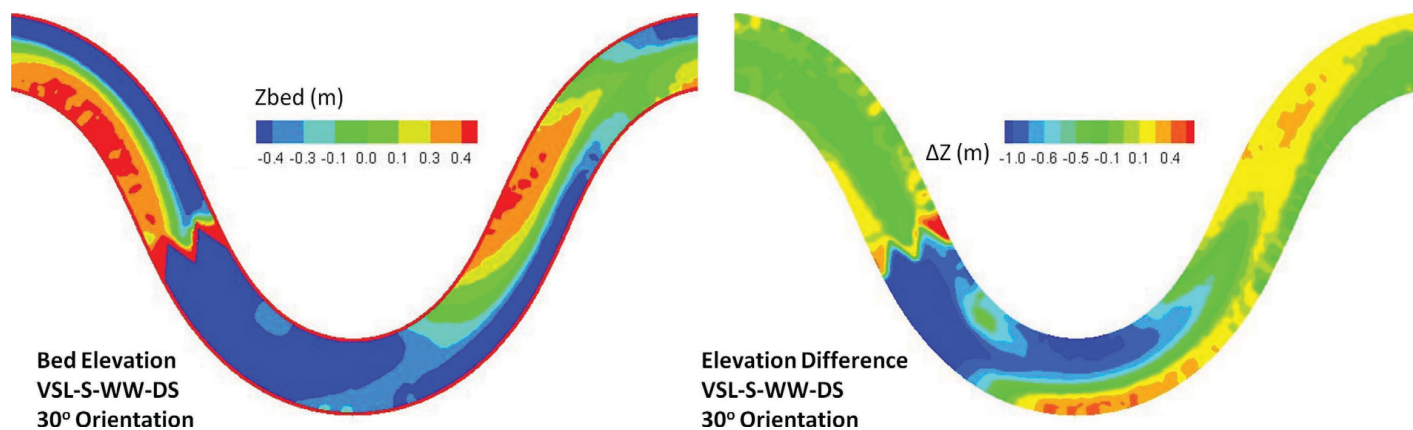


Figure 4-12. Zbed for a single WW located at the downstream end of the straight reach of the VSL-S. The ΔZ represents the Zbed of the baseline case (with no rock structure; Figure 3-2) subtracted from the Zbed of this case. Flow is from left to right.

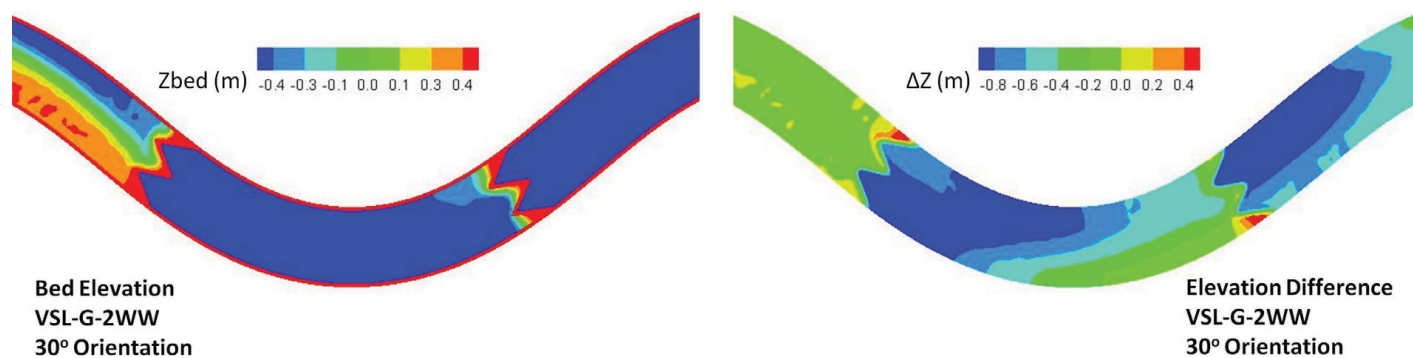


Figure 4-13. Zbed for two WWs in VSL-G. The ΔZ represents the Zbed of the baseline case (with no rock structure; Figure 3-2) subtracted from the Zbed of this case. Flow is from left to right.

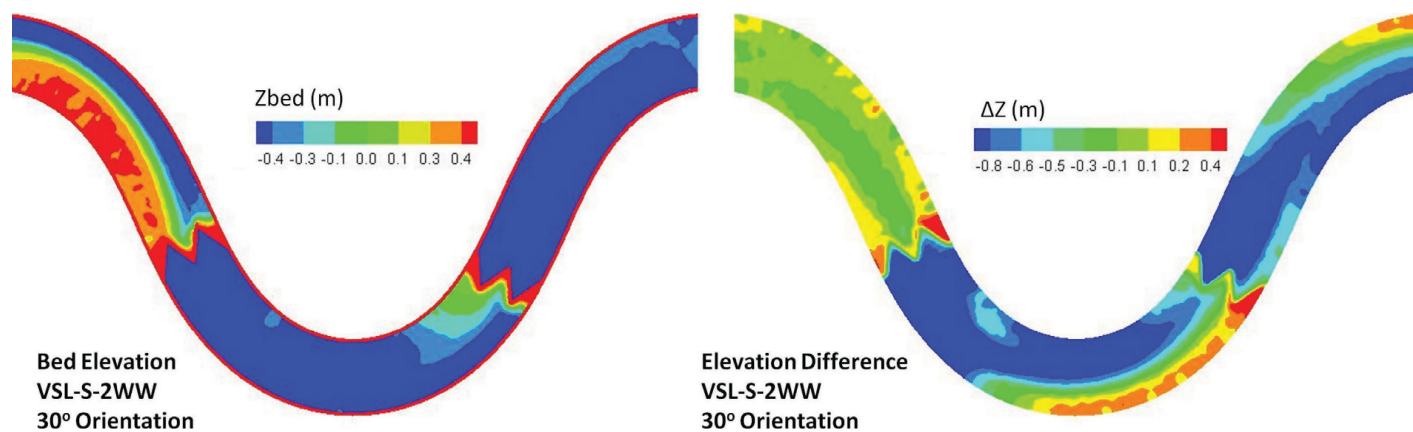


Figure 4-14. Zbed for two WWs in VSL-S. The ΔZ represents the Zbed of the baseline case (with no rock structure; Figure 3-2) subtracted from the Zbed of this case. Flow is from left to right.

CHAPTER 5

Comparison of In-Stream Flow Control Structure Types

5.1 Bank Protection

Pronounced bank erosion has been observed at meander bends due to pressure-driven secondary currents. These are helicoidal flow patterns, directed from the outer to the inner bank along the channel bed, that result from the local imbalance between the curvature-induced transverse pressure gradient and the centrifugal force along the bed. Secondary currents result in an increase in water surface elevation on the outside bank, which is known as superelevation, and redistribute stream-wise momentum within the channel cross-section. Pressure-driven secondary circulation can persist downstream of the apex, leading to undesired scour or deposition (Army Corps of Engineers, 1991). In both meandering and straight reaches, unchecked scour at the toe of banks will eventually lead to failure (Odgaard, 1988); therefore, to evaluate bank protection, scour at the bank toe was analyzed.

Both sill and single-arm structures were evaluated for their ability to provide bank protection. All of the single-arm structures were successful at shifting the channel thalweg toward the center of the channel (Figure 5-1), thus providing some level of bank protection. To compare the applicability of different structure types for bank protection, the length of protected bank for each structure was quantified in terms of the upstream (L_u) and downstream (L_d) length of bank where deposition was calculated relative to the structure-free channel (see Figure 3-3).

The final optimized structure arrays were evaluated for the three single-arm structure types. In general, the BW arrays provided the greatest length of bank protection. In VSL-G, these structures provided consistent bank protection, with little scour along the inner bank and a thalweg located in the middle of the channel. RVs and JHs also provided bank protection in their optimal set-up but with a less consistent thalweg, less consistent bank protection, and risk of scour to the inner bank (Figure 5-2).

For sill-type structures in VSL-G, the length of bank protection was very similar for all structure types. Minimal protection was provided along the outer bank (Figure 5-2) downstream of the apex. However, quasi-equilibrium scour holes downstream of the sill structures extended to the outer bank [also observed in the OSL and indoor StreamLab (ISL) experiments], threatening bank stability on both banks downstream of the structure.

In the VSL-S channel, all single-arm structure arrays provided outer bank protection that extended through the meander test section (Figure 5-3). RVs provide a slightly greater length of bank protection, and BWs and RVs both resulted in a more consistent thalweg than JHs, which created more scouring of the inner point bar.

In VSL-S, CVs and the modified CVA sill-type structures provided a greater length of bank protection than the WW (Figure 5-3). As in the VSL-G, OSL, and ISL channels, the scour hole downstream of the structures extended to either bank, therefore threatening bank stability immediately downstream of sill-type structures.

5.2 Scour Hole Dimensions

The depth and location of scour holes are important for (1) structure stability and (2) the secondary goal of aquatic habitat (see Figure 5-4). In the VSL-G channel, JHs met their stated goal of creating scour holes for aquatic habitat (Rosgen, 2006). RVs created smaller, less deep scour holes, and BWs created the smallest scour hole. All three sill-type structures resulted in a large, deep scour hole downstream of the structures that extended to the outer bank in VSL-G (Figures 5-5 and 5-6). Similar results were seen in the VSL-S channel. JHs fulfilled their intended purpose of creating a scour hole, RVs had smaller scour holes, and BWs created a relatively consistent channel geometry with indistinct scour holes in VSL-S. All three sill-type structures in the VSL-S channel created large scour holes; however, in the more sinuous VSL-S channel, the

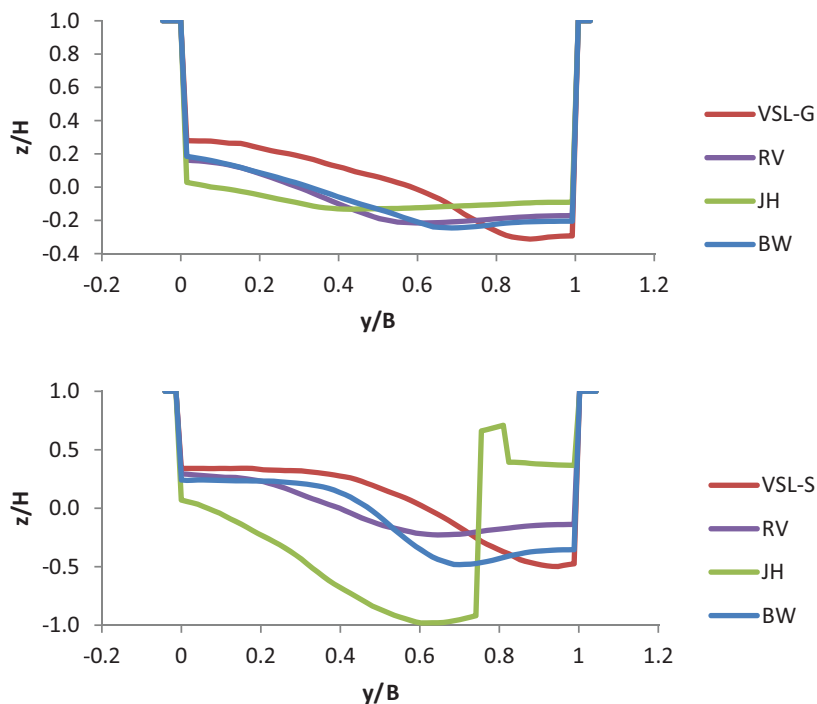


Figure 5-1. Cross-sectional profile just downstream of meander apex for VSL-G (top) and VSL-S (bottom) illustrating the shift of the channel thalweg with single-arm structures installed. Zero on the x-axis is at the inner bank.

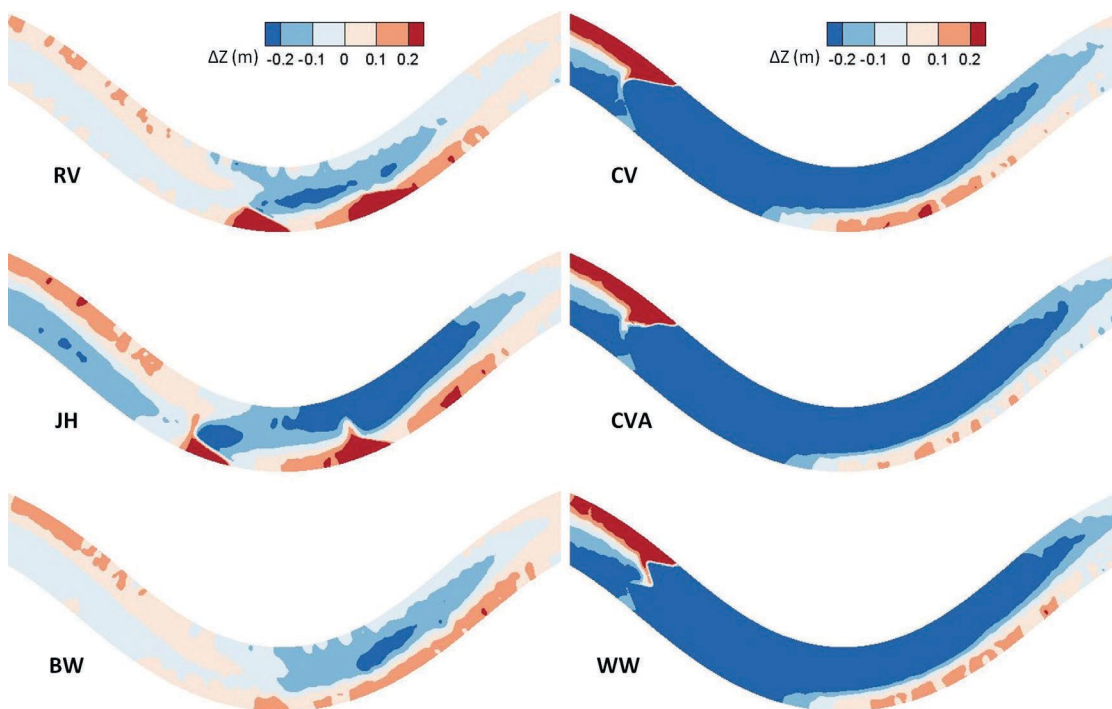


Figure 5-2. Comparison of bank protection for the final design layout for different structure types in VSL-G. The ΔZ represents the quasi-equilibrium bed topography of the baseline case (with no rock structure) subtracted from the quasi-equilibrium bed topography of the case with a rock structure. Flow is from left to right.

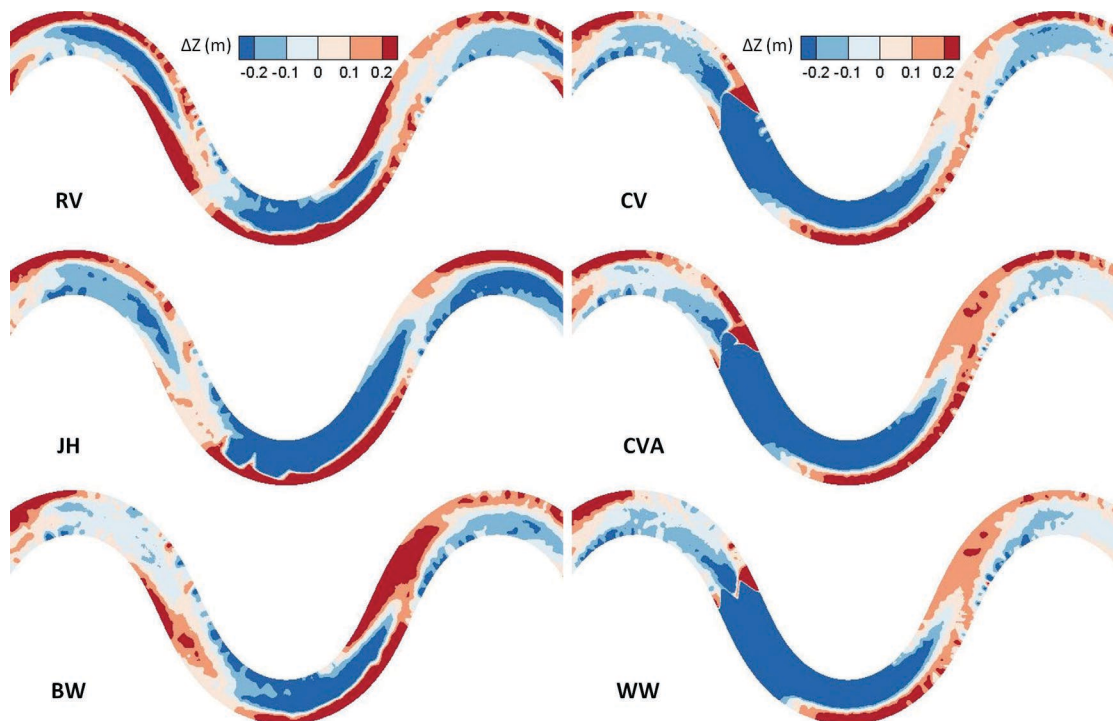


Figure 5-3. Comparison of bank protection for the final design layout for different structure types in VSL-S. The ΔZ represents the quasi-equilibrium bed topography of the baseline case (with no rock structure) subtracted from the quasi-equilibrium bed topography of the case with a rock structure. Flow is from left to right.

scour hole shape varied (See Figures 5-5 and 5-7). Standard CVs created the smallest scour hole, the addition of the step in the modified (A-shape) CVA created a wider scour hole, and the WW had the longest and widest scour hole. Deep scour holes adjacent to the structures are a cause for concern as one of the primary modes of failure of rock structures is the undermining and subsequent shifting of individual rocks.

5.3 Flanking Potential

Flanking was determined to be a major failure mechanism of in-stream flow control structures (see Appendix B for survey results and Appendix C for field case studies). Flanking is the circumvention of flow behind the structure. The risk of flanking was evaluated for each structure type by comparing the ratio of deposition upstream of each structure (compared to the average bed elevation) to flow depth (H) for each structure type. These ratios are shown in Table 5-1. BWs showed the least risk of flanking as there was little to no deposition upstream (Figure 5-8). JHs and sill structures had a moderate risk of flanking, with ratios in the range of 0.3 to 0.4, and RVs showed the greatest risk of flanking, with ratios ranging up to 0.8. Particular care should be used in keying in RV structures to ensure that the structures remain intact.

5.4 Hydrodynamic Forces on Rock Structures

In this section are presented calculated force distributions along the sill and single-arm rock structures for VSL-G and VSL-S. For all of the cases, the Reynolds numbers are over 10^6 , which implies that the major force over any immersed rock can be attributed to form drag, which is calculated using the following relationship (Raudkivi, 1967):

$$F = \frac{1}{2} \cdot C_d \cdot \rho \cdot A \cdot u^2$$

where F is the force on the rocks, ρ is density of water, A is the cross-sectional area of the single rock, u is the local velocity magnitude, and C_d is the drag coefficient. The drag force was calculated for the top row of rocks in each structure using the local velocity magnitude immediately upstream of the center mass of each rock. The rocks nearest the surface are subject to the highest flow velocities and are, therefore, the most likely to be dislodged by flow. For VSL-G and VSL-S with a Reynolds number over 10^6 , C_d is almost constant and roughly equal to 0.2 (Raudkivi, 1967). The calculated forces in this study were non-dimensionalized by the drag force due to the mean velocity in each channel, F_o , on a representative rock

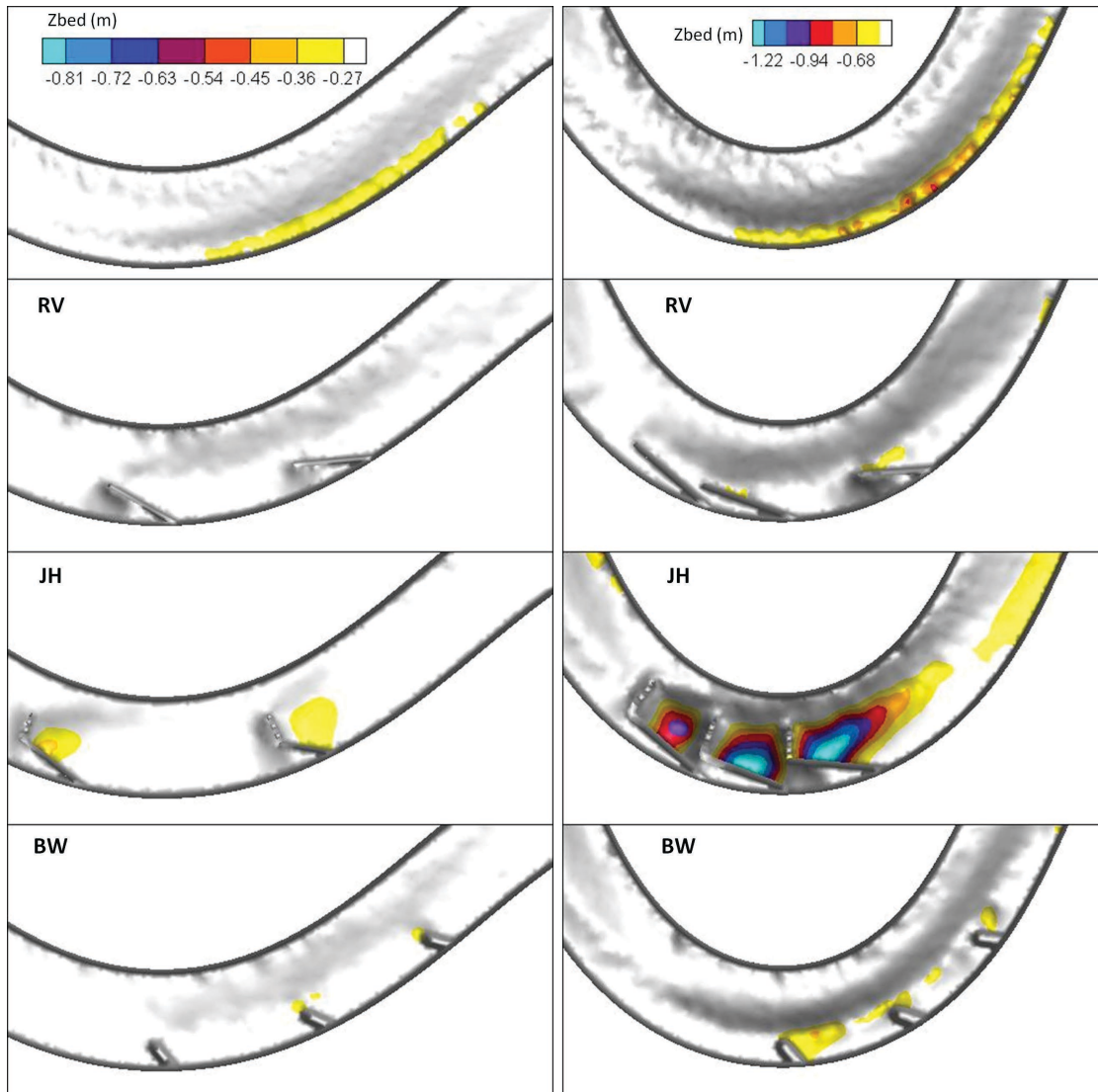


Figure 5-4. Comparison of scour holes for the final design layout for different single-arm structure types in VSL-G (left) and VSL-S (right).

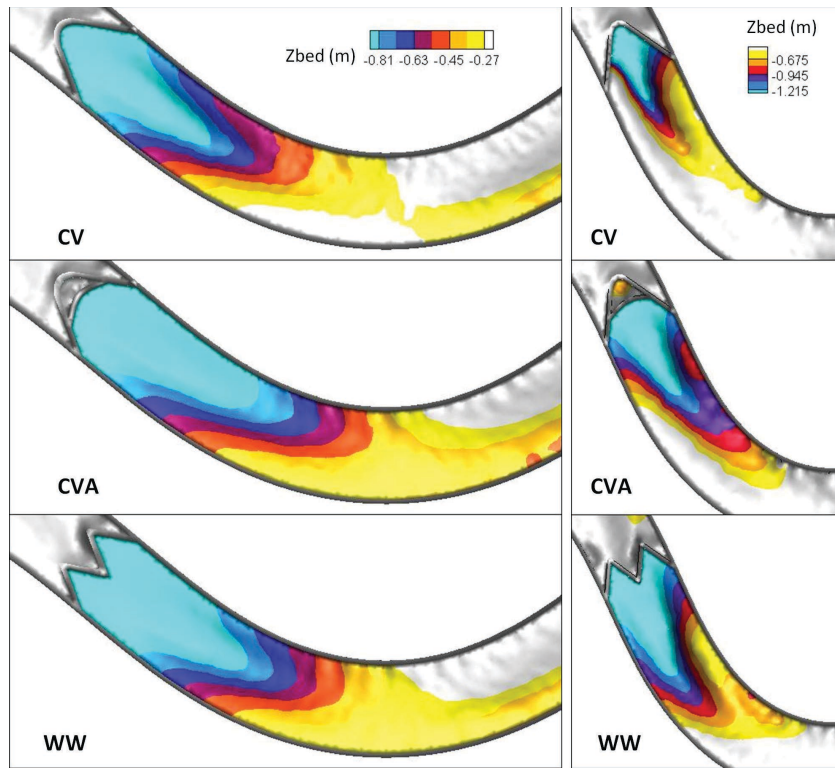


Figure 5-5. Comparison of scour holes for the final design layout for different sill structure types in VSL-G (left) and VSL-S (right).

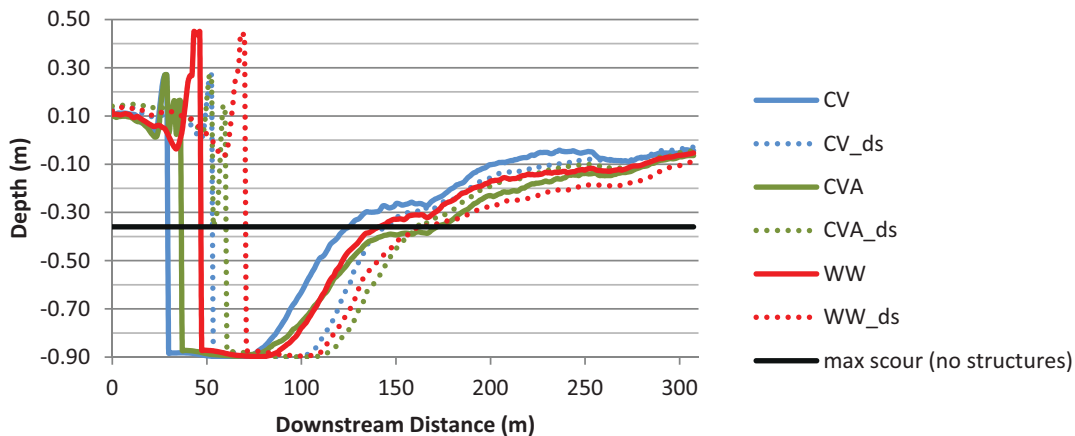


Figure 5-6. Depth distribution illustrating scour hole length along the channel centerline for sill structures in VSL-G. Solid black line represents the maximum depth in VSL-G with no structures.

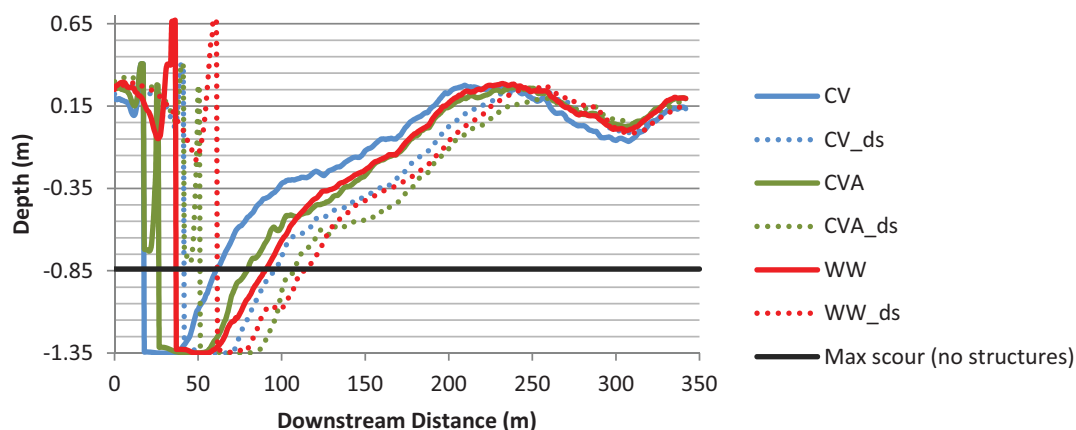


Figure 5-7. Depth distribution illustrating scour hole length along the channel centerline for sill structures in VSL-S. Solid black line represents the maximum depth in VSL-S with no structures.

Table 5-1. Relative susceptibility to flanking for in-stream flow control structures based on the ratio of deposition upstream of each structure to the flow depth (H).

Structure	Deposition/ (H)	Susceptibility to Flanking
RV	0.1-0.8	high
JH	0.3-0.4	medium
BW	0	low
Sill (CV, WW)	0.3	medium

size (D_{100}) for each structure (see Table 3-1 for rock sizes used in VSL3D simulations). The mean velocities for the bankfull flow condition were 1.33 m/s and 1.48 m/s for VSL-G and VSL-S, respectively. The representative area used to calculate F_p , using the force equation earlier in this paragraph, was defined as $A = \pi/4(D_{100})^2$. To calculate the force distribution along each rock structure, the 3-D flow data along the structure length were averaged to calculate the force distribution. The steady-state calculated hydrodynamic results (coincides with the quasi-equilibrium bed bathymetry) were employed to calculate the drag forces on rock structures.

Figures 5-9 and 5-10 show the non-dimensionalized force distribution along a single RV, JH, and BW located at the apex in VSL-G and VSL-S, respectively. The hydrodynamic forces over the rocks in the hook part of a JH structure are drastically bigger than the forces on the rocks in the vane portion of the JH structure or the forces on RV or BW structures (Figures 5-9 and 5-10). Because JHs are constructed with gaps between the rocks in the hook, the forces on these individual rocks will be critical to the structure's stability. Figures 5-9 and 5-10 also show that the rocks located near the RV tip bear most of the

hydrodynamic forces exerted by the turbulent flow. For the rocks in a BW, a roughly uniform distribution can be seen.

In Figures 5-11 and 5-12, the non-dimensionalized force distribution along the rock sill structures, including CV, CVA, and WW, are shown for VSL-G and VSL-S, respectively. The force distribution was calculated along single sill structures located at the downstream end of the straight reach with an angle of 30° (for all of the cases). In Figures 5-11 and 5-12, the force over the key rocks of CVA is significantly higher at the middle of the key (the dashed red line). The solid red line also shows that the force distribution of CVA has two peaks at the points linked to the key. The individual rocks that are located in the middle of the WW and U-shaped CV will experience slightly higher force magnitude than those along the bank (see green and blue lines in Figures 5-11 and 5-12).

5.5 Backwater and Water Surface Elevation Impacts

Since flow-training structures act as obstructions to flow and change the total channel roughness, it is expected that structures will affect the water surface elevation, particularly at flows at or near bankfull. For large floods, the impact of structures will diminish as they become a smaller portion of the total flow depth. The total effect on water surface will be dependent on relative submergence of structures as well as structure geometry and layout. Lower-profile structures, such as bendway weirs, have less influence on water surface elevation than sloping structures that reach the bankfull flow elevation such as rock vanes. This was demonstrated with two sets of simulations computing the turbulent flow and free-surface evolution over the quasi-equilibrium bed geometry in the VSL-S. The VSL3D water surface simulations were carried

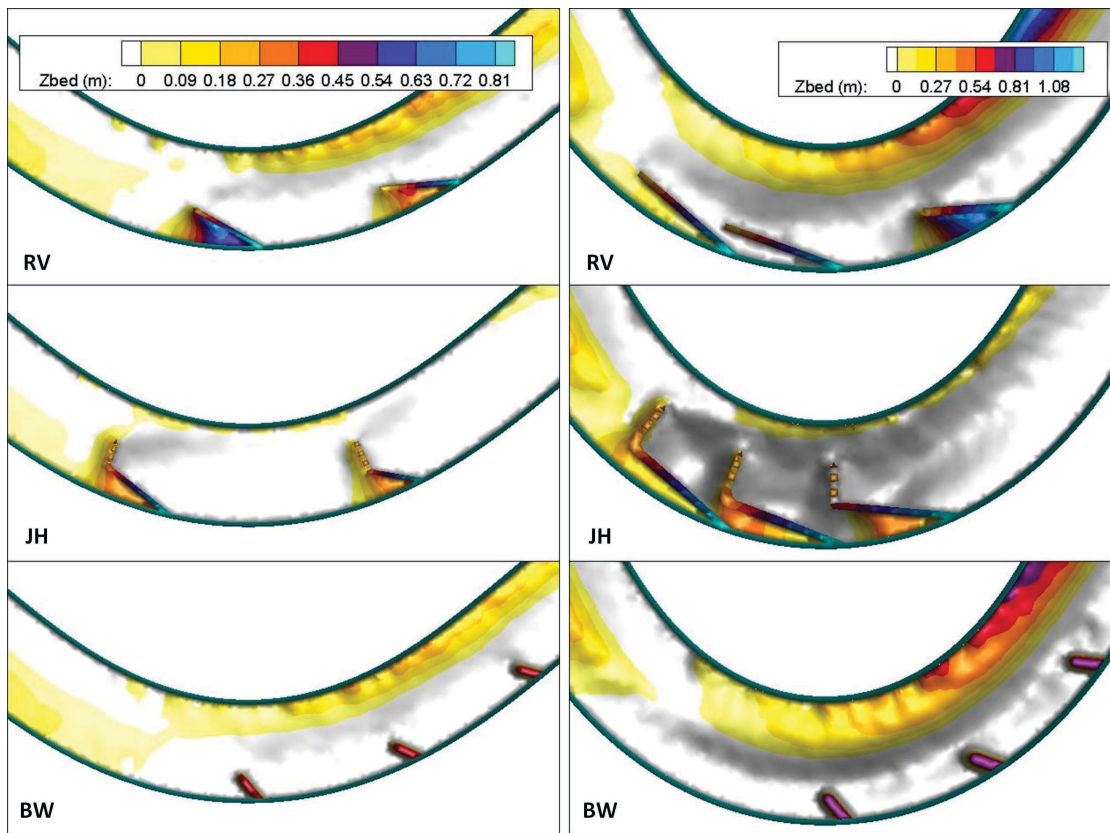


Figure 5-8. Deposition (relative to average bed elevation) upstream of single-arm structures demonstrating risk of flanking in VSL-G (left) and VSL-S (right).

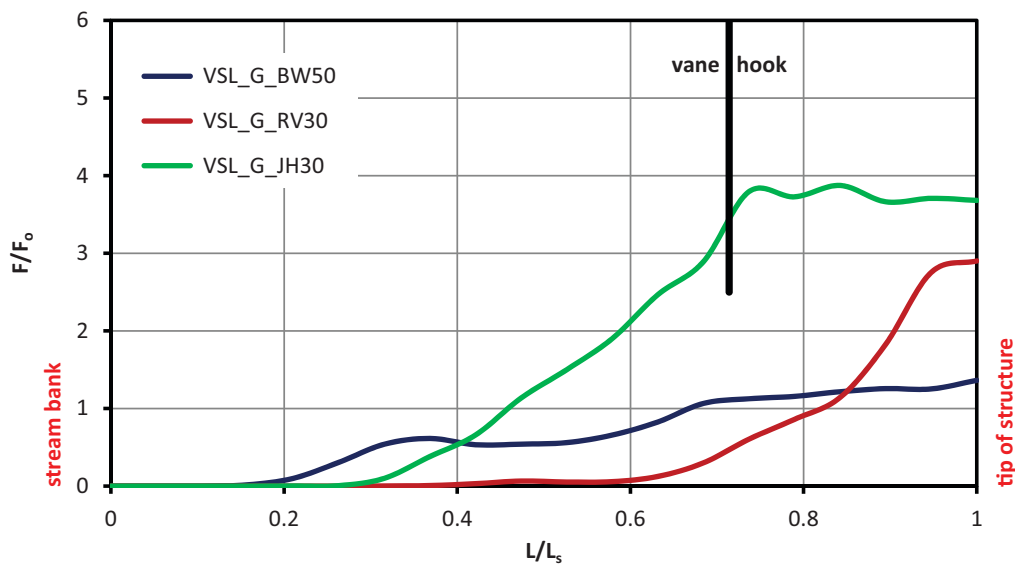


Figure 5-9. Steady-state force distribution over rocks along different structures in VSL-G. Forces are non-dimensionalized using the drag force on a single rock due to the mean flow velocity, F_0 . The vane and hook sections are the hook and vane parts associated with the J-hook vane. Distance, L , is non-dimensionalized by the total length of each structure, L_s .

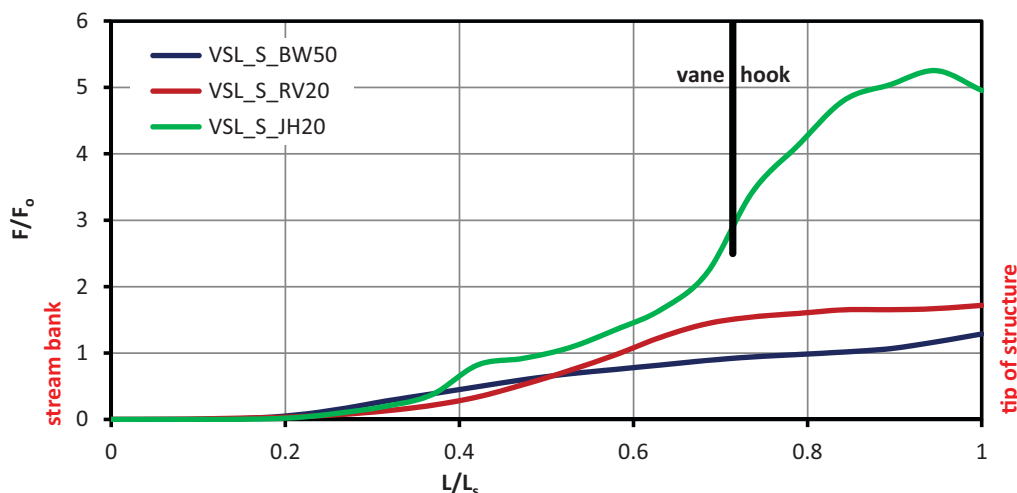


Figure 5-10. Steady-state force distribution over rocks along different structures in VSL-S. Forces are non-dimensionalized using the drag force on a single rock due to the mean flow velocity, F_0 . The vane and hook sections are the hook and vane parts associated with the J-hook vane. Distance, L , is non-dimensionalized by the total length of each structure, L_s .

out with three RVs and three BWs (Figures 5-13 and 5-14). RVs contributed to a maximum difference in water surface elevation of 7.4% (difference in water surface elevation between computed superelevation with structures and computed superelevation without structures divided by the mean flow depth). For BWs, the maximum water surface elevation difference was 5.9%.

A similar comparison was done between all single-arm structures using the OSL water surface measurements (for more information about OSL experiments, see Appendix D). Similar to the VSL-S results, the impact of structures on water surface elevation was local, with backwater just upstream of the structures and a decrease in water surface elevation just downstream of the structures (Figure 5-15).

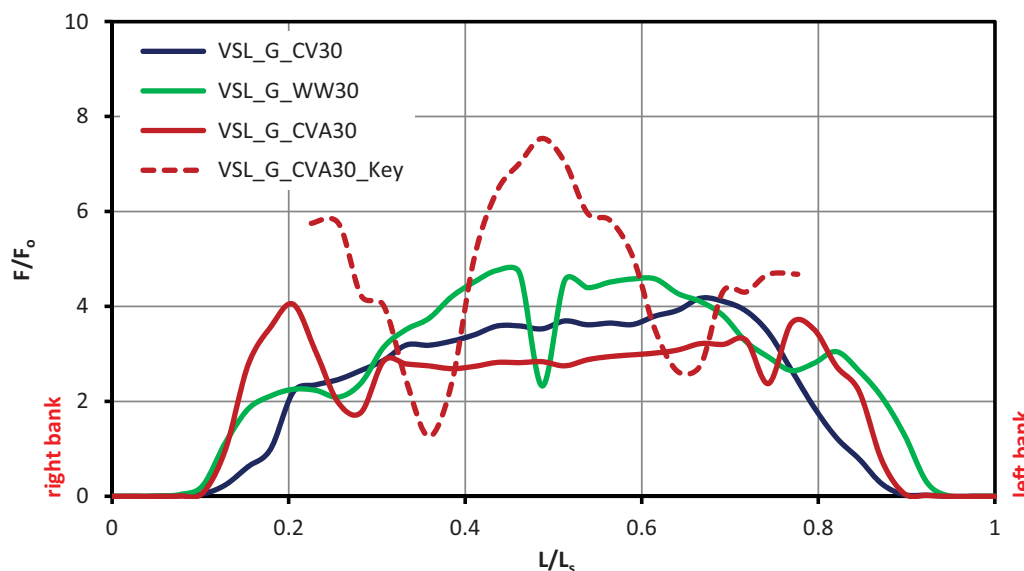


Figure 5-11. Steady-state force distribution over rocks along different structures including cross vanes and a W-weir in VSL-G. The dashed line is the key part of the A-shaped cross vane. Forces are non-dimensionalized using the drag force on a single rock due to the mean flow velocity, F_0 . Distance, L , is non-dimensionalized by the total length of each structure, L_s .

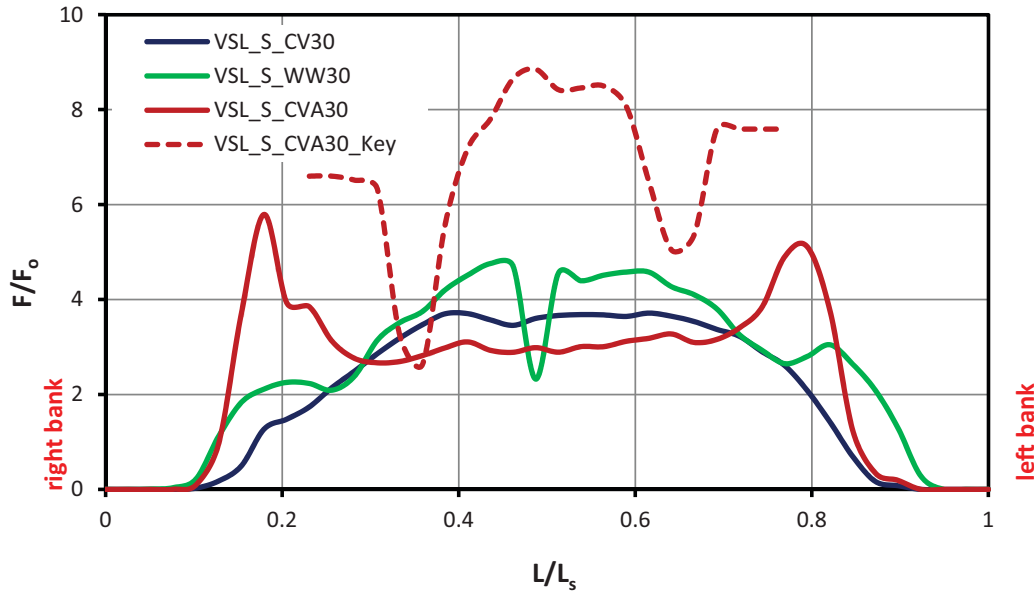


Figure 5-12. Steady-state force distribution over rocks along different structures including cross vanes and a W-weir in VSL-S. The dashed line is the key part of the A-shaped cross vane. Forces are non-dimensionalized using the drag force on a single rock due to the mean flow velocity, F_0 . Distance, L , is non-dimensionalized by the total length of each structure, L_s .

The maximum percent difference was calculated as the water surface with structures minus the baseline water surface normalized by the mean flow depth. Maximum differences were greatest for JHs (16%), then RVs (11%), and finally BWs (5%). While the influence of single-arm structures on water surface elevation is local, for channel-spanning sill

structures such as CVs and WWs, the influence of structure configuration on water surface elevation is expected to be significant and highly dependent on the sill elevation. For more information on the relationships between stage-discharge relationships and sill structure configuration, see Thornton et al. (2011).

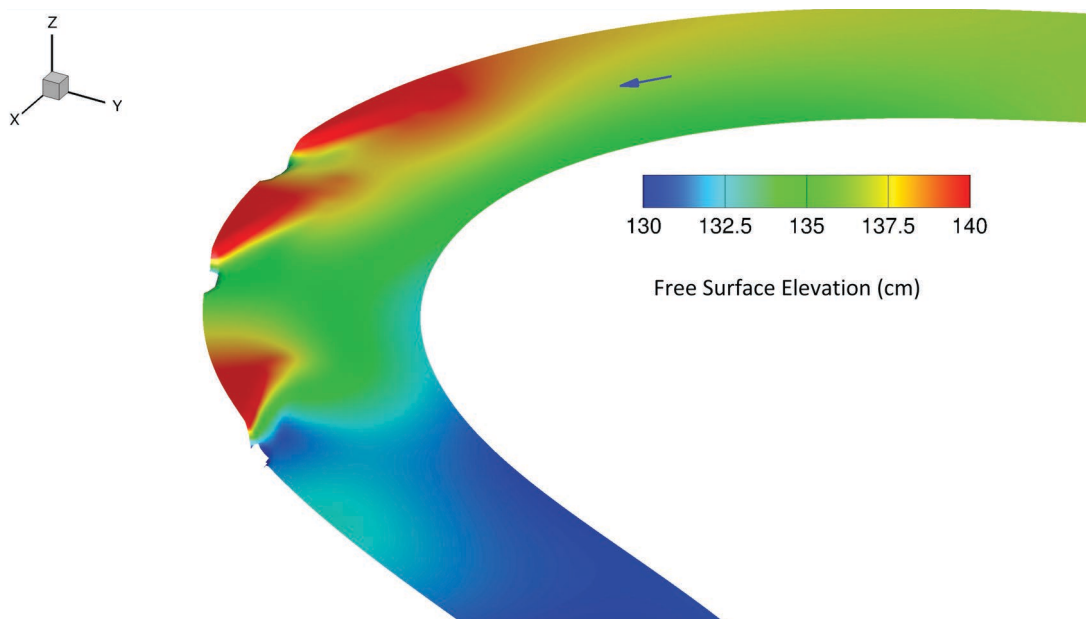


Figure 5-13. Simulation results of water surface elevation for three RVs in VSL-S. Flow direction is from top to bottom. The red zones show the backwater upstream of each rock vane structure.

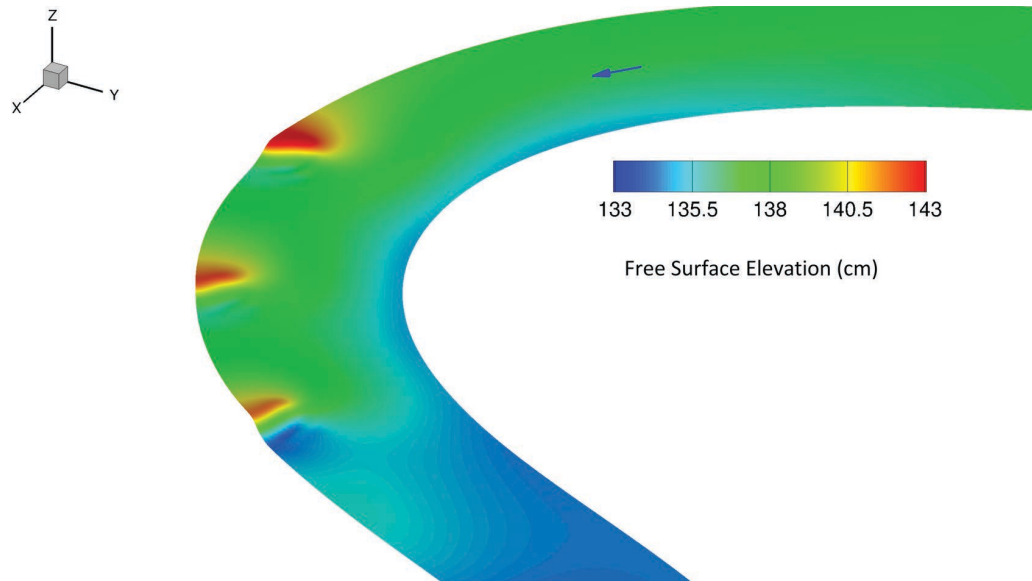


Figure 5-14. Simulation results of water surface elevation for three bendway weirs in VSL-S. Flow direction is from top to bottom. The red zones show the backwater upstream of each bendway weir structure.

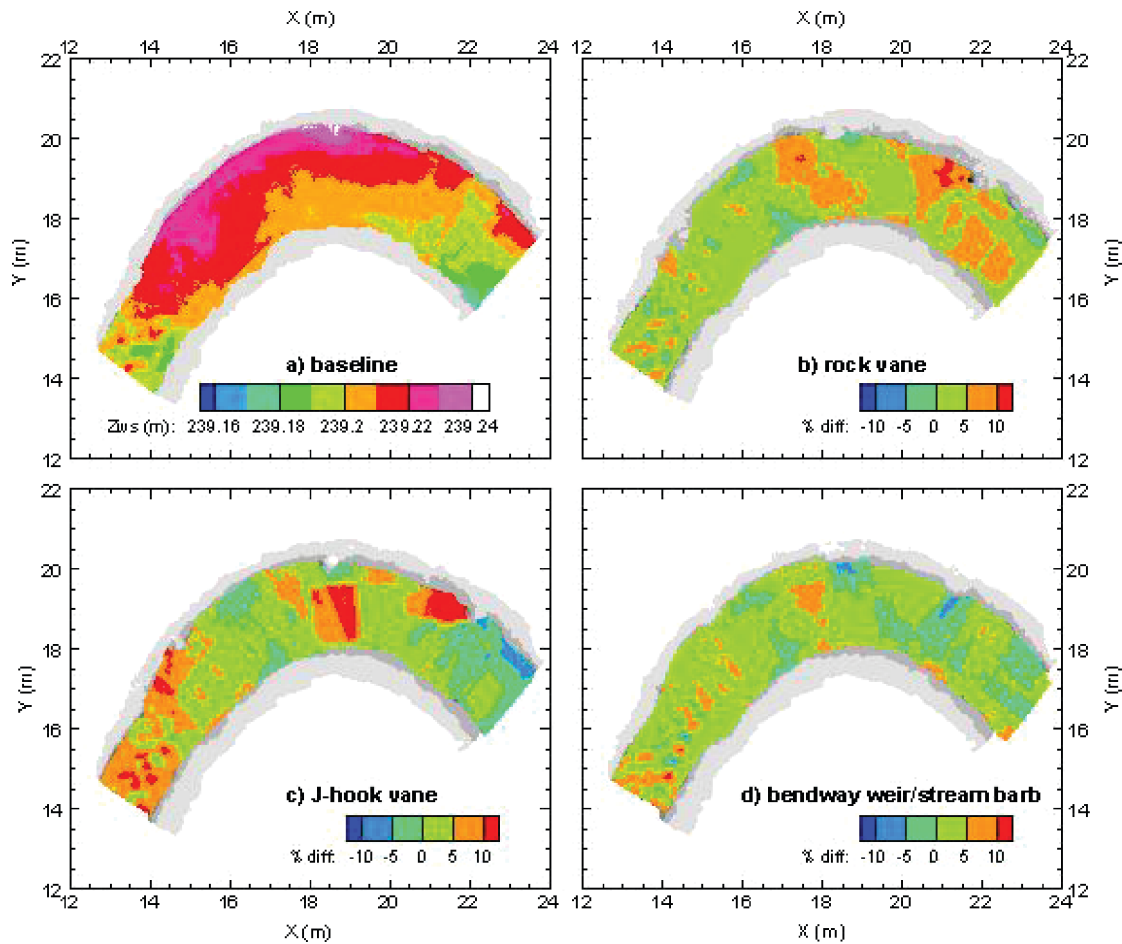


Figure 5-15. Water surface elevation for (a) baseline and percent difference in water surface elevation (normalized by average depth), (b) three RVs, (c) three JH vanes, and (d) three bendway weirs in the OSL.

CHAPTER 6

Evaluation of Current Guidelines

6.1 Length of Bank Protection in Meandering Channels

In meandering channels, the length of bank protection can be determined for approximately sinusoidal channels by determining the tangent points to the meander (Figure 6-1) and identifying a point approximately one channel width (B) upstream and $1.5B$ downstream from these points, as presented in HEC 23 (Lagasse et al., 2009). Both the OSL and VSL3D meandering channel results confirm the guidance for the length of bank that needs to be protected in meandering channels, as shown in Figure 6-1 (Lagasse et al., 2009). All three channels that have been studied herein fall within the radius of curvature to width ratio, R_c/B , range of 2 to 3. This is expected to be the range of ratios at which meander migration is fastest (Johnson et al., 2002b).

6.2 Spacing and Number of Structures

Based on the results of the VSL3D numerical simulations, an interactive method is suggested to determine the optimum structure layout for in-stream flow control structures similar to the methodology presented in NRCS (2007) for BWs. This spacing methodology was based on a detailed analysis of the shear layer reattachment in a meandering channel. These results were compared to guidelines for spacing based on the equations in Rosgen (2006) (Figure 6-2). Based on the Rosgen guidelines, as the ratio of radius of curvature to channel width increases, structure spacing (V_s) should increase. Based on the analysis described previously, the opposite was found, although there was not a channel with an R_c/B equal to 5, and VSL-S had a R_c/B below the threshold of sharp meanders of 3.0, where flow and shear stress distributions behave differently (Kashyap et al., 2012). For example, as the ratio of radius of curvature to channel width increased (R_c/B), the spac-

ing recommended by this study (V_s/B) increased, while the spacing recommended by Rosgen (2006) decreased. This indicates that understanding the flow paths around the site-specific channel meander configuration is essential to optimal placement of structure arrays. Also, as the angle of orientation increased, the spacing recommended in this study increased, while the spacing in the Rosgen (2006) guidelines decreased. For these reasons, a revised spacing methodology based on a vector analysis similar to that described in HEC 23 (Lagasse et al., 2009) for BWs and NRCS (2007) for stream barbs is suggested as an alternative to the spacing described for JH and RV structures in Rosgen (2006) and NRCS (2007).

Typical BW or stream barb spacing is described in HEC 23 (Lagasse et al., 2009) and NRCS (2007). Based on these guidelines, BW spacing should be between 4 and 10 times the effective length, Le , of the structure (ideally 4 to 5 times Le). Spacing can be calculated using the following equation.

$$V_s = 1.5Le \left(\frac{R_c}{B} \right)^{0.8} \left(\frac{Le}{B} \right)^{0.3}$$

And maximum spacing can be calculated by:

$$V_s = Rc \left(1 - \left(1 - \left(\frac{Le}{Rc} \right)^2 \right) \right)^{0.5}$$

These equations produce a spacing of 17.4 m and 12.2 m and a maximum spacing of 34 m and 27 m for VSL-G and VSL-S, respectively. Based on the structure optimization described previously, the average spacing in VSL-G was 45 m (6.7 times Le), and the average spacing in VSL-S was 34 m (5 times Le). The use of high-resolution numerical modeling determined an optimal structure spacing that was greater than the recommendations, thus reducing the number of structures and the cost. A vector analysis (e.g., NRCS, 2007) provides further guidance into BW structure spacing and

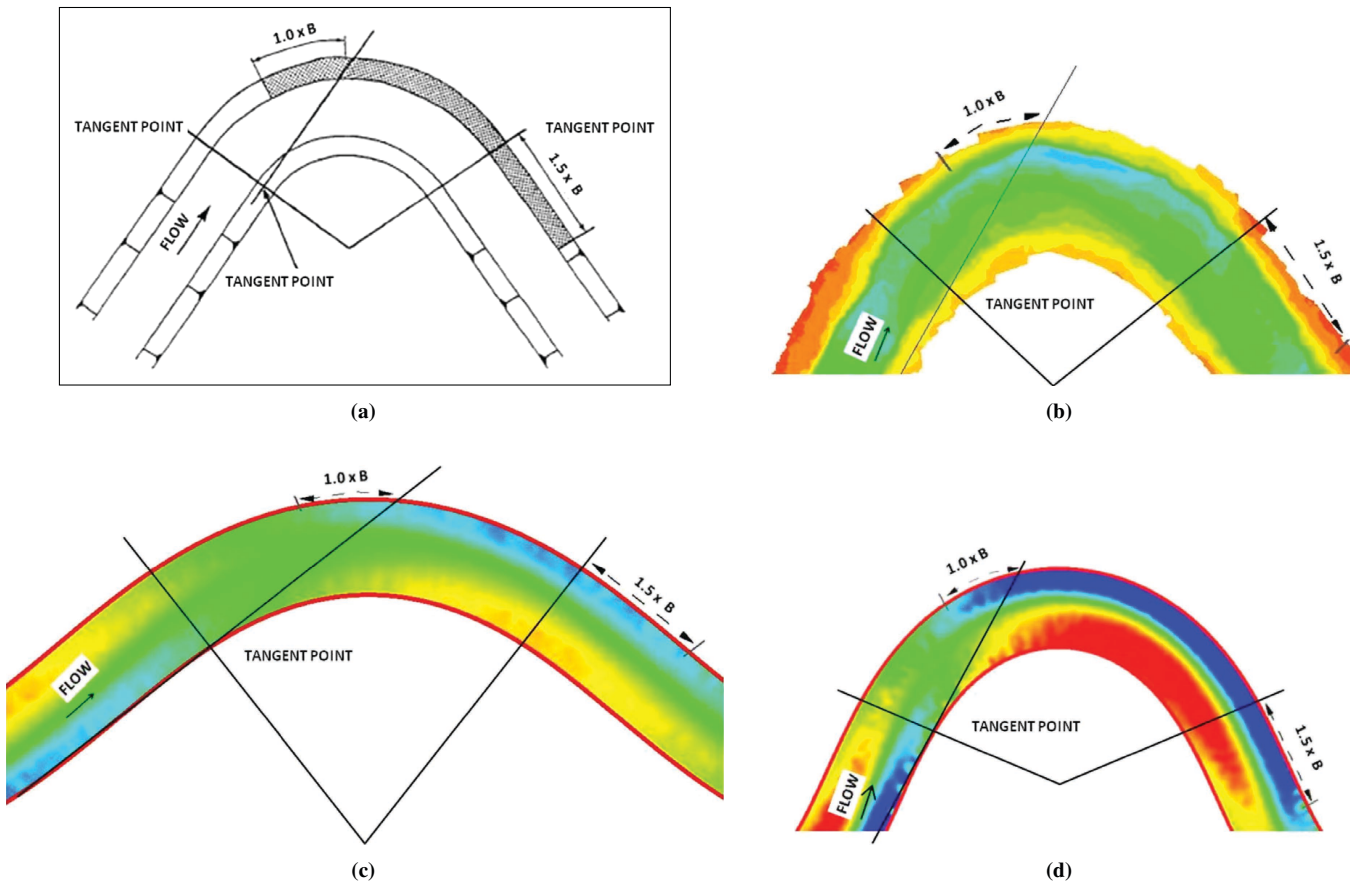


Figure 6-1. Extent of protection required at a channel bend for (a) general guidelines (from HEC 23, Lagasse et al., 2009). The extent of protection applied to (b) the OSL channel with no structures, (c) VSL-G, and (d) VSL-S. Contours show the bed elevations at quasi-equilibrium. Blue and red zones are associated with the regions of significant scour and deposition, respectively.

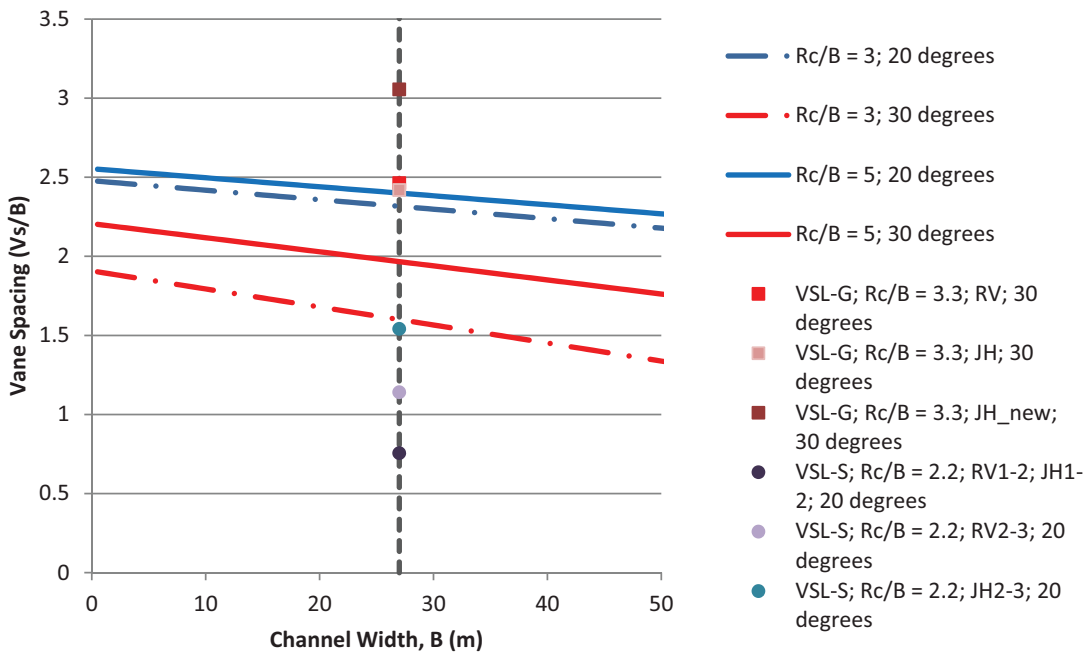


Figure 6-2. Structure spacing based on Rosgen (2006) guidelines and optimized spacing derived from the VSL3D described previously. Gray line indicates channel width of VSL-S and VSL-G.

location around a meander. In this type of analysis, lines are projected from the tip of the upstream structure to the bank to locate the second structure.

Based on the vector analysis commonly used for BWs, the following guidelines are suggested to determine the optimum structure layout for each single-arm structure array described in Chapter 3.

1. Project a line tangent to the bank at the meander apex. Set this line at 0° (horizontal).
2. Place the first structure at the apex. The angle of orientation should be such that it intercepts flow from upstream. This angle is dependent on the sinuosity and curvature of the meander where the structures are being installed (see Figure 6-3).
 - a. RVs and JHs: Greater angles protected more bank length in channels with a larger radius of curvature, and smaller angles protected more bank length in channels with a smaller radius of curvature.
 - b. Bendway weirs/stream barbs: An angle of 50° was determined to be the optimum between cost (length of structure) and length of bank protected.

3. Draw a horizontal line parallel to the first line from the tip of the structure. Draw another line with an offset angle from the parallel line. Where this line intersects the bank, the next structure should be located. The offset angle is a function of stream radius of curvature and channel width (see Chapter 3).

6.3 Footer Rock Depths

To inform the choice of footer rock depth, the maximum scour depth adjacent to each structure type was compared to the maximum scour depth, Sc_{MAX} , in the structure-free channel, as defined in Figure 6-4 as the difference between the maximum scour depth and the average depth across a cross-section. Sill-type structures had the greatest scour, followed by JHs (which perform as a partial sill), followed by RVs and BWs. Dividing the maximum scour in each structure case by Sc_{MAX} from the baseline case resulted in a ratio of 0.6 to 0.7 for RVs, 1.1 to 1.6 for JHs, and 0.8 to 0.9 for BWs. Multiplying these values by a factor of safety of 1.3 results in footer rock depth of 1 to 1.5 Sc_{MAX} , for RVs and BWs, 1.5 to 2 for JHs, and 2 to 3.5 for sill structures.

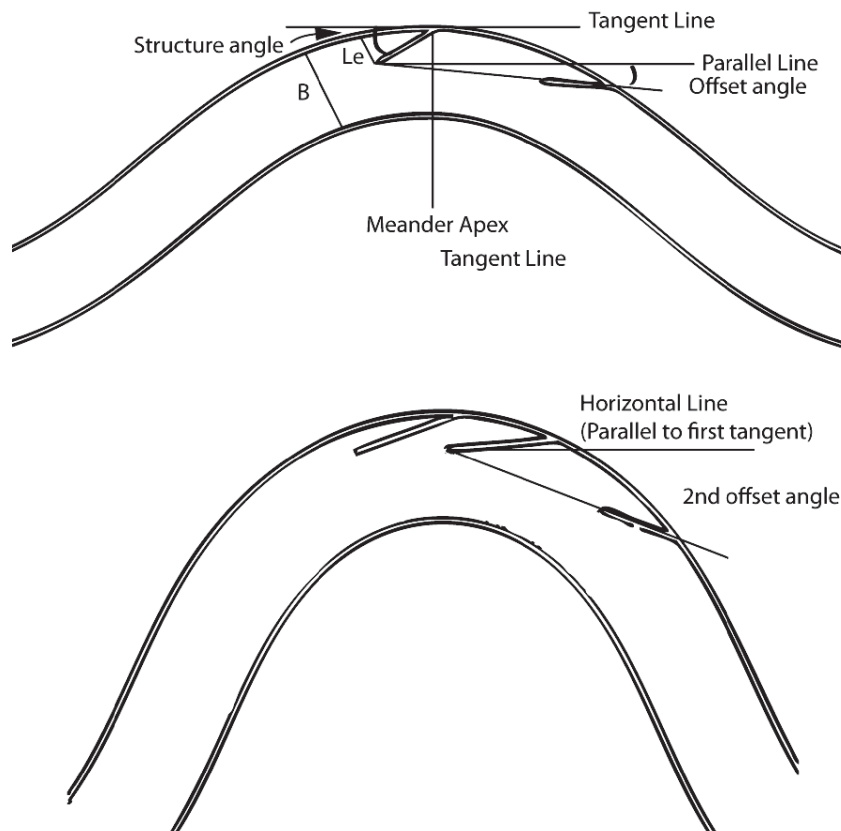


Figure 6-3. Example layout for first structure at apex and second (top) and third (bottom) structure in different meandering channels.

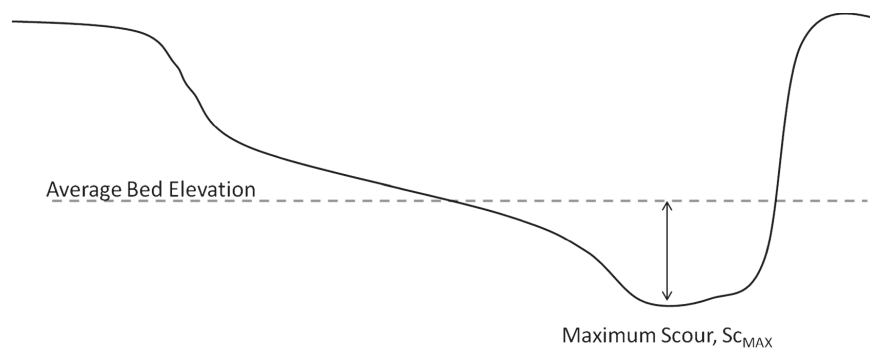


Figure 6-4. Sketch of definition of maximum scour depth, Sc_{MAX} . Dotted line is average bed elevation calculated from field data. Sc_{MAX} is the difference between the maximum scour depth and the average depth.

CHAPTER 7

Compilation of Experimental and Numerical Results to Develop Design Guidelines

What follows is a discussion on design considerations for in-stream structures, starting with current practice and expanding to include new design insights based on the results from the ISL, OSL, and VSL3D experiments. These results address three major components of structure installation: angle of orientation, location and spacing, and footer depth. The range of all stream characteristics (both physical and virtual) used in this project is detailed in Table 7-1. The recommendations in this report and the associated design guidelines are limited to sand and gravel streams and rivers (up to ~30 m in width) with low (2 to 3.3) R/B ratios or straight channels, although many of these guidelines can be applied with an appropriate evaluation of the baseline (pre-structure) hydraulics at the project site.

7.1 Rock Vanes/J-Hooks

Rock vanes direct the faster portion of the flow toward the center of the channel and create quiescent flow conditions near the bank (Johnson et al., 2002a). A series of vanes in the stream-wise direction is required to create a secondary flow cell, or secondary circulation, which creates scour at the middle of the channel while simultaneously backfilling the bank, effectively relocating erosive flow patterns induced by channel curvature (Johnson et al., 2001).

Other structures are slightly modified RVs, including JHs, CVs, and WWs. A JH consists of a RV with additional boulders placed at the tip of the vane in a hooking pattern with gaps between them. This layout creates scour by forcing the flow in the center of the channel to converge between the gaps. While this modification is primarily to create habitat, it also provides energy dissipation (Harman et al., 2001; Rosgen, 2001). The hook portion of the structure provides a longer, deeper, and wider scour pool than that created by a rock vane only (Rosgen, 2001).

RVs can reduce or eliminate the need for armor since high flows are redirected away from banks; additionally, they

compound the effectiveness of vegetative restoration techniques (McCullah and Gray, 2005). Vanes have previously been studied and used in other forms such as submerged (Iowa) vanes and BWs. Odgaard and Kennedy (1983), Odgaard and Spoljaric (1986), Odgaard and Mosconi (1987), and Odgaard and Wang (1991) provide many examples of laboratory work and some case studies associated with submerged vanes. Odgaard and Kennedy (1983) and Odgaard and Wang (1991) suggest that similar hydraulic principles are present in RVs as in submerged vanes and that for a large river with deeper pools they would be an attractive solution. However, Odgaard and Wang (1991) stress that their design guidelines are not valid for RVs.

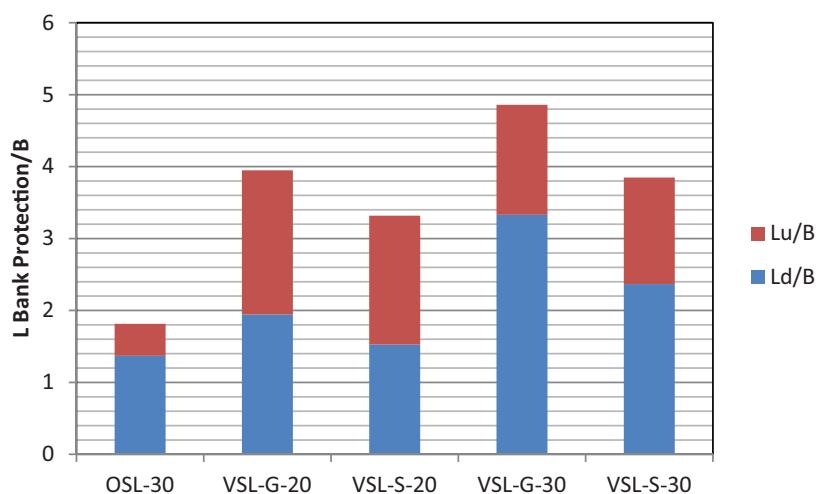
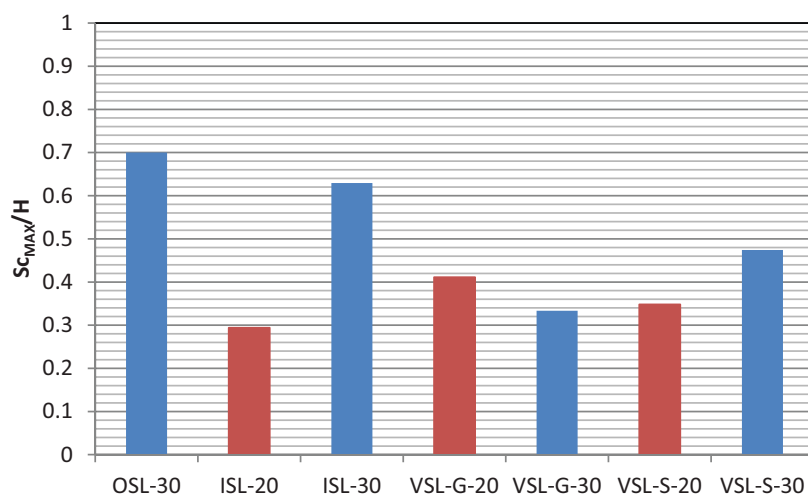
When the results from the ISL, OSL, and VSL3D experiments are combined, a number of trends emerge. First, as the angle of orientation increases, the ratio of protected bank to channel width (B) increases (Figure 7-1). Second, as the angle of orientation increases, the ratio of maximum scour depth to channel depth (H) also tends to increase in the straight and VSL-S channel (Figure 7-2). This was not the case, however, in the VSL-G channel. It should also be noted that for higher angles of orientation, the location of the maximum scour hole is at the structure tip in the vicinity of high bed fluctuations due to passing bed forms, indicating a high potential for structure failure if the footer rocks are not deep enough (see the Z_{rms} in Figures 3-7 and 3-8). For the 20° single RV case, there was no scour at the structure tip for VSL-S or VSL-G.

Straight Channel Recommendations

Velocity data from the ISL experiments (Appendix D) show that altered flow patterns and turbulence from the structures propagate far downstream of the structure location. A larger angle (30° instead of 20°) shifted the higher shear stresses farther away from the bank, thereby creating a longer region of low bank shear stress downstream of the structure along

Table 7-1. Summary of channel parameters for indoor (ISL), outdoor (OSL), and numerical (VSL3D) experiments.

	Depth	Width	Transport Mode	Aspect Ratio	Median Grain Size	Discharge	Bed Slope	Sinuosity	Wavelength	Radius of Curvature	R_c/B
	H	B		B/H	D_{50}	Q	S_0	p	λ	R_c	
	m	m			mm	L/s			m	m	
ISL-fixed	0.17	0.91	Fixed	5	6	36	0.0007	1	–	–	–
ISL-mobile	0.17	0.91	Clear water	5	2	55	0.0003	1	–	–	–
OSL	0.3	2.7	Live bed	9	0.7	280	0.0007	1.3	25	5.7	2.11
VSL-S	1.35	27	Live bed	20	0.5	48400	0.0007	1.5	266.7	57.6	2.13
VSL-G	0.9	27	Live bed	30	30	36000	0.003	1.15	328.1	89.1	3.30

**Figure 7-1. Angle of orientation of rock vanes compared to the ratio of downstream protected bank, L_d , and upstream protected bank, L_u , for OSL, VSL-G, and VSL-S with a single rock vane at the meander apex.****Figure 7-2. Ratio of maximum scour, Sc_{MAX} , to average channel depth, H , for a single rock vane installed in OSL, ISL, VSL-G, and VSL-S channels at 20° or 30°.**

the bank to which it is attached; however, larger angles (30° instead of 20°) produced greater scour depths, which could also create greater risk of structure undermining and failure. All RV angles provided net erosion within the zone one channel width downstream. These structures tended to result in net deposition in zones that were two or more channel widths downstream of their location.

In a straight channel, JHs produced 25% less scour than the RV alone. The J-hook produced a single deep scour hole just downstream of the hook portion of the vane that extended approximately two channel widths downstream of the structure. This scour hole was wider and longer than the scour hole produced for the 30° RV. The 30° JH moved the high shear zone further from the bank toward the center of the channel; however, the bank protection provided by each structure was similar. Based on the ISL straight channel experiments, the following recommendations are made for RV and JH installation in straight channels.

- Monitoring should be conducted well downstream of the structure (>5 channel widths) because the flow structure could initiate scour and erosion of the opposite bank.
- To protect the bank where structures are to be attached, a larger angle (30°) is recommended as it provides a greater length of bank protection.
- Structures should be installed two or more channel widths upstream of the infrastructure they are designed to protect.
- Larger footer rocks should be installed with greater angle of orientation.
- Footer rocks should be sized appropriately at positions of large scour depth and large hydrodynamic forces (e.g., at the structure tip).
- JHs are appropriate in projects where a larger area of scour hole is deemed beneficial to in-stream habitat.
- In low aspect ratio streams, the top slope of RV and JH structures may need to be adjusted to ensure that the structure slopes from the top of the bank to the channel bed.

Meandering Channel Recommendations

Observations from the OSL (Appendix D) and VSL3D (Chapter 3) meandering channel experiments indicated that RVs were successful at protecting a portion of the outer bank from erosive effects due to the 3-D helical flow in meander bends. A single RV structure was not able to protect the entire bank due to the extension of the shear layer from the tip of the RV. With multiple RV structures, the scour hole at the tip of the downstream RV can be significant. RVs downstream of the apex experienced significant scour around the tip of the structure, while RVs installed upstream of the apex experienced very little scour but were subject to deposition. Conversely, the most upstream RV structure was the most likely

to experience excessive deposition and consequential flanking. RVs were successful at moving the high-velocity core away from the outer bank; however, in the OSL experiments, significant local scour was experienced at the downstream RV. RVs placed at the apex of the meander and downstream effectively moved the region of high shear stress away from the outer bank.

In meandering channels, the installation of JHs resulted in both deeper and larger scour holes. JHs were successful at moving the high-velocity core from the outer banks, but in some structure scenarios, threatened the stability of the inner bank. JHs protected a longer zone of the outer bank, but this was not consistent since all VSL3D cases exhibited scour adjacent to the outer bank just downstream of the structure and before the protected area of bank. Based on the OSL and VSL3D experiments, the following recommendations are made for JH and RV structure installation in meandering channels.

- When used for meander bend protection, RVs and JHs should be installed in series of at least two structures to protect the entire region of the outer bank subject to scour.
- Footer rocks should be sized appropriately at positions of large scour depth and large hydrodynamic forces (e.g., at the structure tip).
- For RVs, the structure array should begin at the meander apex in less sinuous channels, but for channels with low radius of curvature to channel width, RV and J-hook arrays should be shifted upstream so that the first structure is located approximately one channel width upstream of the apex. For JHs, structure arrays should be shifted upstream by one channel width.
- In highly sinuous channels, RV spacing should be decreased. A vector analysis with an appropriate offset angle is suggested for determining structure spacing.
- JHs are appropriate in projects where a larger area of scour hole is deemed beneficial to in-stream habitat.
- RVs and JHs pose a high risk of flanking due to deposition upstream of the structure. Bank keys are required to mitigate the risk of flanking, and monitoring should evaluate the sediment deposition upstream of each structure.

7.2 Bendway Weirs/Stream Barbs

Stream barbs and BWs interrupt the helical flow patterns of secondary currents typically associated with channel meanders. The presence of these in-stream structures relocates the erosive flow patterns from the vulnerable outer bank toward the center of the channel (Derrick, 1998). Stream barbs specifically protect the bank by disrupting velocity gradients in near-bed regions, deflecting currents away from the bank

by forcing flow perpendicularly over the weir and shifting the channel thalweg to the stream-wise end of the barbs (Matsuura and Townsend, 2004).

An effective series of barbs will induce a subcritical zone of backwater, which should reach the next upstream barb. This upstream progression of subcritical reaches controls erosion and eventually leads to sediment deposition in the near-bank region (NRCS, 2013). Bendway weirs are primarily used along meanders in larger rivers and tend to work best in high-flow, high-energy conditions but have been observed to function effectively in low-flow events (Derrick, 1998; Abad et al., 2008).

When the results from the ISL and OSL (Appendix D) and VSL3D (Chapter 3) experiments are combined, BWs, which are submerged at most flows, behaved fundamentally differently than RVs. First, as the angle of orientation increases, the ratio of protected bank to channel width (B) decreases. For BWs in VSL-G and VSL-S, smaller angles resulted in greater bank protection, with one exception for the 60° structure in VSL-S. The scour depth was independent of the angle of orientation; however, scour depth in the vicinity of the structure decreased as aspect ratio increased (Figure 7-3).

Straight Channel Recommendations

Velocity data from the ISL experiments show that altered flow patterns and turbulence from the structures propagate far downstream of the structure location. As the angle of orientation increased, the scour depth and scour hole dimensions decreased, with no visible difference in bank protection. In all cases, scour around the structure extended to the upstream side of the structure tip, eventually exposing the footer rocks.

Based on the ISL straight channel experiments, the following recommendations are made for BW structure installation in straight channels.

- Monitoring well downstream (>5 channel widths) of the structure is important because the flow structure could still initiate scour and erosion of the opposite bank.
- In straight channels, a BW with an angle of orientation of 80° will provide bank protection for less material cost because of the shorter structure length.
- Bendway weirs are not recommended in low aspect ratio streams. If they are installed in low aspect ratio (<6) streams, footer rock depths need to be increased since significant scour is expected near the structure.

Meandering Channel Recommendations

Use of a single BW structure at the apex of an outer bend can protect a portion of the outer bank from erosive effect, although, to fully protect an eroding meander, multiple structures will be required. With multiple BW structures, the scour hole at the tip of the downstream structure can be significant. Similar to RVs, BWs downstream of the apex experienced significant scour around the tip of the structure, while BWs installed upstream experienced very little scour but were subjected to deposition. In the OSL experiments, less local scour was experienced at the lower BW than at the lower RV. Scour depth at the BW tip was found to be correlated to channel aspect ratio. Larger aspect ratios had less scour. The practitioner survey indicated that the single reported unsuccessful BW project was in a low aspect ratio channel, although this was true of all rock structures considered (Radspinner et al., 2010). Based on the OSL and VSL3D experiments, the following

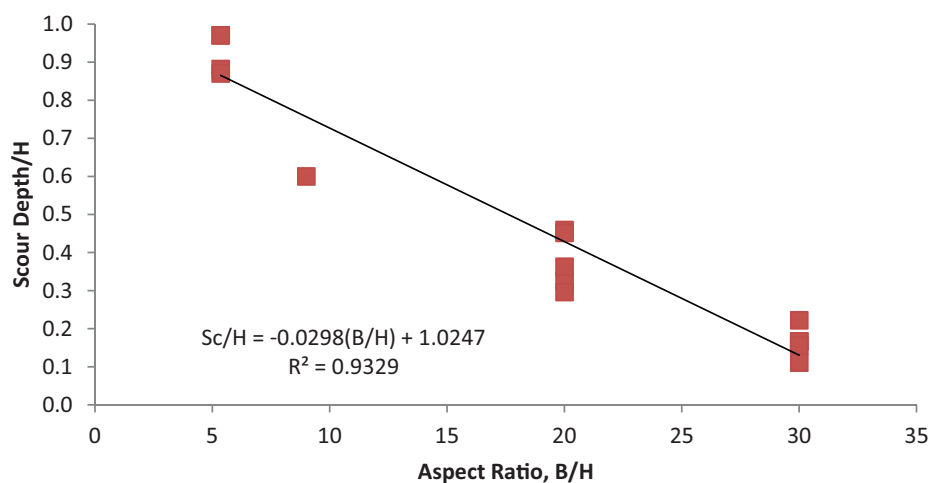


Figure 7-3. Scour depth in the vicinity of BWs normalized by channel depth (H) as a function of aspect ratio (B/H). All results from ISL, OSL, and VSL3D experiments have been superimposed.

recommendations are made for BW structure installation in meandering channels.

- To provide bank protection for a full meander bend, at least three BWs should be used.
- Footer rock depth should be similar to RVs.
- Bendway weirs are less susceptible to flanking from over-bank flows, but structure layout should be such that the bank between and above structures should be protected at high flows.
- Bendway weirs are not recommended in low aspect ratio streams. If they are installed in low aspect ratio (<6) streams, footer rock depths need to be increased since significant scour is expected near the structure.

7.3 Sill Structures (Cross Vanes/W-Weirs)

CVs and WWs are variations of the RV but have a primary function as grade-control structures while still providing a reduction in near-bank shear stress. The structure raises or maintains the bed elevation, so it is normally installed within a section of little or no turbulence for larger streams or at the head of a riffle for smaller streams (Doll et al., 2003). CVs are constructed by connecting the tips of two RVs from opposite banks with rocks arranged perpendicular to the flow. The CV is expected to create a variety of habitat in the channel by increasing flow diversity and substrate complexity (McCullah and Gray, 2005). The vane sections raise the water level in the near-bank area, providing more cover, the scour pool allows a holding area in high- and low-flow periods, flow separation zones become feeding lines, and the downstream end of the scour pool is ideal for spawning beds. Like CVs, the WW is primarily a grade-control structure that facilitates scour pool habitat. WWs are normally only used in larger rivers since they are relatively large structures. The layout of this structure is a “W” shape looking downstream. This arrangement creates dual thalwegs and, therefore, can lead to more flow diversity.

Cross vanes were tested in the ISL and OSL (Appendix D) and VSL (Chapter 3). Because they were installed in straight or crossover reaches in each channel, the recommendations are not divided between meandering and straight channels. Two configurations of cross vanes, a standard U-shaped CV, and an A-shaped CVA, were evaluated. The deepest scour was within the structure for the U-shaped CV, and immediately downstream of the cross piece of the CVA structure.

WWs were tested in the ISL and VSL. WWs were not installed in the OSL because the channel was too small. Because WWs were installed in straight or crossover reaches in each channel, the recommendations are not divided between meandering and straight channels. The deepest scour was within the structure and immediately downstream. At the early stages

of scour, WWs provide some protection from scour downstream of the middle point of the W; however, as the system progresses, this region also scours to a single large scour hole downstream. The results of the physical and numerical experiments led to the following recommendations for CVs and WWs.

- For bank protection, an angle of orientation of 30° should be used instead of 20°.
- A stepped CVA should be used to provide additional protection for the upstream rocks; however, an A-shaped structure poses a greater risk to the stability of banks immediately downstream and should not be used if bank protection is the project goal.
- Monitoring should be focused within and immediately downstream of a CV or CVA (within one channel width) for structure and bank stability. All sill structures showed a risk to the banks in the vicinity of the scour hole in this region.
- Sill structures should be installed a minimum of two channel widths upstream of bridge piers or other infrastructure to be protected. For CVAs, this should be extended to 2.5 to 3 channel widths. An alternative would be to install structures in series to minimize the dimensions of the scour hole immediately downstream of a CV.
- WWs will provide short-term scour protection mid-channel but should not be used for long-term scour protection for bridge piers and other structures installed in the middle of the river channel.
- Sill structures were successful at creating large scour pools downstream of each structure; however, if the project goal includes fish habitat, sill structures need to be evaluated to ensure that the drop height created by the structure does not create a fish passage barrier.
- Sill-type structures created a moderate risk of flanking due to deposition upstream of the structure. This area needs to be monitored to minimize flanking risk.
- Undermining of the structure is expected to be the primary failure mechanism due to the growth of the large scour pool; footer structures should be 2 to 3 times deeper than the maximum scour present in the structure-free channel.

7.4 Structure Selection

Following the detailed evaluation of experimental and numerical results described previously for five structure types (with an additional CV modification, CVA), Table 7-2 compiles these recommendations on structure selection based on site characteristics and project goals. This is a modification of the summary tables presented in the MWCG (Maryland Department of the Environment, 2000).

Table 7-2. Recommendations for in-stream flow control structure selection based on site characteristics and project goals.

	Site Characteristics				Project Goals				
	Steep Streams	Low Aspect Ratio (Low B/H)	Tight Meanders (Low R_c/B)	Fine Bed Material (Sand)	Protect Bank Toe	Redirect Flow (Central Thalweg)	Scour Pool Habitat	Minimize Lateral Channel Adjustments	Grade Control
RV	o	o	o	o	o	o	-	o	-
JH	o	o	o	o	o	o	+	o	o
BW	-	-	-	o	+	+	-	+	-
CV	+	o	o	o	-	o	+	-	+
CVA	+	-	o	-	-	o	+	-	+
WW	+	-	o	-	-	o	+	-	+

- Not appropriate

o Moderately appropriate with design modifications

+ Well suited

Three major categories of structure failure mechanism were identified: flanking (circumvention combined with aggradation), local scour (which can lead to rock displacement), and rock displacement (based on hydrodynamic forces, not local scour). The practitioner survey also reported winnowing (or scour between rocks) as a significant failure mode. This failure mechanism was not evaluated in NCHRP Project 24-33. Table 7-3 compiles the evaluation of the susceptibility to these failure mechanisms for each structure type. Recommendations based on the systematic use of VSL3D to evaluate a range of structure types in typical sand and gravel channels were used to develop updated design guidelines, which are presented in Appendix F. These recommendations are specific to non-cohesive sand or gravel channels with subcritical flow and relatively immobile banks compared to the bed sediment. Structure performance was evaluated at bankfull flow conditions for channels in the ranges of aspect ratio 5 to 30, sinuosity 1 to 1.5, slope 10^{-4} to 10^{-3} , and grain size 0.5 to 30 mm. Each project should be evaluated based on site-specific characteristics.

Table 7-3. Evaluation of susceptibility to failure for in-stream flow control structures.

	Susceptibility to Failure Mechanism		
	Local Scour	Flanking	Rock Displacement
RV	o	+	o
JH	+	o	+
BW	+	-	-
CV	+	o	o
CVA	+	o	+
WW	+	o	+

- Low risk

o Moderate risk

+ High risk

See Section 5.2 for discussion on local scour.

See Section 5.3 for discussion of flanking.

See Section 5.4 for discussion of force distribution.

References

- Abad, J. D., Rhoads, B. L., Guneralp, I., and Garcia, M. H. (2008). "Flow Structure at Different Stages in a Meander-Bend with Bendway Weirs." *J. Hydraul. Eng.*, 134 (8), 1052–1063.
- Army Corps of Engineers (1991). *Engineering and Design-Hydraulic Design of Flood Control Channels*. EM-1110-2-1601. Washington, D.C.
- Bernhardt, E. S., Palmer, M. A., Allan, J. D., Alexander, G., Barnas, K., Brooks, S., Carr, J., Clayton, S., Dahm, C., Follstad-Shah, J., Galat, D., Gloss, S., Goodwin, P., Hart, D., Hassett, B., Jenkinson, R., Katz, S., Kondolf, G. M., Lake, P. S., Lave, R., Meyer, J. L., O'Donnell, T. K., Pagano, L., Powell, B., and Sudduth, E. (2005). "Synthesizing U.S. River Restoration Efforts." *Science*, 308, 636–637.
- Bhuiyan, F., Hey, R. D., and Wormleaton, P. R. (2010). "Bank-Attached Vanes for Erosion Control and Restoration of River Meanders." *Journal of Hydraulic Engineering*, 136(9), 583–596.
- Brown, K. (2000). *Urban Stream Restoration Practices: An Initial Assessment*. U.S. Environmental Protection Agency, Office of Wetlands, Oceans, and Watersheds, Region V. Ellicott City, MD.
- Chang, H. H. (1988). *Fluvial Processes in River Engineering*. John Wiley & Sons, New York, NY.
- Derrick, D. L. (1998). "Four Years Later, Harland Creek Bendway Weir/Willow Post Bank Stabilization Demonstration Project." *Proc.*, 1998 Int. Water Resources Engineering Conf., ASCE, Memphis, TN.
- Dietrich, W. E. (1987). *Mechanics of Flow and Sediment Transport in River Bends*. In: *River Channels: Environment and Process*, K. S. Richards (ed.), Institute of British Geographers Special Publication No. 18, Basil Blackwell, Inc., pp. 179–227.
- Doll, B. A., Grabow, G. L., Hall, K. L., Halley, J., Harman, W. A., Jennings, G. D., and Wise, D. E. (2003). *Stream Restoration: A Natural Channel Design Handbook*. NC State University, Raleigh, NC.
- Ettema, R., Muste, M. (2004). "Scale Effects in Flume Experiments on Flow Around a Spur Dike in a Flatbed Channel." *J. Hydr. Engrg.*, 130(7), pp. 635–646.
- Evans, J. L., and Kinney, W. (2000). "Bendway Weirs and Rock Stream Barbs for Stream Bank Stabilization in Illinois." Technical Presentation for 2000 ASABE Int. Meeting, ASABE.
- Fox, J. F., Papanicolaou, A. N., Hobbs, B., Kramer, C., and Kjos, L. (2005). "Fluid Sediment Dynamics Around a Barb: An Experimental Case Study of a Hydraulic Structure for the Pacific Northwest." NRC Research Press website, <http://cjce.nrc.ca> (May 29, 2008).
- Harman, W. A., Jennings, G. D., Tweedy, K. R., Buck, J. A., Taylor, D. L. (2001). "Lessons Learned from Designing and Constructing In-stream Structures." *Proc.*, *Wetland Engineering and River Restoration Conf.* CD-ROM, ASCE, Reston, VA.
- Johnson, P. A., Hey, R. D., Brown, E. R., and Rosgen, D. L. (2002a). "Stream Restoration in the Vicinity of Bridges." *J. Am. Water Resour. Assoc.*, 38(1), 55–67.
- Johnson, P. A., Tereska, R. L., and Brown, E. R. (2002b). "Using Technical Adaptive Management to Improve Design Guidelines for Urban Instream Structures." *J. Am. Water Resour. Assoc.*, 38(4), 1143–1152.
- Johnson, P. A., Hey, R. D., Tessier, M., and Rosgen, D. L. (2001). "Use of Vanes for Control of Scour at Vertical Wall Abutments." *Journal of Hydraulic Engineering*, 127(9), 772–778.
- Kang, S., Lightbody, A., Hill, C., and Sotiropoulos, F. (2010). "High-Resolution Numerical Simulation of Turbulence in Natural Waterways." *Adv. Water Resources*, 34, 98–113.
- Kang, S., and Sotiropoulos, F. (2011). "Flow Phenomena and Mechanisms in a Field-Scale Experimental Meandering Channel with a Pool-Riffle Sequence: Insights Gained via Numerical Simulation." *J. Geophys. Res.*, 116, F03011.
- Kang, S., and Sotiropoulos, F. (2012a). "Assessing the Predictive Capabilities of Isotropic, Eddy-Viscosity Reynolds-Averaged Turbulence Models in a Natural-Like Meandering Channel." *Water Resour. Res.*, 48, W06505, doi:10.1029/2011WR011375.
- Kang, S., and Sotiropoulos, F. (2012b). "Numerical Modeling of 3D Turbulent Free Surface Flow in Natural Waterways." *Adv. Water Resour.*, 40, 23–36, doi:10.1016/j.advwatres.2012.01.012.
- Kashyap, S., Constantinescu, G., Rennie, C., Post, G., and Townsend, R. (2012). "Influence of Channel Aspect Ratio and Curvature on Flow, Secondary Circulation, and Bed Shear Stress in a Rectangular Channel Bend." *J. Hydraul. Eng.*, 138(12), 1045–1059.
- Lagasse, P. F., Zevenbergen, L. W., Schall, J. D., and Clopper, P. E. (2009). "HEC 23, Bridge Scour and Stream Instability Countermeasures." FHWA HEC-23, U.S. DOT, FHWA.
- Maryland Department of the Environment. (2000). *Maryland's Waterway Construction Guidelines*, Water Management Administration, Baltimore.
- Matsuura, T., and Townsend, R. D. (2004). "Stream-Barb Installations for Narrow Channel Bends—A Laboratory Study." *Canadian Journal of Civil Engineering*, 31(3), 478–486.
- McCullah, J., and Gray, D. 2005. *NCHRP Report 544: Environmentally Sensitive Channel and Bank-Protection Measures*. Transportation Research Board of the National Academies, Washington, D.C.
- NRCS. (2000). "Design of Rock Weirs." Oregon Technical Notes Engineering No. 24, USDA NRCS, Portland, OR.

- NRCS. (2007). *Stream Restoration Design National Engineering Handbook*, Part 654, United States Department of Agriculture, National Resource Conservation Service, Washington, D.C.
- NRCS. (2010). "Design of Stream Barbs for Low Gradient Stream." Minnesota Technical Note No. 8, USDA NRCS, St. Paul, MN.
- NRCS. (2013). "ENG-Design of Stream Barbs." Kansas Engineering Technical Note No. KS-1 (Revision 1), USDA NRCS, Salina, KS.
- Odgaard, A. J. (1988). Construction and Evaluation of Submerged Vanes for Stream Control. Iowa Institute of Hydraulic Research, Iowa City, IA.
- Odgaard, A. J. (2009). River Training and Sediment Management with Submerged Vanes, ASCE, Reston, VA.
- Odgaard, A. J., and Kennedy, J. F. (1983). "River-Bend Bank Protection by Submerged Vanes." *Journal of Hydraulic Engineering*. Vol. 109 No. 8, p. 1161–1173.
- Odgaard, A. J., and Mosconi, C. E. (1987). "Streambank Protection by Submerged Vanes." *Journal of Hydraulic Engineering*, ASCE, Vol. 113 No. 4, p. 520–536.
- Odgaard, A. J., and Spoljaric, A. (1986). "Sediment Control by Submerged Vanes." *J. Hydraul. Eng.*, 112 (12), 1164–1181.
- Odgaard, A. J., and Wang, Y. (1991). "Sediment Management with Submerged Vanes. I: Theory." *J. Hydraul. Eng.*, 117 (3), 267–283.
- Papanicolaou, A. N., M. Elhakeem, and B. Wardman. (2011). "Calibration and Verification of a 2D-Hydrodynamic Model for Simulating Flow Around Bendway Weir Structures." *Journal of Hydraulic Engineering*. 137:75–89.
- Radspinner, R. R., Diplas, P., Lightbody, A. F., Sotiropoulos, F. (2010). "River Training and Ecological Enhancement Potential Using In-Stream Structures." *Journal of Hydraulic Engineering*. 136(12), 967–980.
- Rajaratnam, N., and Nwachukwu, B. A. (1983). "Flow Near Groin-Like Structures." *J. Hydraul. Eng.* 109 (3), 463–480.
- Raudkivi, A. J. (1967). "Loose Boundary Hydraulics." pp. 175–221, Pergamon, New York.
- Rosgen, D. L. (2001). "The Cross-Vane, W-Weir and J-Hook Vane Structures . . . Their Description, Design and Application for Stream Stabilization and River Restoration." *Wetlands Engineering & River Restoration 2001*: pp. 1–22.
- Rosgen, D. L. (2006). Cross-Vane, W-Weir, and J-Hook Vane Structures. Wildland Hydrology, Pagosa Springs, CO.
- Sharma, K., and Mohapatra, P. (2012). "Separation Zone in Flow Past a Spur Dyke on Rigid Bed Meandering Channel." *J. Hydraul. Eng.*, 138(10), 897–901.
- Simon, A., Doyle, M., Kondolf, M., Shields, Jr., F. D., Rhoads, B., and McPhillips, M. (2007). "Critical Evaluation of How the Rosgen Classification and Associated 'Natural Channel Design' Methods Fail to Integrate and Quantify Fluvial Processes and Channel Response." *J. Am. Water Resour. Assoc.* 43(5), 1117–1131.
- Slate, L. O., Shields, Jr., F. D., Schwartz, J. S., Carpenter, D. D., and Freeman, G. E. (2007). "Engineering Design Standards and Liability for Stream Channel Restoration." *Journal of Hydraulic Engineering*. 133(10), 1099–1102.
- Thornton, C. I., Heintz, M. L., Abt, S. R., Baird, D. C., and Padilla, R. S. (2005). *Effects of Bendway Weir Characteristics on Resulting Flow Conditions*. Environmental and Water Resources Institute, ASCE, Reston, VA.
- Thornton, C. I., Meneghetti, A. M., Collins, K., Abt, S. R., and Scurlock, S. M. (2011). Stage-Discharge Relationships for U-, A-, and W-Weirs in Un-submerged Flow Conditions. *Journal of the American Water Resources Association*, 47: 169–178.
- U.S. Department of the Interior, Bureau of Reclamation. (2009). "Quantitative Investigation of the Field Performance of Rock Weirs." U.S. Department of the Interior, Bureau of Reclamation. SRH-2009-46. Denver, CO.

APPENDIX F

Design Guidelines for In-Stream Flow Control Structures

In-stream structures, constructed of rock or wood in various configurations, are often used to limit lateral migration, reduce bank erosion, and create diverse aquatic habitat (Radspinner et al., 2010). In-stream structures can be classified in two fundamental categories: sills and single-arm structures (Figure F-1). Sills are structures that span the entire channel width, while single-arm structures extend from one bank into the channel without reaching the opposite bank. Single-arm structures can be further subdivided into deflector, redirective, and retard types, depending on the function of each structure configuration (NRCS, 2007).

Proper structure design and placement are necessary to avoid channel aggradation, local bed scour, and bank erosion, all of which can result in structure failure and cause significant harm to the stream and nearby property. Furthermore, failure of these structures will accelerate the adverse effects they were initially installed to prevent, such as lateral migration and infrastructure endangerment (see Table F-1). Design approaches need to incorporate the unsteady, 3-D character of the flow in the vicinity of structures and the complex interactions of turbulence in the water column with streambed sediments. The design guidelines in the following sections were developed with the multi-pronged approach described in Chapter 2, combining information from a comprehensive literature review (Appendix A), practitioner survey (Appendix B), field case studies (Appendix C), physical experiments (Appendix D), and numerical simulations (Appendix E and Chapter 3). Figure F-2 lays out the general flowchart for using the following design guidelines. Structure type is selected based on project goals and channel characteristics (Tables F-2 and F-3). An appropriate angle of orientation is selected based on the site characteristics. A vector analysis is used to map out optimum structure location. Ideally, 2-D or 3-D modeling approaches, such as VSL3D, will be used to further refine the design of the structure layout and evaluate its performance for the specific site under consideration. One-dimensional models will not provide adequate information

to evaluate structure layout and, therefore, are not suggested as a tool for in-stream structure design.

Three major categories of structure failure mechanism were identified: flanking (circumvention combined with aggradation), local scour (which can lead to rock displacement), and rock displacement (based on hydrodynamic forces, not local scour). The practitioner survey (Appendix B) also reported winnowing (or scour between rocks) as a significant failure mode. This failure mechanism, however, was not explicitly evaluated in NCHRP Project 24-33, although the effects of this process were likely in the field case studies (Appendix C). Table F-3 compiles the evaluation of the susceptibility of each structure type to these failure mechanisms.

F.1 Determining the Length of Outer Bank Protection in Meandering Channels

In meandering channels, the length of bank protection can be determined for approximately sinusoidal channels by determining the tangent points to the meander (Figure F-3) and identifying a point approximately one channel width (B) upstream and $1.5B$ downstream from these points, as presented in U.S. Army Corps of Engineers (1991) and HEC 23 (Lagasse et al., 2009).

F.2 Rock Vane Design Guidelines

The term “rock vane” applies to single vane rock structures that extend out from a stream bank into the flow. These structures gradually slope from the bank to the bed such that, even at low-flow conditions, the tip of the structure remains submerged (Radspinner et al., 2010). Rock vanes are installed with an upstream angle to minimize erosive flow patterns near the bank by diverting high-velocity flow away from the bank (Maryland Department of the Environment, 2000; Johnson et al., 2002a; see Figure F-4). Often, rock vanes and other in-stream rock

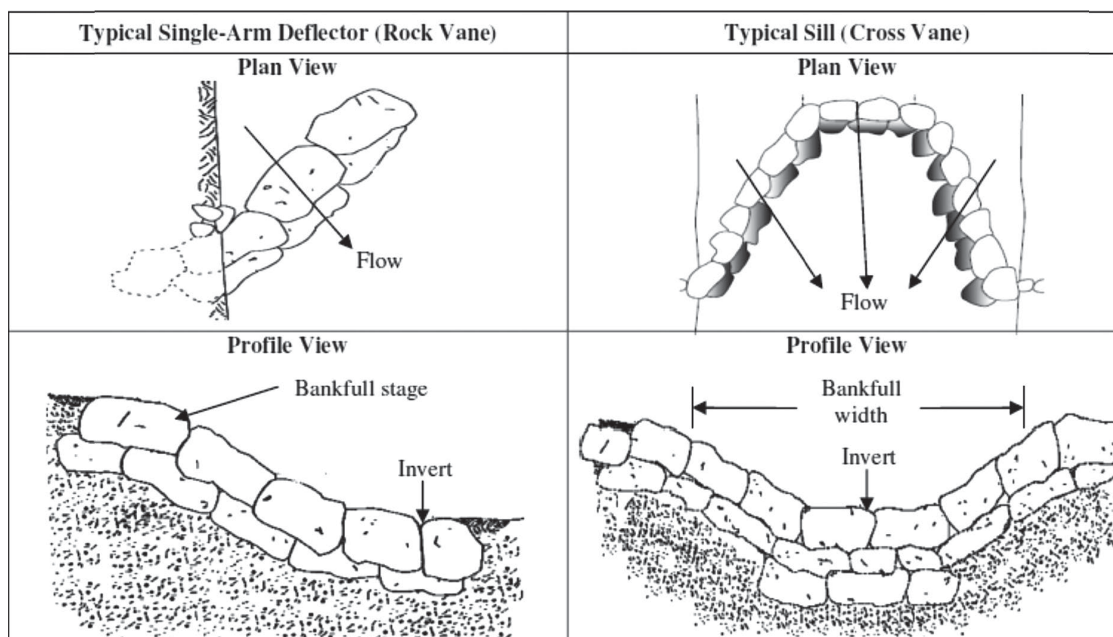


Figure F-1. Illustrations of typical single-arm deflector structure and typical sill rock structure (from Radspinner et al., 2010).

structures are installed with a secondary goals of improving aquatic habitat by creating flow diversity through the formation of scour pools (Rosgen, 2006). A series of vanes installed for bank protection is intended to move scour to the middle of the channel and enhance deposition along the bank (e.g., Johnson et al., 2001; Bhuiyan et al., 2010). Rock vanes and other in-stream rock structures can reduce or eliminate the need for bank armoring on unstable banks and can improve the effec-

tiveness of other erosion protection measures such as vegetation restoration (McCullah and Gray, 2005). Current guidelines for placement and spacing of rock vanes, however, are based primarily on practitioner experience (e.g., Maryland Department of the Environment, 2000; Doll et al., 2003; NRCS, 2007).

The Maryland Department of the Environment's Water Management Administration included design guidelines for rock vanes in the MWCG (Maryland Department of the

Table F-1. Reasons and modes of failure reported in the practitioner survey published in Radspinner et al. (2010).

Structure Type	Channel Characteristics			Failure	
	Aspect Ratio	Sinuosity	Slope	Reasons	Modes
Deflector					
Rock vane (RV)	7–33	n/a	0.003–0.008	Not keyed properly; rock size and shape	Lateral circumvention; winnowing; local scour; aggradation
J-hook vane (JH)	8.8–36	1.1–1.5	0.003–0.02	Not keyed properly; rock size and shape	Lateral circumvention; winnowing; local scour; aggradation
Bendway weir (BW)	8.6–33	1.3–1.5	<0.003	Footer size; build depth	Local scour
Sill					
Cross vane (CV or CVA)	7.3–19.6	1.1–1.5	0.001–0.03	Faulty installation; rock size and shape	Lateral circumvention; winnowing; local scour; aggradation; displacement
W-weir (WW)	n/a	n/a	n/a	Faulty installation; rock size and shape	Lateral circumvention; winnowing; local scour; aggradation; displacement

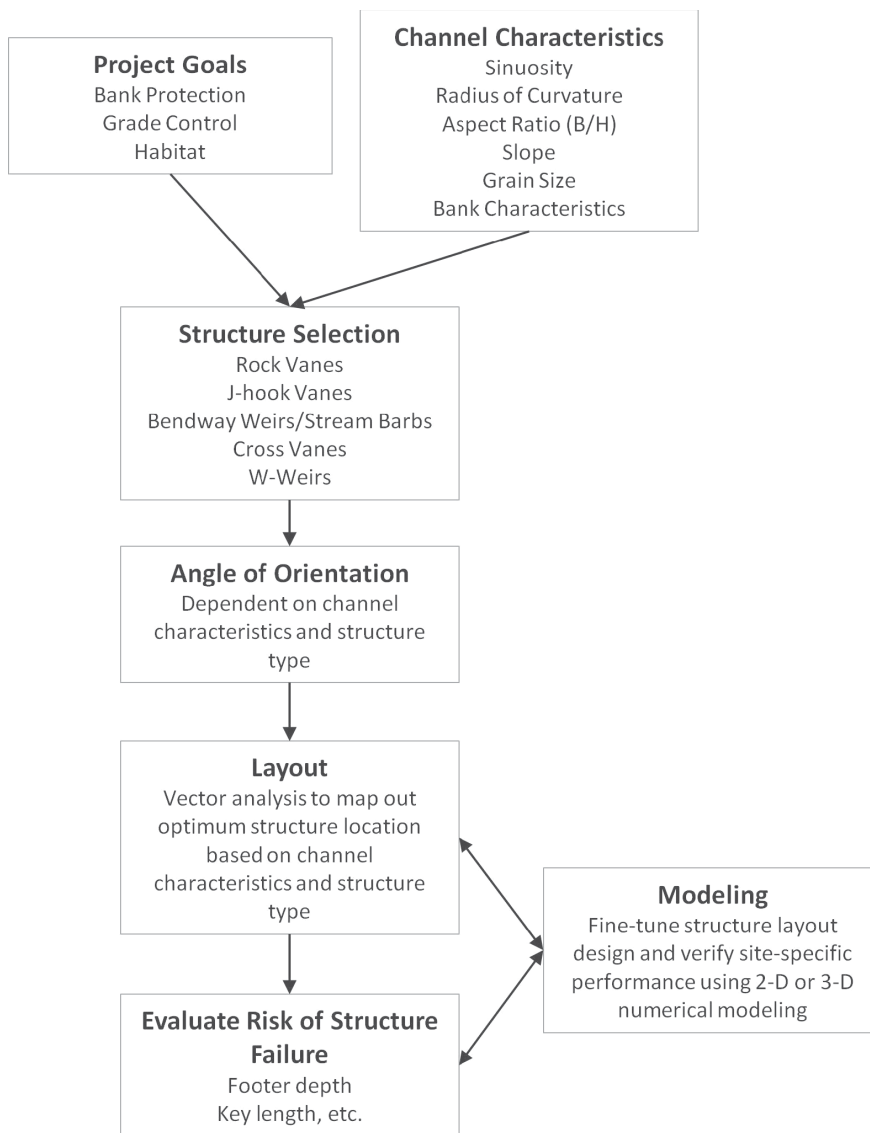


Figure F-2. Design flow process for the design and layout of in-stream flow control structures.

Table F-2. Recommendations for in-stream flow control structure selection based on site characteristics and project goals.

	Site Characteristics				Project Goals				
	Steep Streams	Low Aspect Ratio (Low B/H)	Tight Meanders (Low R _c /B)	Fine Bed Material (Sand)	Protect Bank Toe	Redirect Flow (Thalweg)	Scour Pool Habitat	Minimize Lateral Channel Adjustments	Grade Control
RV	o	o	o	o	o	o	-	o	-
JH	o	o	o	o	o	o	+	o	o
BW	-	-	-	o	+	+	-	+	-
CV	+	o	o	o	-	o	+	-	+
CVA	+	-	o	-	-	o	+	-	+
WW	+	-	o	-	-	o	+	-	+

- Not appropriate

o Moderately appropriate with design modifications

+ Well suited

Table F-3. Evaluation of susceptibility to failure mechanisms for in-stream flow control structures.

	Susceptibility to Failure Mechanism		
	Local Scour	Flanking	Rock Displacement
RV	o	+	o
JH	+	o	+
BW	+	-	-
CV	+	o	o
CVA	+	o	+
WW	+	o	+

- Low risk

o Moderate risk

+ High risk

Environment, 2000). Included in this document is a summary of the uses of these structures in common restoration and stabilization practices. Within this summary, applications for which rock vanes are well suited (e.g., protecting bank toe, and redirecting flows), moderately well suited (e.g., providing in-stream habitat), and not well suited (e.g., stabilizing bed and use in bedrock channels) are discussed. Based on the practitioner experience reported in the MWCG, caution should be used in steep stream reaches with gradients that exceed 3%. It is also important to note that the stream bank opposite the rock vane structures should be monitored closely after installation for any increase in erosion occurring due to the presence of the rock vane and its ability to direct flow away from the outer bank, towards the center of the channel, and, on occasion, negatively affecting the opposite bank.

Several structures use the rock vane as the key component and modify it for various situations. All structures from the rock vane family can be subjected to failure by lateral circumvention, winnowing, local scour, aggradation, and displacement (Johnson et al., 2002b). In addition to the MWCG (Maryland Department of the Environment, 2000), rock vane design guidelines can be found in the USDA NRCS *Stream*

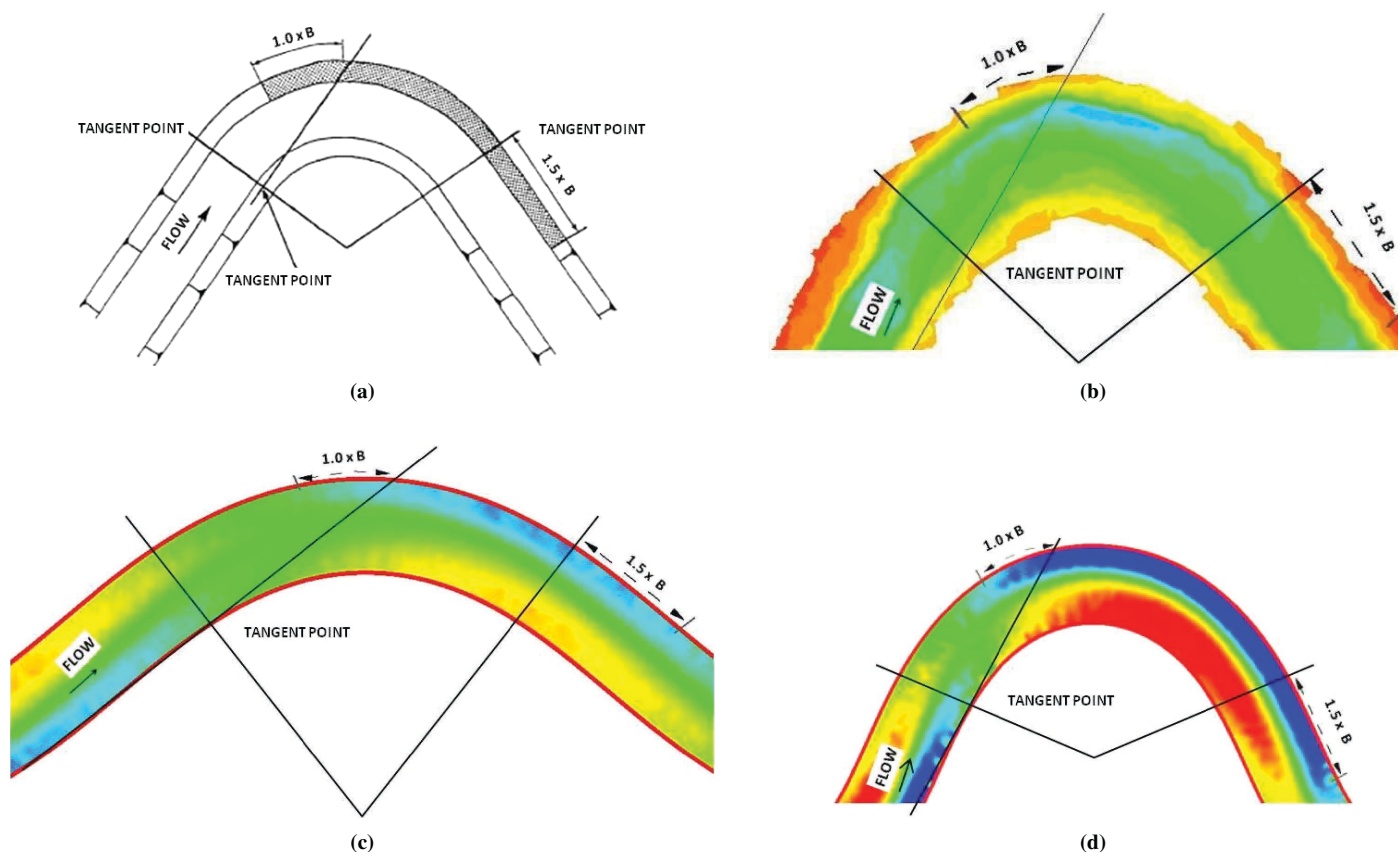


Figure F-3. Extent of protection required at a channel bend for three different channels: (a) general guidelines (from U.S. Army Corps of Engineers, 1991), (b) the SAFL Outdoor StreamLab (OSL) channel with no structures, (c) VSL-G, and (d) VSL-S. Blue and red zones are associated to the regions with significant scour and deposition, respectively.

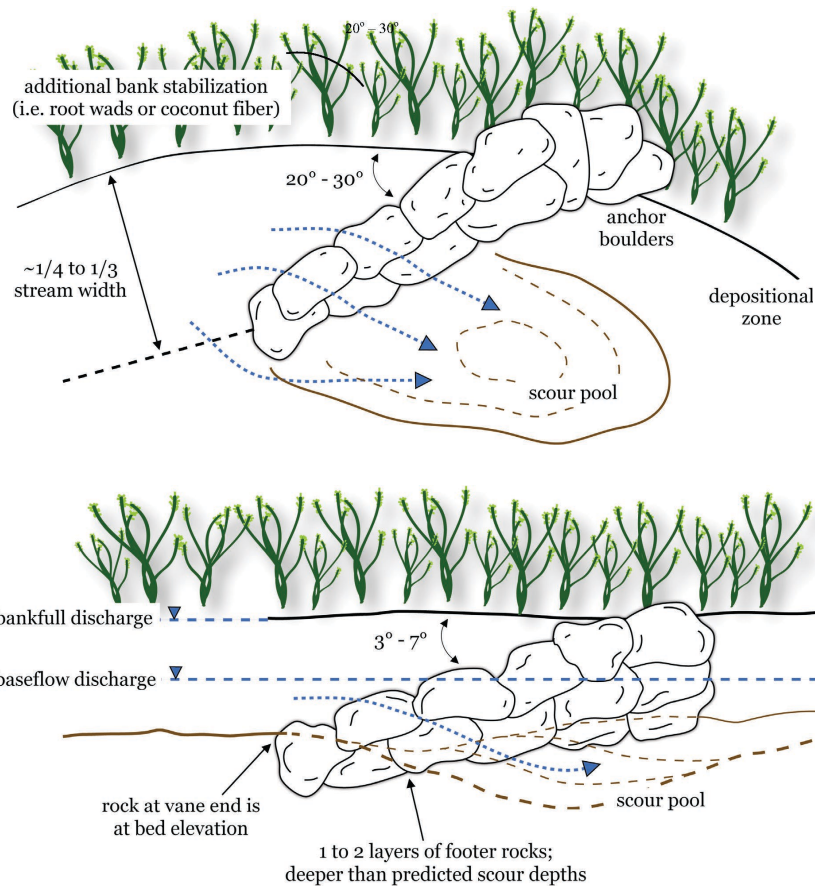


Figure F-4. Typical rock vane installation (after Rosgen, 2006 and Radspinner et al., 2010).

Restoration Design National Engineering Handbook, Part 654 (NRCS, 2007). Chapter 11 of this design manual, “Rosgen Geomorphic Channel Design,” focuses on the design guidelines for cross vanes, J-hook vanes, and W-weir structures; however, all of these structures are rock vane variations. The following section builds on existing rock vane guidance with input from the comprehensive physical and numerical experiments described in previous sections.

F.2.1 Structure Geometry

Vane Slope

General guidelines suggest that the vane arm should slope from the bankfull water surface elevation on the attached bank to the bed with a slope of between 2% to 7% (Maryland Department of the Environment, 2000; NRCS, 2007), although this can vary up to 20% in channels with low aspect ratios (Doll et al., 2003). In general, longer, flatter vanes will offer greater lengths of bank protection.

Vane Length

Vane length is typically designed such that the vane tip is located between $\frac{1}{4}$ and $\frac{1}{3}$ of the bankfull width, B_{bf} , across the

channel (Brown, 2000; NRCS, 2007), or $<\frac{1}{2}$ of base-flow channel width (Doll et al., 2003). For very large rivers where it is impractical to extend the vane at the desired angle to $\frac{1}{3} B_{bf}$, shorter vane lengths are appropriate, following vane slope and angle guidelines. The experiments and simulations considered in NCHRP Project 24-33 evaluated rock vane structures installed at $\frac{1}{3} B_{bf}$.

F.2.2 Structure Layout

Angle of Orientation

By definition, rock vanes have a shallow upstream angle of between 20° and 30° from the tangent to the upstream bank. The vane tip points in the upstream direction, with 0° aligned with the bank and 90° perpendicular to the bank (NRCS, 2007; Doll et al., 2003; Maryland Department of the Environment, 2000; Brown, 2000). Results from NCHRP Project 24-33 experiments and simulations indicate that larger angles provide a greater length of bank protection across a range of channel characteristics (aspect ratio 5–30, sinuosity 1–1.5, slope 10^{-4} – 10^{-3} , grain size 0.5–30 mm) but also typically result in a deeper scour hole adjacent to the rock vane tip. In low R_c/B channels, a rock vane installed with a 30° angle at the outer bend apex threatens the stability of the inner bank.

Based on NCHRP Project 24-33 results, the angle of orientation for rock vanes for bank protection should be 30° from the tangent to the bank channels in typical gravel rivers and 20° from the tangent to the bank in more sinuous typical sand rivers (see Chapter 3 for more information).

Vane Location and Spacing

Rock vanes should be installed in series of at least two structures to protect the entire region of the outer bank subject to scour (Johnson et al., 2001). Specific guidelines on vane spacing and vane placement are sparse. Doll et al. (2003) suggest that rock vanes should be located just downstream of where the flow intercepts the bank at acute angles. Bhuiyan et al. (2010) give an example of a circular meander with vanes spaced such that the whole bank is covered. The Maryland Department of the Environment guidelines (2000) suggest spacing of one or more channel widths for habitat considerations, depending on the pattern of scour pools, in reference reaches, or five to seven bankfull widths if the restoration goal is to initiate meandering. Chapter 11 of the NRCS manual provides empirical equations for calculating spacing based on the channel radius of curvature and width (NRCS, 2007; Table 12). Based on the results of NCHRP Project 24-33, a vector analysis approach is suggested, as described in the structure layout section (Section F.7). Based on the numerical results of NCHRP Project 24-33, for projects where outer bank protection is the primary project goal, a rock vane structure array should begin at the meander apex in large radius of curvature channels ($R_c/B > 3$) to minimize the number of structures installed. For smaller radius of curvature channels, the final structure array should be shifted upstream by approximately one channel width to provide adequate bank protection and minimize the risk of structure failure due to excessive local scour or flanking.

If rock vanes are installed to protect specific infrastructure in a large R/B or straight channel, the vane should be installed two or more channel widths upstream of the infrastructure they are designed to protect (Johnson et al., 2001; Johnson et al., 2002a)

F.2.3 Construction

Footer Rocks

To prevent structure failure due to local scour around the rock vane base, substantial footer rocks should be installed below the stream grade. Typically, footer rocks are one to two large rocks underneath the top rock. Footer rocks should be downstream of the top rock to minimize structure failure by rocks falling into a downstream scour hole (Doll et al., 2003). Gaps between footer rocks up to $\frac{1}{3}$ of the stone diameter can enable interlocking (Brown, 2000). Footer rock size should be at least three times the protrusion height of the vane. This depth should be doubled for sand-bed streams (NRCS, 2007). Based

on the numerical results from NCHRP Project 24-33, footer rocks should be installed at an elevation that is 1 to 1.5 times deeper than the maximum scour along the outer bank of the channel (Sc_{MAX}).

Johnson et al. (2001) suggest the use of geotextile fabric or well-graded material to mitigate structural porosity. Doll et al. (2003) recommend that geotextile fabric always be used for any rock vane or modified rock vane structure.

Rock Size

Rock vanes are typically constructed from rock much larger than the rock size for other redirective flow training structures such as bendway weirs or stream barbs. Rocks in bendway weirs and stream barbs are commonly sized using riprap sizing equations with a factor of safety (i.e., NRCS guidance suggests two times the median grain size, D_{50} , for stream-bank riprap). The rock used to construct rock vanes is typically much larger than riprap equations suggest as the rocks are not interlocking. One method for sizing individual boulders is based on a balance of the forces on an individual rock (Fischenich and Seal, 2000); however, these equations also undersize the rock. The rock size needs to be large enough to withstand local scour around the base of the structure. Many other guidelines suggest large rock sizes regardless of local stream-channel characteristics (i.e., 1 to 2 tons, Doll et al., 2003; or >200 lbs, Maryland Department of the Environment, 2000). Rosgen (2006) provides a general reference for minimum rock size based on a limited number of rivers.

$$D_{min} = 0.174Ln(\tau) + 0.6349$$

where τ = bankfull shear stress in kg/m^3 . This relationship results in a much larger rock size than other rock-sizing methods.

Rock shape depends on local availability but typically should be flat to allow interlocking, and vane rocks should be touching (Doll et al., 2003; Maryland Department of the Environment, 2000). Large rocks and boulders can be placed on the downstream side of the structure to enhance stability (Maryland Department of the Environment, 2000). For rock vanes, rocks placed at the tip of the structure are subject to forces that are approximately 1.5 to 3 times the force on rocks closer to the stream bank. This is compounded by the fact that the deepest scour occurs near the structure tip. Therefore, rocks placed at the tip of the structure need to be large enough to account for the forces exerted by the turbulent flow.

Sills (Bank Key)

Sills consisting of two to three large rocks built into the stream bank can help mitigate erosion behind rock vanes, especially on new channels (Maryland Department of the Environment, 2000; NRCS, 2007). Experimental and numerical results from

NCHRP Project 24-33 indicated that a large amount of sediment was transported and stored upstream of rock vanes. This additional sediment may lead to bank overtopping and flanking of the structure as sediment deposition becomes vegetated under low flows, increasing local roughness and redirecting flow around and behind the structure.

F.2.4 Maintenance and Monitoring

To ensure proper structure performance, installed structures need to be monitored for signs of structure failure, particularly after the first large flood event. The following suggestions are included based on the results from NCHRP Project 24-33 for monitoring and maintenance of rock vanes.

- Structures should be monitored for local scour, particularly near the tip of the structure where the large hydro-

dynamic forces could combine with undermining of the footer rock to shift rocks at the structure tip.

- Structures should be monitored for signs of excessive deposition and potential flanking following large flow events. Over time, vegetation can begin to grow on this deposited material, shifting flow around the outside of the structure.
- The opposite bank should be monitored for signs of unacceptable scour well downstream of the structure (>5 channel widths).

F.3 J-Hook Vane Design Guidelines

J-hook vanes are a variation on the single-arm rock vane that includes a hook that extends from the tip of the vane approximately perpendicular to the flow (Figure F-5). Similar to the rock vane, the vane portion of these structures gradually slopes from the bank to the bed such that, even at low-flow

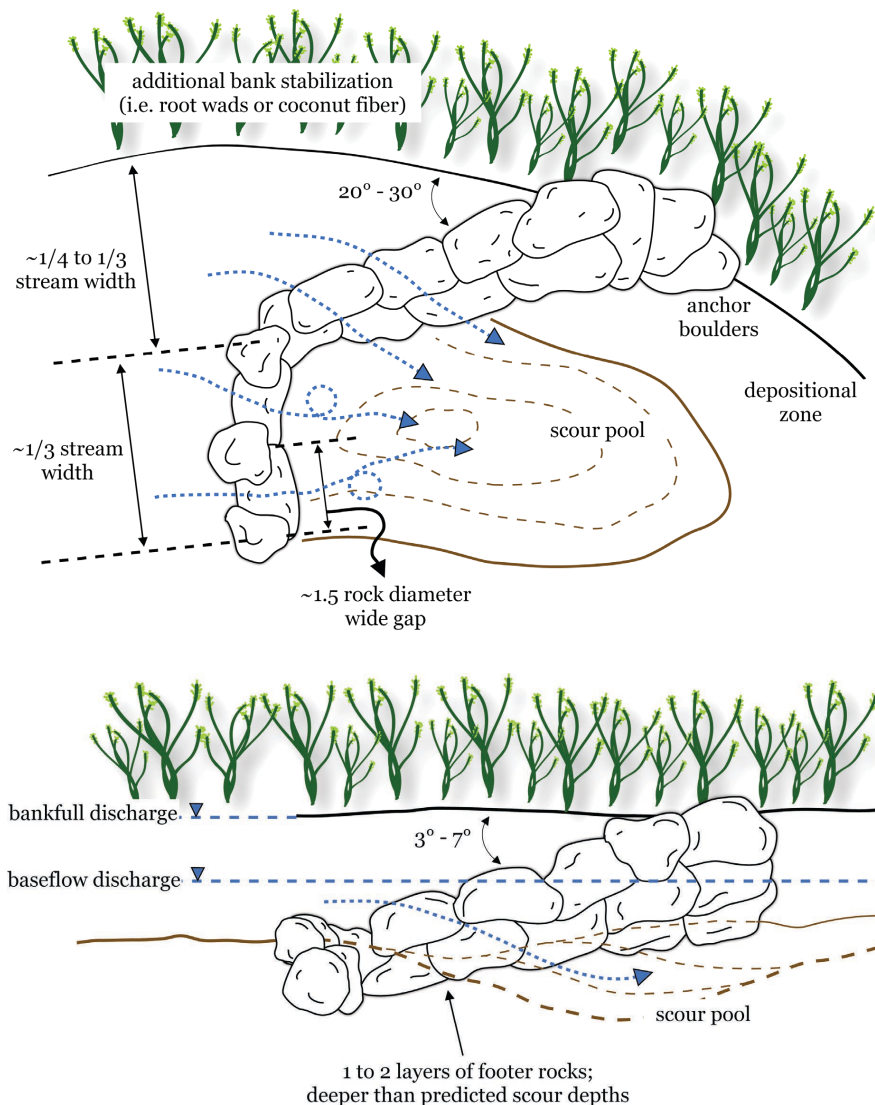


Figure F-5. Typical J-hook vane installation (after Rosgen, 2006).

conditions, the tip of the structure remains submerged (Radspinner et al., 2010). J-hook vanes are also installed with an upstream angle to minimize erosive flow patterns near the bank by diverting high-velocity flow away from the bank (Maryland Department of the Environment, 2000; Johnson et al., 2002a). Often, rock vanes and other in-stream rock structures are installed with a secondary goal of improving aquatic habitat by creating flow diversity through the formation of scour pools (Rosgen, 2006), and J-hook vanes are expected to provide additional in-stream habitat enhancement in the form of a mid-channel scour pool (Maryland Department of the Environment, 2000). Current guidelines for placement and spacing of J-hook vanes are similar to those developed for rock vanes, based primarily on practitioner experience (e.g., Maryland Department of the Environment, 2000; Doll et al., 2003; NRCS, 2007).

Applications for J-hook vanes are similar to those for rock vanes, with the exception that J-hook vanes are expected to provide better in-stream habitat in the form of a deep scour hole (Maryland Department of the Environment, 2000). Limitations of J-hook vanes are similar to those of rock vanes. These structures should not be used in steep stream reaches (greater than 3%). With any flow-redirection structure, the stream bank opposite the structures should be monitored closely after installation for any increase in erosion occurring due to the presence of the structure. All structures from the rock vane family can be subjected to failure by lateral circumvention, winnowing, local scour, aggradation, and displacement (Johnson et al., 2002b). J-hook design guidelines can be found in the MWCG (Maryland Department of the Environment, 2000) and the USDA NRCS *Stream Restoration Design National Engineering Handbook*, Part 654 (NRCS, 2007). Chapter 11 of this design manual, “Rosgen Geomorphic Channel Design,” focuses on the design guidelines for cross vanes, J-hook vanes, and W-weir structures. The following section builds on existing J-hook vane guidance with input from the comprehensive physical and numerical experiments from NCHRP Project 24-33.

F.3.1 Structure Geometry

Vane Slope

See Structure Geometry section (Section F.2.1) for guidelines.

Vane Length

J-hook vane length is typically designed such that the vane tip is located between $\frac{1}{4}$ and $\frac{1}{3}$ of the bankfull width, B_{bf} , across the channel (Brown, 2000, NRCS, 2007) or $<\frac{1}{2}$ of base-flow channel (Doll et al., 2003), and the hook portion of the J-hook vane extends to no greater than $\frac{2}{3}$ of the channel

width. For very large rivers where it is impractical to extend the vane at the desired angle to $\frac{1}{3} B_{bf}$, shorter vane lengths are appropriate, following the vane slope and angle guidelines.

F.3.2 Structure Layout

Angle of Orientation

By definition, J-hook vanes have a shallow upstream angle of between 20° and 30° from the tangent to the upstream bank (NRCS, 2007; Doll et al., 2003; Maryland Department of the Environment, 2000; Brown, 2000). In general, larger angles provide greater bank protection across a range of channel characteristics (aspect ratio 5–30, sinuosity 1–1.5, slope 10^{-4} – 10^{-3} , grain size 0.5–30 mm), but 20° angles present significant risk to the inner bank. Based on the experimental and numerical results from NCHRP Project 24-33, 30° from the tangent to the bank is an appropriate angle of orientation for J-hook vanes in typical gravel rivers, and 20° is appropriate for more sinuous sand rivers (see Chapter 3 for more information).

Vane Location and Spacing

When used for meander bend protection, J-hook vanes should be installed in series of at least two structures to protect the entire region of the outer bank subject to scour (Mooney et al., 2007). Specific guidelines on vane spacing and vane placement are sparse. Similar to rock vanes, the Maryland Department of the Environment guidelines (2000) suggest spacing of one or more channel widths for habitat considerations, depending on the pattern of scour pools, in reference reaches, or 5 to 7 bankfull widths if the restoration goal is to initiate meandering. Chapter 11 of the NRCS manual provides empirical equations for calculating spacing based on the channel radius of curvature and width (NRCS, 2007; Table 12). Based on the results of NCHRP Project 24-33, a vector analysis approach is suggested as described in Section F.7. Based on the numerical results of NCHRP Project 24-33, for large radius of curvature to width ratio channels ($R_c/B > 3$), where outer bank protection is the project goal, the structure array should begin at the meander apex to minimize the number of structures installed. For smaller radius of curvature channels, the final structure array should be shifted upstream by approximately one channel width to provide adequate bank protection and minimize the risk of structure failure due to excessive local scour or flanking.

If J-hook vanes are installed to protect specific infrastructure in a large R_c/B or straight channel, the vane should be installed two or more channel widths upstream of the infrastructure they are designed to protect.

F.3.3 Construction

Footer Rocks

To prevent structure failure due to local scour around the J-hook vane base, substantial footer rocks should be installed below the stream grade. Typically, footer rocks are one to two large rocks underneath the top rock. Footer rocks should be downstream of the top rock to minimize structure failure by rocks falling into a downstream scour hole (Doll et al., 2003). Gaps between footer rocks up to $\frac{1}{3}$ of the stone diameter can enable interlocking (Brown, 2000). Footer rock size should be at least three times the protrusion height, and this depth should be doubled for sand-bed streams (NRCS, 2007). Based on the numerical results from NCHRP Project 24-33, footer rocks for J-hook vanes should be installed at an elevation that is 1.5 to 2 times deeper than the maximum scour along the outer bank of the channel ($S_{c_{MAX}}$; see Chapter 6).

Rock Size

J-hook vanes are typically constructed from rock much larger than the rock used for other redirective flow training structures such as bendway weirs or stream barbs (see the Rock Size subsection in Section F.2.3 for more information).

Excessive gaps between rocks can lead to winnowing and subsequent failure of the structure. Johnson et al. (2001) suggest that field procedures such as the use of geotextile fabric or well-graded material be used to mitigate structural porosity. Doll et al. (2003) recommend that geotextile fabric always be used for any rock vane or modified rock vane structure. Alternatively, grouting structures can help them survive high-flow events. NCHRP Project 24-33 evaluated structures where gaps between rocks were limited to the tip of the hook portion of the vane. Gaps in the hook were found to significantly alter sediment transport through the structure.

For J-hook vanes, rocks placed at the tip of the structure are subject to forces that are approximately 4 to 5 times the force on rocks closer to the stream bank. This is compounded by the fact that the deepest scour occurs near the structure tip. Therefore, rocks placed at the tip of the structure need to be large enough to account for the forces exerted by the turbulent flow.

Sills (Bank Key)

Sills consisting of two to three large rocks built into the stream bank can help mitigate erosion behind rock vanes, especially in new channels (Maryland Department of the Environment, 2000; NRCS, 2007). Experimental and numerical results from NCHRP Project 24-33 indicated that a

moderate amount of sediment was transported and stored upstream of J-hook vanes. This additional sediment may lead to bank overtopping and flanking of the structure as sediment deposition becomes vegetated under low flows, increasing local roughness and redirecting flow around the structure.

F.3.4 Maintenance and Monitoring

To ensure proper structure performance, installed structures need to be monitored for signs of structure failure, particularly after the first large flood event. The following suggestions are included based on the results from NCHRP Project 24-33 for monitoring and maintenance of rock vanes.

- Structures should be monitored for local scour, particularly near the tip and on the hook of the structure. Large hydrodynamic forces could combine with undermining of the footer rock to shift rocks at the structure tip or displace the rocks that form the hook part of the structure.
- Structures should be monitored for signs of excessive deposition and potential flanking following large flow events. Over time, vegetation can begin to grow on this deposited material, shifting flow around the outside of the structure.
- The opposite bank should be monitored for signs of unacceptable scour well downstream of the structure (>5 channel widths).

F.4 Bendway Weir/Stream Barbs

The terms “bendway weir” and “stream barb” refer to single-arm rock structures extending from the bank that are submerged in all but low flows and are designed to mitigate erosive flow patterns through weir mechanics (Derrick, 1998; Evans and Kinney, 2000; see Figure F-6). Several state agencies have published technical notes and case studies for bendway weir use under a variety of stream characteristics (e.g., NRCS, 2010). Stream barbs are designed to protect the bank by disrupting velocity gradients in the near-bed regions, deflecting currents toward the tip of the weirs (Matsuura and Townsend, 2004).

F.4.1 Structure Geometry

Weir Slope and Weir Height

Bendway weirs are typically installed with a nearly flat (Lagasse et al., 2009) or slightly sloping weir slope. The transverse slope along the centerline should be no steeper than 1V:5H (1 vertical to 5 horizontal); however, care should be taken that the slope does not redirect flow toward the bank to be protected. The flat weir section normally transitions into

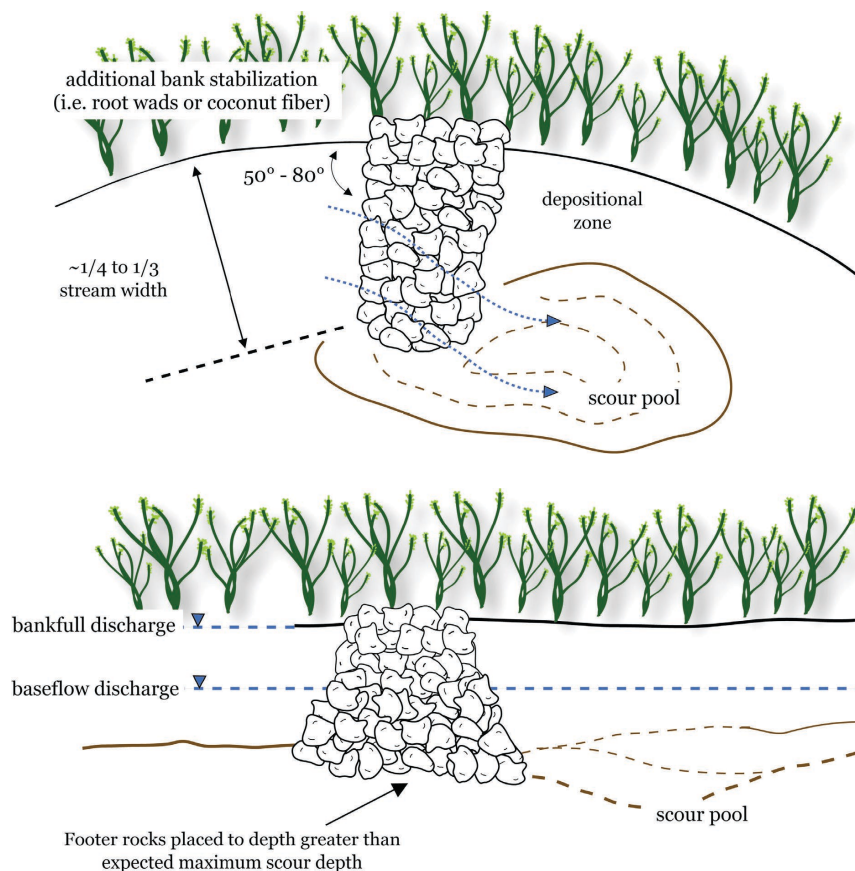


Figure F-6. Typical bendway weir installation (after NRCS, 2007 and Radspinner et al., 2010).

the bank on a slope of 1V:1.5H to 1V:2H. The height of the weir should meet the following criteria (Lagasse et al., 2009):

- Between 30% and 50% of the mean annual high-water level (or bankfull level) (NRCS, 2007),
- Below the normal or seasonal mean water level,
- Equal to or above the mean low-water level, and
- Of adequate height to intercept a large enough percentage of the flow to produce the desired results.

Weir Length

Suggested weir lengths range from $\frac{1}{10}$ to $\frac{1}{4}$ of the channel width, not to exceed $\frac{1}{3}$ of the channel width (NRCS, 2007; Lagasse et al., 2009).

F.4.2 Structure Layout

Angle of Orientation

Guidelines for the angle of orientation for bendway weirs vary greatly from 20° to 80° from the tangent to the outer bank (e.g., NRCS, 2007; Lagasse et al., 2009). NCHRP Project 24-33 found that the optimum angle should be selected

by evaluating the combined effect of multiple structures and longer vane length. Results from this project suggest that a moderate angle of 50° balanced the length of bank protection provided by longer weirs with the smaller cost of installation of higher angle (shorter weirs).

Weir Location and Spacing

The furthest upstream barb should be placed near or just upstream of the area first affected by erosion and should not be placed downstream of $\frac{3}{4}$ of the turn length (Castro and Sampson, 2001). Based on numerical simulations from NCHRP Project 24-33, placing the first bendway weir at the meander apex sufficiently protected the toe of the bank on the outer bank of the meander. Typical bendway weir spacing should range from 5 to 10 times the effective structure length, and ideally 4 to 5 times the effective length (NRCS, 2007; Lagasse et al., 2009). A vector analysis (e.g., NRCS, 2007; described in Section F.7) provides guidance into bendway weir structure spacing around a meander. In this type of analysis, lines are projected from the tip of the upstream structure to the bank to determine where to place the second structure.

F.4.3 Construction

Footer Depth

Bendway weir structures should be installed during low-flow periods, with rock placement beginning at the upstream end of the structure (Castro and Sampson, 2001). Footer rocks installed in the streambed need to be at least D_{100} or 2.5 times the exposed rock height for gravel and 3 to 3.5 times exposed rock height for sandy streams. Based on the numerical results from NCHRP Project 24-33, footer rocks should be installed at an elevation that is 1 to 1.5 times deeper than the maximum scour along the outer bank of the channel (Sc_{MAX} ; see Chapter 6).

Rock Size

Rock size is typically determined using riprap sizing criteria for turbulent flow (NRCS, 2007; West Lane method). In addition, the following criteria should be met (Lagasse et al., 2009; NRCS, 2007):

- D_{50} , stream barb = $2 \times D_{50}$, as determined for stream bank riprap.
- D_{100} , stream barb = $2 \times D_{50}$, stream barb.
- $D_{min} = 0.75 \times D_{50}$, as determined for stream bank riprap.
- Rock in the barb should be well graded in the D_{50} to D_{100} range for the weir section; the smaller material may be incorporated into the bank key. The largest rocks should be used in the exposed weir section at the tip and for the bed key (footer rocks) of the barb.
- The Isbash curve (NEH-650.16; NEH = National Engineering Handbook) is not appropriate for sizing rock for stream barbs since it results in sizes too small for this application.
- Stone should be angular, and not more than 30% of the stones should have a length exceeding 2.5 times their thickness.
- No stones should be longer than 3.5 times their thickness.
- Typically, the size should be 20% greater than computed from nonturbulent riprap sizing formulas.
- The minimum rock size should not be smaller than the D_{100} of the streambed.

Sills (Bank Key)

Bendway weirs/stream barbs have a relatively low risk of flanking from overbank flows compared to rock vanes or J-hook vanes. However, guidelines suggest that bendway weirs should be keyed into the bank at least 1.5 times bank height (NRCS, 2007). More specific bank key guidelines based on a 20° angle of expansion can be found in HEC 23 (Lagasse et al., 2009) and are listed as follows.

When the channel radius of curvature is large ($R_c > 5B$):

$$LK = Vs \tan(20) - Le$$

where:

- Vs = spacing,
- LK = length of key, and
- Le = effective length of weir.

When the channel radius of curvature is small ($R_c < 5B$):

$$LK = (Le/2)(B/Le)^{0.3} (Vs/R_c)^{0.5}$$

F.4.4 Maintenance and Monitoring

To ensure proper structure performance, installed structures need to be monitored for signs of failure, particularly after the first large flood event. The following suggestions are included based on the results from NCHRP Project 24-33 for monitoring and maintenance of bendway weirs.

- Structures should be monitored for local scour, particularly near the tip of the structure where the large hydrodynamic forces could combine with undermining of the footer rock to shift rocks.
- Structures should be monitored for signs of excessive deposition and potential flanking following large flow events. Over time, vegetation can begin to grow on this deposited material, shifting flow around the outside of the structure.
- The opposite bank should be monitored for signs of unacceptable scour well downstream of the structure (>5 channel widths).

F.5 Cross Vane Design Guidelines

Cross vanes are low-profile, channel-spanning structures designed to provide grade control, divert flow away from unstable banks, and create scour pools for aquatic habitat (Maryland Department of the Environment, 2000). Cross vanes have also been installed upstream of bridge piers to reduce scour. There are two types of cross vanes. The first is a U-shaped structure, which has two arms angled upstream at 20° to 30° from the banks that slope downward to the streambed cross piece (Figure F-7). The second type, an A-shaped structure, is a modified cross vane with a step located in the upper $\frac{1}{3}$ to $\frac{1}{2}$ of the arm. This step is designed to dissipate energy, thereby reducing footer scour and protecting the structure from failure (Rosgen, 2006). Cross vanes are well suited for use in moderate- and high-gradient streams and should be avoided in bedrock channels, streams with unstable bed substrates, and naturally well-developed pool-

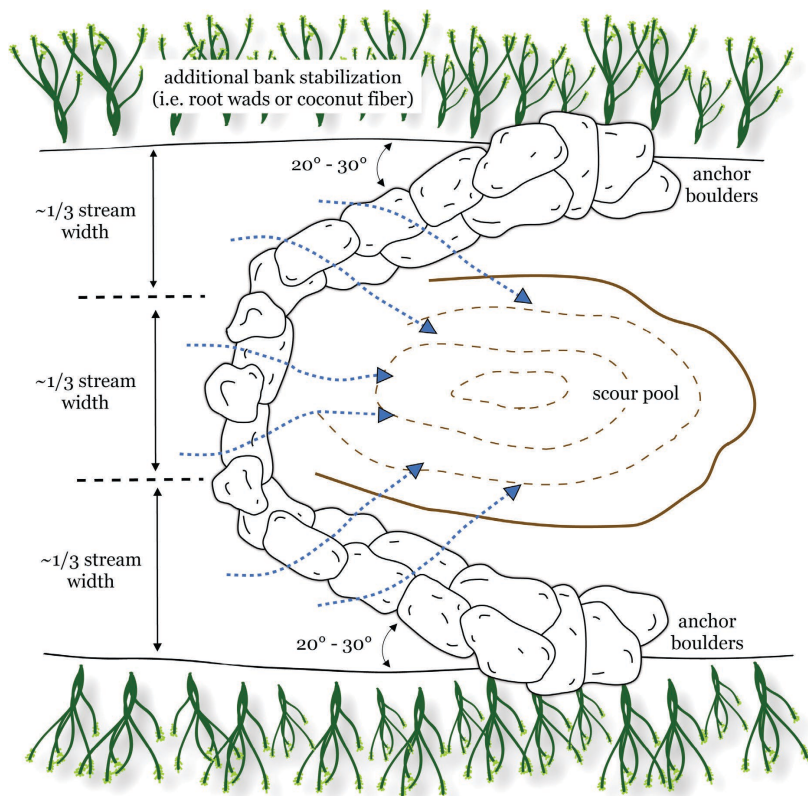


Figure F-7. Typical cross vane installation (after Rosgen, 2006).

riffle sequences (Maryland Department of the Environment, 2000). Cross vane design guidelines can be found in Rosgen (2006), the MWCG (Maryland Department of the Environment, 2000), and the USDA NRCS *Stream Restoration Design National Engineering Handbook*, Part 654 (NRCS, 2007). Chapter 11 of this design manual, “Rosgen Geomorphic Channel Design,” focuses on the design guidelines for cross vanes, J-hook vanes, and W-weir structures.

F.5.1 Structure Geometry

Cross Vane Step

Two variations of cross vane were tested in NCHRP Project 24-33: a standard U-shaped cross vane, and a cross vane with a step (a A-shaped cross vane). A stepped, A-shaped cross vane should be used to provide additional protection for the upstream rocks; however, an A-shaped structure poses a greater risk to the stability of banks immediately downstream and should not be used if bank protection is the project goal.

Vane Slope

See Structure Geometry section (Section F.2.1) for guidelines.

Vane Length

Vane length is typically designed such that the vane tip is located between $\frac{1}{4}$ and $\frac{1}{3}$ of the bankfull width, B_{bf} , across the channel (Brown, 2000, NRCS, 2007), or $<\frac{1}{2}$ of base-flow channel (Doll et al., 2003), and the cross portion extends over the middle $\frac{1}{3}$ of the channel width. For very large rivers where it is impractical to extend the vane at the desired angle to $\frac{1}{3} B_{bf}$, other structure configurations, such as a W-weir, could be considered.

F.5.2 Structure Layout

Angle of Orientation

By definition, cross vanes have a shallow upstream angle of between 20° and 30° from the tangent to the upstream bank (NRCS, 2007; Doll et al., 2003; Maryland Department of the Environment, 2000; Brown, 2000). Results from this research indicate that larger angles provide greater bank protection across a range of channel characteristics (aspect ratio 5–30, sinuosity 1–1.5, slope 10^{-4} – 10^{-3} , grain size 0.5–30 mm), and smaller angles present significant risk to the banks downstream of the cross vane structure. Based on these results, the angle of orientation for cross vanes for bank protection should be 30° from the tangent to the bank. Cross vanes with

large angles (generally greater than 30°) have shown indicators of partial and full failure in field investigations (U.S. Department of the Interior, Bureau of Reclamation, 2009).

Vane Location and Spacing

While it is suggested that cross vanes can be used to protect unstable banks, very little information exists on the optimal placement of vanes to meet this goal. Based on the results from NCHRP Project 24-33, sill structures should be installed a minimum of two channel widths upstream of bridge piers or other infrastructure due to scour immediately downstream of these structures. For A-shaped cross vanes, this should be extended to 2.5 to 3 channel widths. An alternative would be to install structures in series to minimize the dimensions of the scour hole immediately downstream of a cross vane. A sill structure raises or maintains the bed elevation, so it is normally installed within a section of little or no turbulence for larger streams or at the head of a riffle for smaller streams (Doll et al., 2003). The Maryland Department of the Environment guidelines (2000) suggest spacing depending on the pattern of scour pools in reference reaches.

F.5.3 Construction

Footer Rocks, Rock Size, and Sills

See Construction section (Section F.2.3) for guidelines. Footer rocks should be large enough to resist movement from shear stresses during the design flow. Long and flat rocks tend to perform better in the field (U.S. Department of the Interior, Bureau of Reclamation, 2009).

F.5.4 Maintenance and Monitoring

To ensure proper structure performance, installed structures need to be monitored for signs of failure, particularly after the first large flood event. The following suggestions are included based on the results from NCHRP Project 24-33 for monitoring and maintenance of cross vanes.

- Structures should be monitored for local scour, particularly downstream of cross members of the A- or U-shaped cross vane where the large hydrodynamic forces could combine with undermining of the footer rock to shift rocks.
- Structures should be monitored for signs of excessive deposition and potential flanking following large flow events. Over time, vegetation can begin to grow on this deposited material, shifting flow around the outside of the structure.
- The bank within two channel widths downstream should be monitored for signs of scour as the scour hole downstream widens. Additional bank protection may be required in this zone.

F.6 W-Weirs

Like cross vanes, W-weirs are low-profile, channel-spanning structures designed to provide grade control, direct flow away from unstable banks, create scour pools for aquatic habitat, and protect downstream bridge piers (see Figure F-8). W-weirs are similar to a double cross vane and are typically applicable in larger channels (>12 m or 40 ft in width). They are well suited to protect the bank toe, redirect flow, create flow diversity, and stabilize bed and lateral channel adjustments in channels with highly erodible and steep banks, high design velocity, flashy flows, and high-bedload transport. With proper support, W-weirs can be used with rigid or fixed banks with limited backwater effects. W-weirs are not suited for slow-flow or pooled reaches with silt or fine sand bed (Maryland Department of the Environment, 2000). W-weir design guidelines can be found in Rosgen (2006), the MWCG (Maryland Department of the Environment, 2000), and the USDA NRCS *Stream Restoration Design National Engineering Handbook*, Part 654 (NRCS, 2007). Chapter 11 of this design manual, “Rosgen Geomorphic Channel Design,” focuses on the design guidelines for cross vanes, J-hook vanes, and W-weir structures.

F.6.1 Structure Geometry

Vane Slope

See Structure Geometry section (Section F.2.1) for guidelines.

Vane Length

Vane length is typically designed such that the vane tip is located $\frac{1}{4}$ of the bankfull width, B_{bf} , across the channel (Brown, 2000, NRCS, 2007). The middle V portion of the W-weir extends across the middle $\frac{1}{2}$ of the channel width unless an asymmetrical W-weir is being designed for a specific project goal.

F.6.2 Structure Layout

Angle of Orientation

By definition, W-weirs have a shallow upstream angle of between 20° and 30° from the tangent to the upstream bank (NRCS, 2007; Doll et al., 2003; Maryland Department of the Environment, 2000; Brown, 2000). Results from this research indicate that larger angles provide greater bank protection across a range of channel characteristics (aspect ratio 5–30, sinuosity 1–1.5, slope 10^{-4} – 10^{-3} , grain size 0.5–30 mm), and smaller angles present significant risk to the banks downstream of the W-weir structure. Based on these results, the angle of orientation for W-weirs for bank protection should be 30° from the tangent to the bank. Channel-spanning structures, including cross vanes and W-weirs with large angles (generally greater than 30°), have shown indicators

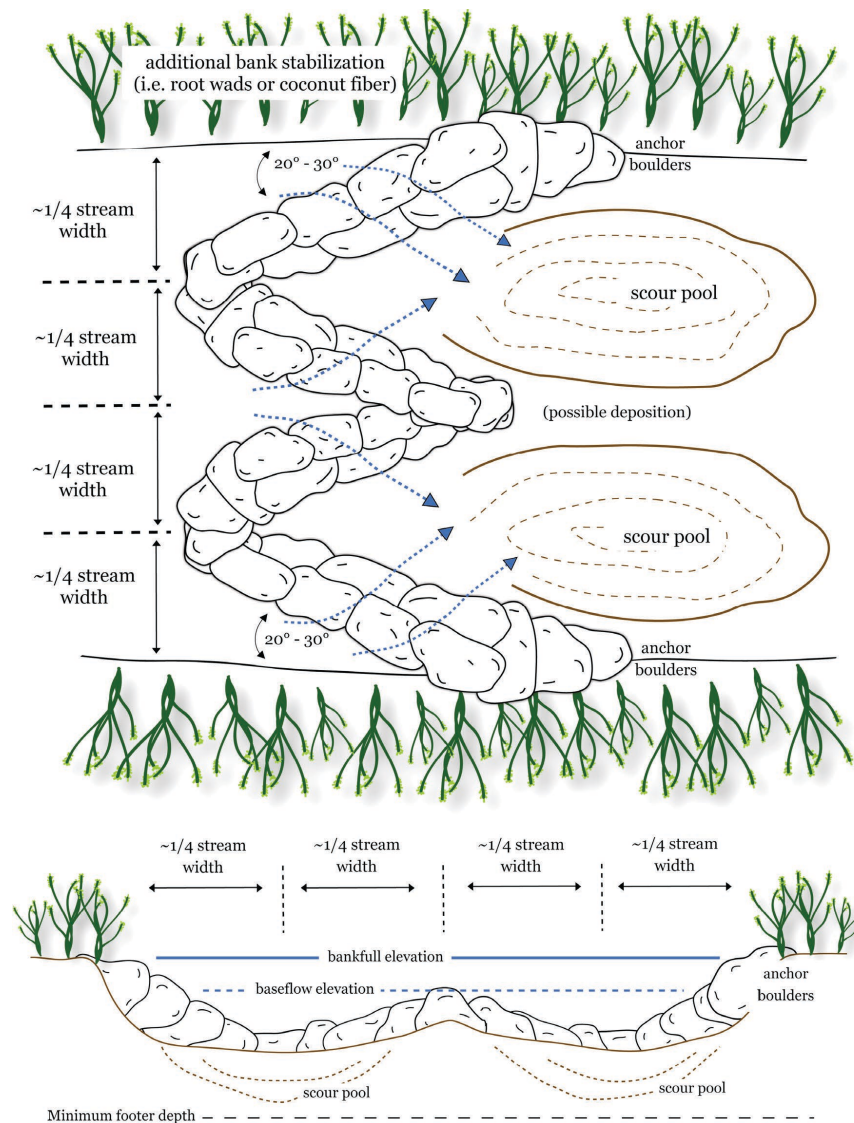


Figure F-8. Typical W-weir installation (after NRCS, 2007).

of partial and full failure in field investigations (U.S. Department of the Interior, Bureau of Reclamation, 2009).

Vane Location and Spacing

The downstream end of the riffle zone and the glides leading into the riffles are the most desirable locations since those areas will offer minimal interference with sediment transport capability (Bhuiyan et al., 2010). Results from NCHRP Project 24-33 indicate that W-weirs performed similarly in these locations; however, sill structures installed at the downstream end of a riffle zone resulted in greater interference with the meander bend mechanics and altered the bed topography in this region. The Maryland Department of the Environment guidelines (2000) suggest spacing depending on the pattern of scour pools in reference reaches or desired step pool spacing. Sill structures should be installed a minimum of two channel widths upstream of bridge piers or other infrastructure to

be protected. An alternative would be to install structures in series to minimize the dimensions of the scour hole immediately downstream of a W-weir.

F.6.3 Construction

Footer Rocks, Rock Size, and Sills

See Construction section (Section F.2.3) for guidelines. Footer rocks should be large enough to resist movement from shear stresses during the design flow. Long and flat rocks tend to perform better in the field (U.S. Department of the Interior, Bureau of Reclamation, 2009). Johnson et al. (2001) suggest that field procedures such as the use of geotextile fabric or well-graded material be used to mitigate structural porosity. Doll et al. (2003) recommend that geotextile fabric always be used for any rock vane or modified rock vane structure.

F.6.4 Maintenance and Monitoring

To ensure proper structure performance, installed structures need to be monitored for signs of structure failure, particularly after the first large flood event. The following suggestions are included based on the results from NCHRP Project 24-33 for monitoring and maintenance of W-weirs.

- Structures should be monitored for local scour, particularly downstream of the W portion of the weir.
- Structures should be monitored for signs of excessive deposition and potential flanking following large flow events. Over time, vegetation can begin to grow on this deposited material, shifting flow around the outside of the structure.
- The bank within two channel widths downstream should be monitored for signs of scour as the scour hole downstream widens. Additional bank protection may be required in this zone.

F.7 Structure Layout for Single-Arm Structures

Using a modified vector analysis commonly employed for bendway weirs or stream barbs (Lagasse et al., 2009; NRCS, 2007), the following guidelines are suggested to determine

the optimum structure layout for each in-stream flow control structure array described in Sections F.2 to F.6.

1. Project a line tangent to the bank at the meander apex. Set this line at 0° (horizontal).
2. Place the first structure at the apex. The angle of orientation should be such that it intercepts flow from upstream. This angle is dependent on the sinuosity and curvature of the meander where the structures are being installed (see Figure F-9).
 - a. Rock vanes and J-hooks: Greater angles protect more channel length in larger radius of curvature streams, and smaller angles protect more bank in smaller radius of curvature, more sinuous channels.
 - b. Bendway weirs/stream barbs: An angle of 50° was determined to be the optimum between cost (length of structure) and length of bank protected. Greater angles may provide greater bank protection, but at the cost of decreased structure stability.
3. Draw a horizontal line parallel to the first line from the tip of the structure. Draw another line with an offset angle from the parallel line. Where this line intersects the bank, the next structure should be located. The offset angle is a function of stream radius of curvature and channel width (Table F-4; see Chapter 3 for specifics).

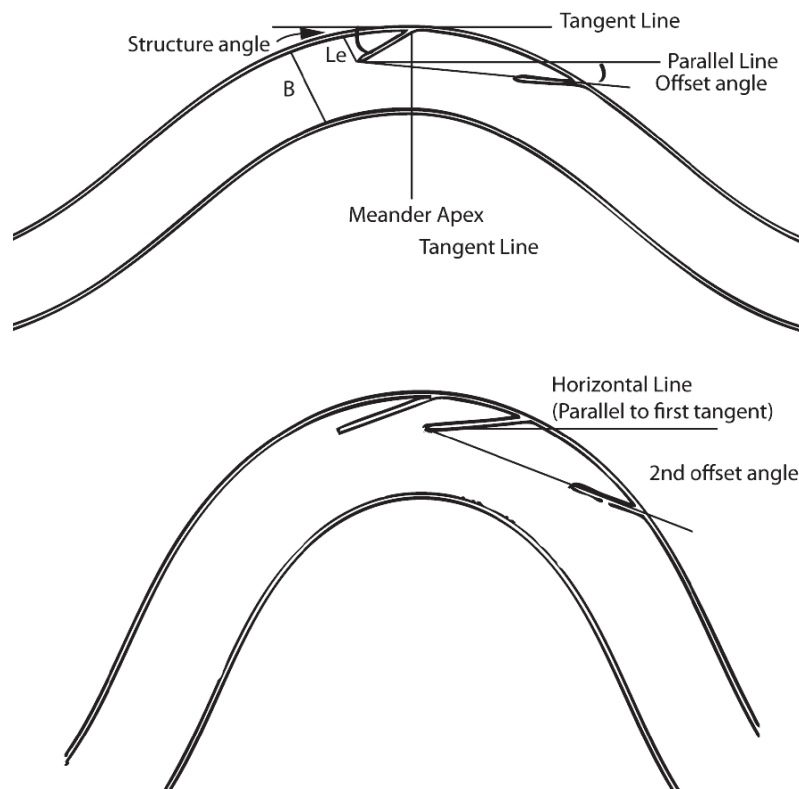


Figure F-9. Example layout for first structure at apex, second structure (top), and third structure (bottom) in two different channels.

Table F-4. Offset angles for additional structure placement based on the intersection of the shear layer of the first structure with the outer bank.

Structure Type	2 nd Structure Offset (Degrees)	3 rd Structure Offset (Degrees)
RV	-5 to 5	20 (if needed)
JH	-5 to 5*	20* (if needed)
BW	5	25 to 30

*For JH structures, the second structure offset begins at the first JH vane tip for sharp meanders and at the second structure hook tip for the third structure offset. For other meanders, the second structure offset begins at the first JH hook tip (see Section 3.2 for more information).

- Shift array upstream if necessary (see Chapter 3 or Sections F.2 to F.6).

F.8 Design Examples

F.8.1 Design Example 1: JHs in a Small Meandering Stream

Step 1. Define Project Goals and Channel Characteristics

For this example, the project goals are to (1) create scour pool habitat, and (2) protect the outer bank of a meandering stream. For this project, there is a significant buffer between the outer bank and a road, so outer bank protection is selected as a secondary goal. Based on these criteria, J-hook vanes are selected from Table F-5.

Site characteristics for this project are listed in Table F-6. This is a low-gradient meandering sand-bed stream. The project site is a sharp meander. Bed topography data were collected to map out the length of bank erosion and the apex of the meander and to calculate the slope and radius of curvature, R_c (see Figure F-10). Additional data were collected to define the maximum scour ($S_{c_{MAX}}$) around the outer meander bank (Figure F-11).

Step 2. Structure Selection

Based on the site characteristics and project goals, JHs were selected for this project (see Tables F-2 and F-3 for more information on selection criteria).

Table F-6. Site characteristics for Design Example 1, small meandering stream.

Bed material (D_{50})	Non-Cohesive Sand, 0.7 mm
Slope	7×10^{-3}
Sinuosity	1.3
Radius of curvature (R_c)	5.7 m
Width (B)	2.7 m
Depth (H)	0.3 m
Bankfull discharge (Q_{bf})	0.28 m ³ /s
Maximum velocity (outside of meander)	0.6–0.8 m/s

Step 3. Angle of Orientation

Based on the moderate sinuosity and low R_c/B ratio, this is a sharp meander bend; therefore, a smaller angle of orientation should be selected for JHs. An angle of 20° is selected.

Step 4. Layout

Vector analysis is used to map out the optimum structure location based on the channel characteristics and structure type. This process is described in Figure F-12.

Step 4a. Numerical Modeling (Recommended)

Fine-tune structure layout design and verify site-specific performance using 2-D or 3-D numerical modeling. Select a model that will allow for examination of flow paths. The VSL3D model developed in this work can serve this purpose. The goal of the modeling is to verify that this structure layout will shift the high-velocity core away from the outer bank.

Step 5. Evaluate Potential for Structure Failure and Create Monitoring Plan

Footer rock depth should be 1.5 to 2 times $S_{c_{MAX}}$ (Figure F-13). The rocks in the hook portion of a JH structure are subject to the largest hydrodynamic forces and are most susceptible to undermining from excessive scour. Therefore, monitoring plans for JHs should include a stability analysis focused on the hook portion of the structure. In addition, JHs have a moderate potential for flanking based on sediment

Table F-5. Project goal matrix for single-arm rock structures.

Primary Goals		Outer Bank Protection	Enhanced Habitat Diversity/Scour Pools	Grade Control
Secondary Goals	Outer bank protection	BW, RV	RV, JH	—
	Enhanced habitat diversity/scour pools	JH, RV	JH, CW, WW, RV	CV, WW
	Grade control	—	CV, WW	CV, WW

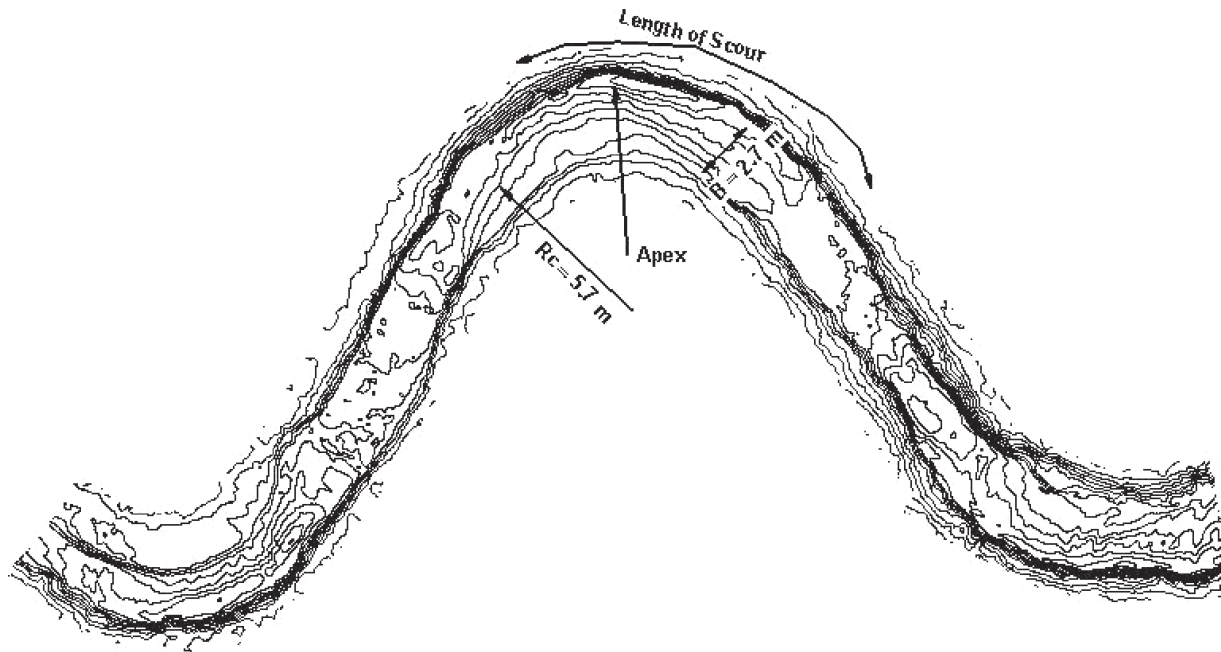


Figure F-10. Bed topography for Design Example 1 for a small meandering stream. Flow is from left to right.

deposition upstream of each structure. Monitoring should also be focused here, especially if vegetation begins to grow on this sediment.

Footer rocks: 1.5 to 2 times $S_{C_{MAX}} = 0.36 \text{ m} - 0.46 \text{ m}$

F.8.2 Design Example 2: BWs in a Meandering River

Step 1. Define Project Goals and Channel Characteristics

Primary goal: Bank protection for an eroding bank on the outside of a meander. Site characteristics are listed in Table F-7.

Step 2. Structure Selection

Based on the site characteristics and project goals, BWs were selected for this project (see Tables F-2 and F-3 for more information on selection criteria).

Step 3. Angle of Orientation

An optimum angle of 50° will be selected for the BW.

Step 4. Layout

Vector analysis will be used to map out the optimum structure location based on the channel characteristics and

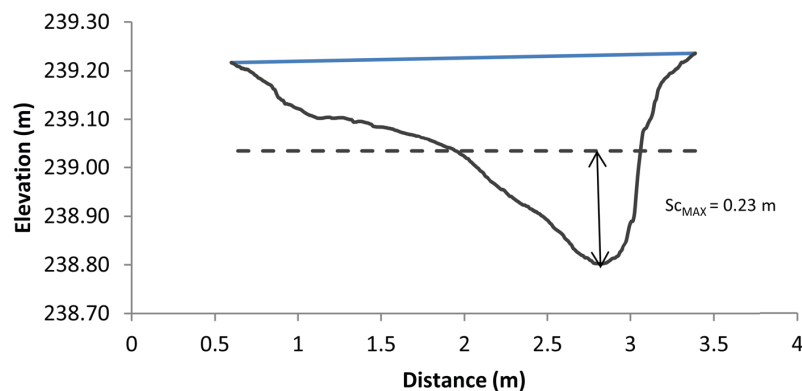


Figure F-11. Example cross section for Design Example 1 for a small meandering stream. Dotted line is average bed elevation calculated from field data. $S_{C_{MAX}}$ is the difference between the maximum scour depth and the average depth.

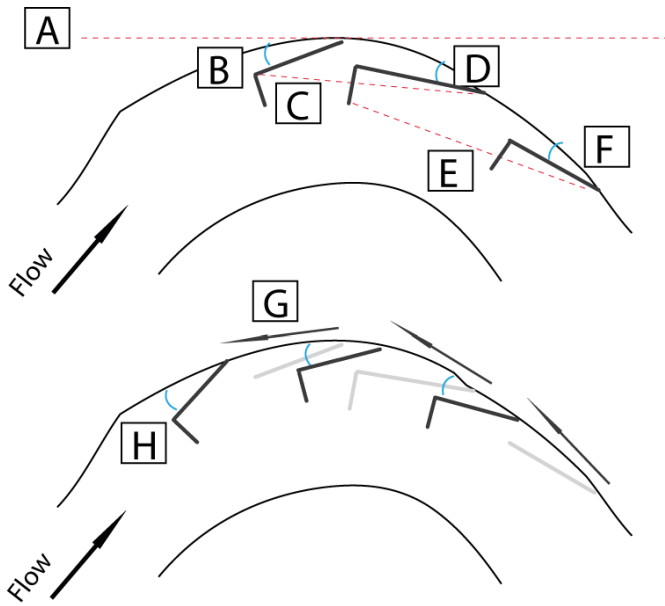


Figure F-12. Example layout for Design Example 1 for a small meandering stream. Steps A through H are described in the following.

- A. Draw a line tangent to the outer bank at the meander apex. Orient the layout so that this line is 0°, or horizontal.
- B. Draw the first JH structure at an angle of orientation of 20° to the tangent to the bank. The structure length is selected so that the vane effective length, L_e , is equal to $\frac{1}{3} B$. The hook part of the structure is another $\frac{1}{3} B$ so that the entire L_e is $\frac{2}{3} B$.
- C. Extend a line from the vane portion of the first JH at an angle of -5° from horizontal.
- D. Place the second JH where this line intersects the outer bank. This structure should be 20° from the tangent to the bank, with $L_e = \frac{2}{3} B$.
- E. Extend a line from the hook portion of the second JH at an angle of 20° from the horizontal.
- F. Place the third JH where this line intersects the outer bank.
- G. Because this is a sharp meander, JHs function better if shifted a channel width, B , upstream. Shift the entire array upstream by B .
- H. Finalize JH dimensions according to Figure F-5. The angle of orientation for each structure should be 20° from the tangent to the bank, with $L_e = \frac{2}{3} B$ (vane $L_e = \frac{1}{3} B$).

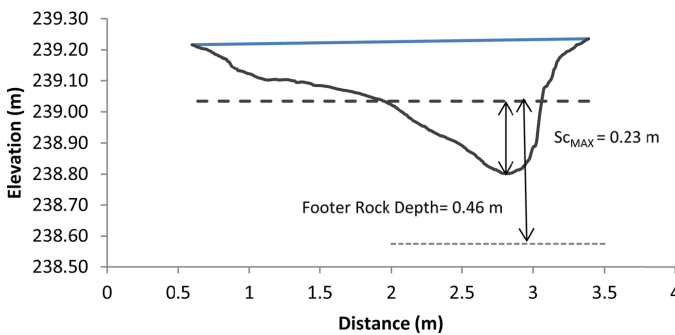


Figure F-13. Example of footer rock depth, Design Example 1 for a small meandering stream.

Table F-7. Site characteristics for Design Example 2 for a meandering river.

Bed material (D_{50})	Non-cohesive sand, 0.4 mm
Slope	3×10^{-4}
Sinuosity	1.4
Radius of curvature (R_c)	36 m
Width (B)	12 m
Depth (H)	1.0 m
Bankfull discharge (Q_{bf})	$27 \text{ m}^3/\text{s}$

Table F-8. Geometrical characteristics of BW structures based on design guidelines provided in Section F.4. B , H , and ϕ in the table are river width, flow depth, and rock's angle of repose, respectively.

	Bendway Weir
Top slope	0%
Side slope	1:2
Slope at the tip	\emptyset
Top width	$2D_{100}$
Bottom width	$2H + D_{100}$
Max. height of structure	$H/2$
Effective length span	$B/4$
Single rock size (D_{100})	0.569 m

structure type. An array of at least three BWs is needed for most channels.

The general steps are as follows:

1. Install the first BW with a 50° angle of orientation at the apex of the meander [on the outer bank of the meander (Figure F-14)].
2. Install the second BW with a 50° angle of orientation with a 5° offset from a horizontal line drawn from the first BW tip (Figure F-14).
3. Install the third BW with a 50° angle of orientation with a 30° offset from a horizontal line drawn from the second BW tip (Figure F-15).

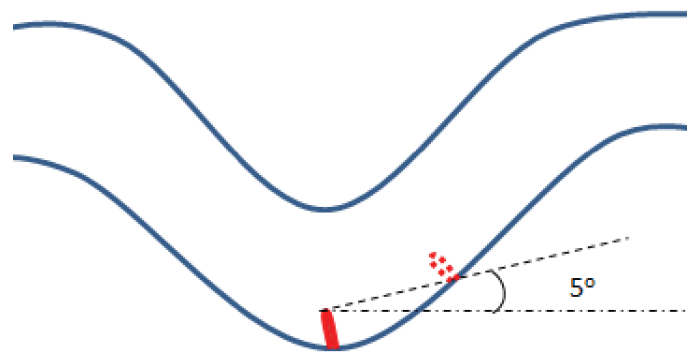


Figure F-14. Schematic of the placement of the second BW. Place the first BW at the meander apex. Set location of second BW with 5° offset from horizontal.

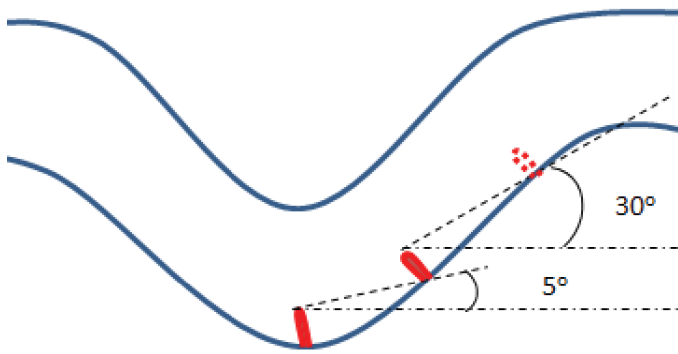


Figure F-15. Schematic of the placement of the third BW. Set location of the third BW with 30° offset from horizontal.

Step 4a. Numerical Modeling (Recommended)

This arrangement should provide the maximum protection with the least number of structures for this channel. The effectiveness of this layout should be verified using a 2-D or 3-D numerical flow model to verify that the structures redirect the high-velocity core away from the outer bank and disrupt the helical flow paths around this meander (the mechanism for outer bank scour in meandering channels).

Step 5. Evaluate Potential for Structure Failure and Create Monitoring Plan

BWs have the least risk of flanking, smallest hydrodynamic forces, lowest backwater effects, and smaller scour holes than the other single-arm structures. Therefore, maintenance is expected to be minimal. Monitoring, however, should be conducted to ensure performance, and should be done specifically for scour between structures or signs of structure instability.

F.9 Appendix F References

- Bhuiyan, F., Hey, R. D., and Wormleaton, P. R. (2010). "Bank-Attached Vanes for Erosion Control and Restoration of River Meanders." *Journal of Hydraulic Engineering*. 136(9), 583–596.
- Brown, K. (2000). *Urban Stream Restoration Practices: An Initial Assessment*. U.S. Environmental Protection Agency, Office of Wetlands, Oceans, and Watersheds, Region V. Ellicott City, MD.
- Castro, J., and Sampson, R. (2001). "Incorporation of Large Wood into Engineering Structures." Natural Resource Conservation Service Engineering Technical Note No. 15, USDA, Boise, ID.
- Derrick, D. L. (1998). "Four Years Later, Harland Creek Bendway Weir/Willow Post Bank Stabilization Demonstration Project." Proc., 1998 Int. Water Resources Engineering Conf., ASCE, Memphis, TN.
- Doll, B. A., Grabow, G. L., Hall, K. L., Halley, J., Harman, W. A., Jennings, G. D., and Wise, D. E. (2003). *Stream Restoration: A Natural Channel Design Handbook*. NC State University, Raleigh, NC.
- Evans, J. L., and Kinney, W. (2000). "Bendway Weirs and Rock Stream Barbs for Stream Bank Stabilization in Illinois." Technical Presentation for 2000 ASABE Int. Meeting, ASABE.
- Fischenich, C., and Seal, R. (2000). "Boulder Clusters." EMRRP Technical Notes Collection (ERDC TN-EMRRP-SR-11), U.S. Army Engineer Research and Development Center, Vicksburg, MS. www.wes.army.mil/el/emrrp.
- Johnson, P. A., Hey, R. D., Brown, E. R., and Rosgen, D. L. (2002a). "Stream Restoration in the Vicinity of Bridges." *J. Am. Water Resour. Assoc.*, 38(1), 55–67.
- Johnson, P. A., Tereska, R. L., and Brown, E. R. (2002b). "Using Technical Adaptive Management to Improve Design Guidelines for Urban Instream Structures." *J. Am. Water Resour. Assoc.*, 38(4), 1143–1152.
- Johnson, P. A., Hey, R. D., Tessier, M., and Rosgen, D. L. (2001). "Use of Vanes for Control of Scour at Vertical Wall Abutments." *Journal of Hydraulic Engineering*. 127(9), 772–778.
- Lagasse, P. F., Zevenbergen, L. W., Schall, J. D., and Clopper, P. E. (2009). "HEC 23, Bridge Scour and Stream Instability Countermeasures." FHWA HEC-23, U.S. DOT, FHWA.
- Maryland Department of the Environment. (2000). *Maryland's Waterway Construction Guidelines*. Water Management Administration, Baltimore.
- Matsuura, T., and Townsend, R. D. (2004). "Stream-Barb Installations for Narrow Channel Bends—A Laboratory Study." *Canadian Journal of Civil Engineering*. 31(3), 478–486.
- McCullah, J., and Gray, D. 2005. *NCHRP Report 544: Environmentally Sensitive Channel and Bank-Protection Measures*. Transportation Research Board of the National Academies, Washington, D.C.
- Mooney, D., Holmquist-Johnson, C., and Holburn, E. (2007) *Qualitative Evaluation of Rock Weir Field Performance*. Bureau of Reclamation, Technical Service Center, Sedimentation and River Hydraulics Group, Denver, CO.
- NRCS (2000). "Design of Rock Weirs." Oregon Technical Notes Engineering No. 24, USDA NRCS, Portland, OR.
- NRCS (2007). *Stream Restoration Design National Engineering Handbook*, Part 654. United States Department of Agriculture, National Resource Conservation Service, Washington, D.C.
- NRCS (2010). "Design of Stream Barbs for Low Gradient Stream." Minnesota Technical Note No. 8, USDA NRCS, St. Paul, MN.
- Rosgen, D. L. (2006). *Cross-Vane, W-Weir, and J-Hook Vane Structures*. Wildland Hydrology, Pagosa Springs, CO.
- Radspinner, R. R., Diplis, P., Lightbody, A. F., Sotiropoulos, F. (2010). "River Training and Ecological Enhancement Potential Using In-Stream Structures." *Journal of Hydraulic Engineering*. 136(12), 967–980.
- U.S. Army Corps of Engineers. (1991). "Hydraulic Design of Flood Control Channels." EM 1110-2-1601, Army Corps of Engineers, Department of the Army, Washington, D.C.
- U.S. Department of the Interior, Bureau of Reclamation. (2009). "Quantitative Investigation of the Field Performance of Rock Weirs." U.S. Department of the Interior, Bureau of Reclamation. SRH-2009-46. Denver, CO.

Abbreviations and acronyms used without definitions in TRB publications:

A4A	Airlines for America
AAAAE	American Association of Airport Executives
AASHO	American Association of State Highway Officials
AASHTO	American Association of State Highway and Transportation Officials
ACI-NA	Airports Council International-North America
ACRP	Airport Cooperative Research Program
ADA	Americans with Disabilities Act
APTA	American Public Transportation Association
ASCE	American Society of Civil Engineers
ASME	American Society of Mechanical Engineers
ASTM	American Society for Testing and Materials
ATA	American Trucking Associations
CTAA	Community Transportation Association of America
CTBSSP	Commercial Truck and Bus Safety Synthesis Program
DHS	Department of Homeland Security
DOE	Department of Energy
EPA	Environmental Protection Agency
FAA	Federal Aviation Administration
FHWA	Federal Highway Administration
FMCSA	Federal Motor Carrier Safety Administration
FRA	Federal Railroad Administration
FTA	Federal Transit Administration
HMCRRP	Hazardous Materials Cooperative Research Program
IEEE	Institute of Electrical and Electronics Engineers
ISTEA	Intermodal Surface Transportation Efficiency Act of 1991
ITE	Institute of Transportation Engineers
MAP-21	Moving Ahead for Progress in the 21st Century Act (2012)
NASA	National Aeronautics and Space Administration
NASAO	National Association of State Aviation Officials
NCFRP	National Cooperative Freight Research Program
NCHRP	National Cooperative Highway Research Program
NHTSA	National Highway Traffic Safety Administration
NTSB	National Transportation Safety Board
PHMSA	Pipeline and Hazardous Materials Safety Administration
RITA	Research and Innovative Technology Administration
SAE	Society of Automotive Engineers
SAFETEA-LU	Safe, Accountable, Flexible, Efficient Transportation Equity Act: A Legacy for Users (2005)
TCRP	Transit Cooperative Research Program
TEA-21	Transportation Equity Act for the 21st Century (1998)
TRB	Transportation Research Board
TSA	Transportation Security Administration
U.S.DOT	United States Department of Transportation